The Speed of Waves

M.H.N. van Velzen

THE SPEED OF WAVES

Measuring the velocity of pressure pulse waves traveling through peripheral blood vessels

Marit H.N. van Velzen

THE SPEED OF WAVES

Measuring the velocity of pressure pulse waves traveling through peripheral blood vessels

DE SNELHEID VAN Ggolven

Het meten van de snelheid van bloeddrukgolven die door perifere bloedvaten bewegen

Proefschrift

ter verkrijging van de graad van doctor aan de
Erasmus Universiteit Rotterdam
op gezag van de
rector magnificus

Prof.dr. R.C.M.E. Engels

en volgens besluit van het College voor Promoties.
De openbare verdediging zal plaatsvinden op

dinsdag 7 mei 2019 om 13:30 uur
door

Marit Heleen Nicolette van Velzen
geboren te Heesch

Erasmus University Rotterdam

Promotiecommissie

Promotor	Prof. dr. R.J. Stolker
Overige leden	Prof. dr. J. Dankelman Prof. dr. I.K.M. Reiss Prof. dr. H.J.M. Verhagen
Copromotoren	Dr. E.G. Mik Dr. ing. S.P. Niehof

Title The Speed of Waves
Author Marit H.N. van Velzen
Print Ridderprint | www.ridderprint.nl.
ISBN 978-94-6385-331-9

Thesis Photography & Cover Design: dr. ir. Arjo J. Loeve | www.arjoloeve.nl

Financial support for this thesis was generously provided by: Jeroen Bosch Ziekenhuis & Verder Met Kwaliteit.
Financial support by the Dutch Heart Foundation for the publication of the thesis is gratefully acknowledged.

Start the day with a smile

Table of contents

Chapter 1

Introduction

1.1 The necessity for early detection of divergent arterial stiffness

Globally, cardiovascular diseases (CVDs) are the number one cause of death. In 2014, an estimated 20 million people died from CVDs, representing 30% of all global deaths [1]. Smoking, unhealthy diet, physical inactivity and excessive use of alcohol are the most important behavioral risk factors of CVDs. As an effect, individuals may develop hypertension, diabetes, heart failure or atherosclerosis, most of which are related to a change in arterial stiffness. Considering the wide spread of CVDs in the world, there is a strong need for an easy and quick prognostic indicator to determine divergent arterial stiffness to support in early diagnosis of CVDs.

1.2 Pulse wave velocity as arterial stiffness measure

Arterial stiffness is most commonly used to express the viscoelastic property of the arterial wall, which describes the relationship between change in pressure and change in arterial volume [2]. Therefore, arterial stiffness, or its inverse the arterial compliance, is a reliable prognostic indicator of cardiovascular morbidity and mortality in the adult population [3-5]. The compliance (C) is a measure of the elasticity of the arteries and is defined as

$$C = \frac{\Delta V}{\Delta P} \tag{1.1}$$

where ΔV is the change in arterial volume and ΔP the change in blood pressure [6]. At any given pressure change, the volume of stiffer vessels change less than that of more compliant vessels. The arterial stiffness of a blood vessel is of crucial importance because the elastic walls of the arteries attenuate the systolic pressure wave of each heartbeat. The potential energy stored in the vessel walls during systole is used to continue to continue propeling the blood during the diastole between successive heartbeats [2].

The effect of increased arterial stiffness, and thus reduced arterial compliance, is a decreased propagation time of pressure pulse waves (PWs) through the vessels and thus an increase of the velocity (PWV) of the PWs [7, 8]. Therefore, the gold standard for determining arterial stiffness is measuring the PWV[9]. The PWV is inversely related to arterial distensiblility [10-12] and is directly related to the incremental elastic modulus $E_{inc,vessel}$ and vessel wall thickness h_{vessel}, and inversely

related to the vessel radius r_{vessel} by the Moens-Korteweg equation (with ρ_{blood} the density of blood) [13]:

$$PWV = \sqrt{\frac{E_{inc} \cdot h}{2r \cdot \rho_{blood}}} \tag{1.2}$$

As a consequence, PWV is widely used as an index of elasticity of the vessel wall and arterial stiffness [12]. The PWV is commonly measured as an average speed of a PW between two locations on the body or along an arterial trajectory. The assessment of the PWV involves measurement of two quantities:

- the distance between both recording sites (d)
- the transit time of the PW along that distance (t)

$$PWV = \frac{d}{\Delta t} \tag{1.3}$$

Note that the PWV is not the speed of blood, but the speed of the pressure pulse traveling through the (usually also moving) blood. Therefore, a PW is comparable to a sound wave. For the evaluation of cardiovascular (CV) risk, the PWV can be measured both invasively and non-invasively and is highly reproducible [14].

In clinical practice, the PWV is generally determined over the carotid-femoral trajectory or the brachial-ankle trajectory. Depending on age, in healthy subjects the PWV is about 6-10 m/s over the carotid-femoral trajectory. In cardiovascular risk patients the PWV can be as high as 20 m/s over the same trajectory [8, 15, 16], which is two to three times as high as in healthy subjects.

1.3 State of the art

Several non-invasive techniques for measuring PWV are currently clinically available, such as [17-19]:

- the SphygmoCor system (AtCor Medical, West Ryde, Australia), which measures PWV via carotid tonometry and a thigh sphygmomanometer cuff,
- the Arteriograph system (Tensiomed, Budapest, Hungary), which measures PWV by analysis of the oscillometric pressure curves registered on the upper arm,

- and the Complior system (Alam Medical, Saint Quentin Fallavier, France), which measures PWV by means of piezo-electronic pressure transducers placed at the neck and at the groin.

The Arteriography system uses the pressure curves on the upper arm to analyze the time difference between the beginning of a PW and the beginning of the succeeding PW, related to the distance from the jugulum to the symphysis [18]. This provides a PWV value as a global measurement of the PWV over the whole body and not the PWV of a particular section of an arterial vascular trajectory.

The drawback of the Sphygmocor and Complior systems is that they require two separate and rather large sensors to be placed on the patients. Limitations of these techniques include the difficulty of accurately positioning the sensors, and the discrepancy between the measured distance between the sensors and the actual path length travelled by the PWs. For this purpose magnetic resonance imaging could can be used. However, measuring the actual path length with the aid of such medical imaging techniques is too expensive and time-consuming in clinical practice.

The systems described above are sub-optimal for use in clinical practice. The sensor clip used with the Complior is placed around the neck, which may be experienced as uncomfortable, and the system requires placement of two sensors on different locations of the body. With the SphygmoCor system it is not possible to fix the sensor on the patient's carotic artery: it has to be kept steady by an operator. These aspects limit the suitability of these systems as monitoring devices. When using a sphygmomanometer cuff to measure the PWV, the blood flow will temporarily be disturbed, causing an unknown impact on the PWV measurements during monitoring. Other disadvantages of the existing systems are their prolonged learning periods for becoming an experienced operator and that the devices lack versatility [19].

1.4 Goal

It would be beneficial if PWV measurements could be performed while integrated into currently available medical devices. One of the simplest potentially suitable devices broadly used in the clinic are the commonly available finger clip PPG-sensors used for SpO_2 and pulse rate monitoring. Clinical practice could benefit from such a device that can measure the PWV over a short distance, using

a simple technique that is already familiar to clinicians, while being comfortable for patients and easy-to-use.

Therefore, the goal of this Ph.D. study was to develop and validate a non-invasive, PPG-based device for peripheral measurement of the PWV on the finger. To that purpose, the following aims were formulated:

- to confirm the value of peripheral PWV measurements,
- to design and technically validate a PPG-based device for measuring PWV in the finger,
- to validate the developed device in clinical studies.

1.5 Approach & Outline

This thesis consists of two main parts. Part I - Substantiation, shows the value of peripheral PWV measurements and provides a platform-independent and measurement technique independent algorithm for improvement of PWV measurements. Part II - Development & Validation, describes the design, technical validation, testing, further improvement and final validation of the Multi Photodiode Array, the PWV measurement device developed during this Ph.D. study. A more detailed outline is provided below.

Part I Substantiation

Chapter 2: During pilot measurements and earlier studies using existing techniques for PWV and PTT (Pulse Transit Time, the time a PW takes to travel from one point to another: PWV=distance/PTT) measurements, it appeared that many PWs get distorted when patients move or have severe vascular disease. These distorted PWs affect PWV and PTT values, undermining the reliability of such metrics in clinical practice. Therefore, a '7-Step PW Filter' was developed with the aim to eliminate pulse waves that are unsuitable for common PWV and PTT analysis methods from PPG signals.

Chapter 3: Several PWV and PTT measuring methods are based on assessing the time between the ECG R-peak of a heartbeat and the successive arrival of the PWV at a peripheral point on a vascular trajectory. However, this time consists of two parts: the pre-ejection period (PEP), which is the time between the ECG R-peak and the moment the PW actually leaves the heart, and the Vascular Transit Time (VTT), the time needed by the PW to travel from the heart to the peripheral measurement point. If the PEP were of the same or larger order of magnitude than

the VTT, as these values may reflect more how fast the heart can built up pressure than the state of the vascular system. After all, in such cases these values may tell more about how fast the heart can build up pressure, than about the state of the vascular system. A study on healthy volunteers and patients was done in order to estimate the variability of PEP at rest and to establish the accuracy or PTT as an approximation for VTT.

Chapter 4: Before upper limb surgery under locoregional anesthesia, an axillary brachial plexus block is used to desensitise and demobilize the arm, which also releases vascular tone. Currently, testing whether a patient can sense a cold-pack on the upper limb's skin is used to verify the effect of the axillary brachial plexus block. In this chapter, peripheral measurements were used to explore whether PTT can be used to objectively, reliably, and quickly establish the state of the vascular system.

Chapter 5: Pain is a sensation that is highly subjective, but also has objective aspects. Tests for determining whether a patient experiences pain are based on obtaining feedback from an individual and therefore require individuals to be conscious and able to communicate. Therefore, having an objective measure for nociception (which, simply put, is the objective part of pain caused by physical stimuli), would be of great value in many clinical settings, such as to determine whether patients under anesthesia experience nociception during surgery. A study on healthy volunteers was done to investigate whether an effect of heat-induced pain stimuli on PTT and pulse wave amplitude could be measured using a PPG-based technique.

Part II Development & Validation

Chapter 6: This chapter describes the design and validation of the Multi Photodiode Array (MPA), a PPG-based system for PWV measurements on the finger that also measures heart rate, pulse wave amplitude and peripheral PTT, and could also measure SpO_2. The accuracy of the MPA system was determined through an experiment with a focused light dot scanning over the MPA with known velocity. The tested velocities matched the broad range of PWVs known from literature to have been measured in volunteers and patients. The aim of this study was to verify the functionality of the MPA.

Chapter 7: An experiment was conducted on healthy volunteers between 20 and 30 years old. PWVs were measured with, two different systems (Biopac and

Complior) over two different trajectories. to investigate whether these provided comparable results. This was done because in clinical practice it is crucial to know whether using different devices for the same purpose provides the same outcome.

Chapter 8: During one volunteers study and two patient studies (described in Appendices 8.A to 8.C) it was noticed that the technically validated MPA provided extremely varying and unlikely PWV values in practice. A systematic investigation was conducted to discover the cause of these outcomes and to determine a standardized, optimal use condition for the MPA sensor that would provide reliable and consistent PWV measurements.

Chapter 9: A final clinical validation study was done by applying the optimal use condition of the MPA determined in Chapter 8 to measure PWV in healthy volunteers of two age groups (18-35 years old and 55+). The measurements were done both in baseline situations and during application of a 'flow mediated dilation'-technique, a standard test for measuring endothelial dysfunction. This was done to investigate whether the MPA results correspond with gold-standard PWV and to validate the optimal use condition from Chapter 8.

Chapter 10: The technical software and hardware developments and validations, the four studies on healthy volunteers and four patient studies that formed this Ph.D. study are discussed in this final chapter. Advice is given about the application of the MPA and suggestions for future research are given to guide the further development of the MPA into an elegant, economical, easy-to-use medical device for measuring all sorts of PPG-based physiological parameters at the finger.

1.6 References

1. Organization, W.H., *Global status report on noncommunicable diseases 2010*. 2011, Geneva: Geneva, Switzerland : World Health Organization.
2. Quinn, U., L.A. Tomlinson, and J.R. Cockcroft, *Arterial stiffness.* JRSM Cardiovasc Dis, 2012. 1(6): p. 1:18.
3. Blacher, J., et al., *Impact of aortic stiffness on survival in end-stage renal disease.* Circulation, 1999. 99(18): p. 2434-2439.
4. Laurent, S., et al., *Aortic stiffness is an independent predictor of all-cause and cardiovascular mortality in hypertensive patients.* Hypertension, 2001. 37(5): p. 1236-1241.
5. Cruickshank, K., et al., *Aortic pulse-wave velocity and its relationship to mortality in diabetes and glucose intolerance: An integrated index of vascular function?* Circulation, 2002. 106(16): p. 2085-2090.

6. O'Rourke, M.F., et al., *Clinical applications of arterial stiffness; definitions and reference values.* Am J Hypertens, 2002. 15(5): p. 426-444.
7. Laurent, S., et al., *Expert consensus document on arterial stiffness: methodological issues and clinical applications.* Eur Heart J, 2006. 27(21): p. 2588-605.
8. Boutouyrie, P. and S.J. Vermeersch, *Determinants of pulse wave velocity in healthy people and in the presence of cardiovascular risk factors: Establishing normal and reference values.* European Heart Journal, 2010. 31(19): p. 2338-2350.
9. Bramwell, J.C. and A.V. Hill, *Velocity of transmission of the pulse-wave. And elasticity of arteries.* Lancet, 1922. 199(5149): p. 891-892.
10. Cavalcante, J.L., et al., *Aortic stiffness: Current understanding and future directions.* Journal of the American College of Cardiology, 2011. 57(14): p. 1511-1522.
11. McDonald, D.A., *Regional pulse-wave velocity in the arterial tree.* Journal of applied physiology, 1968. 24(1): p. 73-78.
12. Asmar, R., et al., *Assessment of arterial distensibility by automatic pulse wave velocity measurement: Validation and clinical application studies.* Hypertension, 1995. 26(3): p. 485-490.
13. Bramwell, J.C. and A.V. Hill, *The Velocity of the Pulse Wave in Man.* Proceedings of the Royal Society of London Series B, Containing Papers of a Biological Character, 1922. 93(652): p. 298-306.
14. Wilkinson, I.B., et al., *Reproducibility of pulse wave velocity and augmentation index measured by pulse wave analysis.* Journal of Hypertension, 1998. 16(12 SUPPL.): p. 2079-2084.
15. Mancia, G., et al., *2013 ESH/ESC guidelines for the management of arterial hypertension: The Task Force for the management of arterial hypertension of the European Society of Hypertension (ESH) and of the European Society of Cardiology (ESC).* European Heart Journal, 2013. 34(28): p. 2159-2219.
16. Meaume, S., et al., *Aortic pulse wave velocity predicts cardiovascular mortality in subjects >70 years of age.* Arteriosclerosis, Thrombosis, and Vascular Biology, 2001. 21(12): p. 2046-2050.
17. Jatoi, N.A., et al., *Assessment of arterial stiffness in hypertension: Comparison of oscillometric (Arteriograph), piezoelectronic (Complior) and tonometric (SphygmoCor) techniques.* Journal of Hypertension, 2009. 27(11): p. 2186-2191.
18. Baulmann, J., et al., *A new oscillometric method for assessment of arterial stiffness: Comparison with tonometric and piezo-electronic methods.* Journal of Hypertension, 2008. 26(3): p. 523-528.
19. Calabia, J., et al., *Doppler ultrasound in the measurement of pulse wave velocity: agreement with the Complior method.* Cardiovasc Ultrasound, 2011. 9: p. 13.

Substantiation

Part I

Chapter 2

Increasing accuracy of pulse transit time measurements by automated elimination of distorted photoplethysmography waves

Marit H.N. van Velzen, Arjo J. Loeve, Sjoerd P. Niehof, Egbert G. Mik

Medical & Biological Engineering & Computing, March 2017

Photoplethysmography (PPG) is a widely available non invasive optical technique to visualize pressure pulse waves (PWs). Pulse transit time (PTT) is a physiological parameter that is often derived from calculations on ECG- and PPG signals and is based on tightly defined characteristics of the PW shape. PPG-signals are sensitive to artefacts. Coughing or movement of the subject can affect PW shapes that much that the PWs become unsuitable for further analysis. The aim of this study was to develop an algorithm that automatically and objectively eliminates unsuitable PWs. In order to develop a proper algorithm for eliminating unsuitable PWs, a literature study was conducted. Next, a '7Step PW Filter' algorithm was developed that applies 7 criteria to determine whether a PW matches the characteristics required to allow PTT calculation. To validate whether the '7Step PW-Filter' eliminates only and all unsuitable PWs, its elimination results were compared to the outcome of manual elimination of unsuitable PWs. The '7Step PW-Filter' had a sensitivity of 96.3% and a specificity of 99.3%. The overall accuracy of the '7Step PW-Filter' for detection of unsuitable PWs was 99.3%. Compared to manual elimination, using the '7Step PW Filter' reduces PW elimination times from hours to minutes and helps to increase the validity, reliability and reproducibility of PTT data.

2.1 Introduction

Photoplethysmography (PPG) is a widely available non-invasive optical technique that uses infrared light and photodiodes to visualize the pressure pulse waves (PWs) in blood vessels by measuring the volumetric changes of pulsating blood and thus the expansion and contraction of the vessels. These PWs result from the contraction of the heart when the blood is pumped through the body [1].

PPG enables continuous measurement of the PWs [2, 3] and is routinely used in everyday medicine for measuring physiological parameters such as heart rate, blood oxygen saturation (SpO_2), Pulse Wave Velocity (PWV) and Pulse Transit Time (PTT) [1]. PTT is usually defined as the propagation time of a PW going from the heart to the peripheral arteries and is calculated as the time between the R-peak of the ECG and a reference point on the PW measured using PPG (see Figure 2.1). PTT is commonly used for assessing arterial stiffness, vessel compliance and sympathetic activity in sleep apnoea patients [4], for measuring endothelial function [5] and as indicator for arterial blood pressure [6]. Generally, PTT is inversely related to PWV [7]. PWV may be considered as the gold standard measure of arterial stiffness [8, 9], which is a very reliable prognostic parameter for cardiovascular diseases [10-12]. Therefore, PTT is considered to be very useful for studying cardiovascular diseases.

The calculation of PTT is based on tightly defined characteristics of the PW-shape.

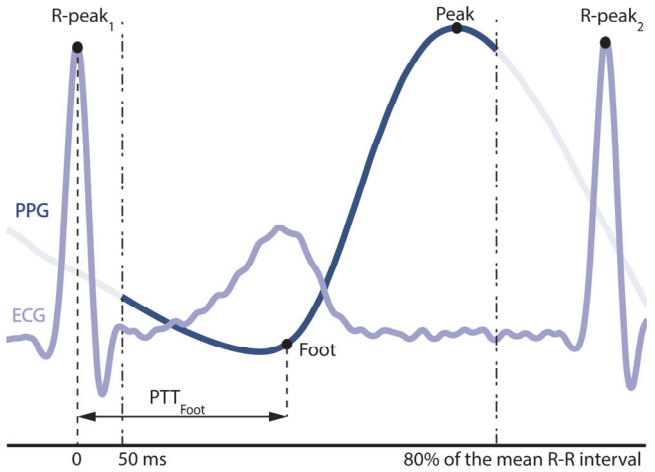

Figure 2.1: Graphical explanation of PTT calculation when using the PW foot as the landmark that indicates arrival of the PW. PTT = Pulse Transit Time, ECG = Electrocardiogram, PPG = Photoplethysmography

PWs measured using PPG are artefact sensitive to talking, moving, breathing and temperature-changes [1]. These artefacts can disturb the shapes of the PWs in such a way that the PWs become unsuitable for further analysis. However, when such unsuitable PWs are nevertheless used for further analysis, nonactual values of calculated parameters may result, which may lead to misinterpretation or even misdiagnosis in clinical practice. Such nonactual values may easily be left unnoticed as these may still fall within the range of commonly encountered values.

Using an algorithm to eliminate unsuitable PWs based on their shape, instead of using, for example, the bandpass-filtering-method [13] probably gives more reliable results. The bandpass-filtering-method ignores the fact that a PW within that band is not always suitable, and a PW outside that band is not always unsuitable, which easily results in false positive and false negative filtering results. In addition, the bandpass-filtering-method does not exclude unsuitable PWs. This paper describes and evaluates an algorithm for assessing the suitability of a PW for PTT-analyses based on the reference points detected on the PW.

During PTT-measurement in clinical experiments, thousands of PWs may be recorded and may have to be checked manually, as is often done in studies described in literature (see Table 2.1), which is obviously highly time consuming. Furthermore, manual assessment of PWs is prone to cause variations due to subjective interpretations.

The goal of this study was to develop an automated filtering method to quickly and objectively eliminate unsuitable PWs. This algorithm should provide consistent and reproducible results and increase the reliability of PTT-values that are calculated based on PW characteristics. Although, ECG-signal artefacts may also cause nonactual PTT-values, this article focuses on the PW-shape.

2.2 Materials and methods

2.2.1 Literature study

In order to develop a proper algorithm for eliminating unsuitable PWs, it should first be clear how the suitability of a PW for PTT calculation should be defined. In literature, the foot, minimum value, point of steepest ascend, or peak or maximum value of a pulse wave are the locations on the PW that are commonly used to calculate the PTT. These locations are all used under the assumption that every PW has a certain characteristic shape and that the arrival of such a location on the PW indicates the arrival of the PW. In order to enable automated extraction of

such data, it should be well defined where a PW starts and how the characteristic shape of this wave should be described.

For PTT calculations, there are several definitions of PTT, each of which using a different location on a PW as the reference point indicating the arrival of the PW. A literature study was done to get an overview of methods that are being used to calculate the PTT in clinical experiments and to see if and how unsuitable PWs are being eliminated. The literature study was conducted in PubMed for studies up to 25 June 2015 and using the search query: *"photoplethysmography" [MeSH Terms] OR "photoplethysmography" [All Fields]) AND "pulse transit time" [All Fields] AND ("humans" [MeSH Terms] AND English[lang]) NOT Review[ptyp].* The query returned 53 studies, of which the relevant ones are listed in Table 2.1. Nine studies were eliminated because PTT was measured using a different technique than PPG or because the study focussed on monitoring devices. Four characteristics of the studies were extracted and listed in Table 2.1:

- Population;
- Period over which PTT was averaged;
- Definition of PTT used;
- Method of filtering applied to the data;

Table 2.1: Results of the literature review showing how the PTT was determined in the respective studies. The studies are sorted by year and grouped by filtering method.

Reference	Population study	Average period	Definition of PTT	Filtering
[14]	patients	1, 2min	foot :maximum of 2nd derivative; 50% is maximum of 1st derivative; peak: maximum of PW	algorithm
[15]	healthy volunteers	The first 50consective PWs	25% peak of PW	algorithm
[16]	children	>30 heartbeats	onset of PW	algorithm
[17]	healthy volunteers	1min, 5min	upstroke of PW	algorithm
[18]	children	30 motion free heartbeats	upstroke of PW	algorithm
[19]	healthy volunteers	50 heartbeats	25% peak point of PW	algorithm
[20]	healthy volunteers	8s	upslope of PW	algorithm
[21]	healthy volunteers	5min	slope of PW	algorithm

[22]	patients	1min	peak of PW	filtered, not specified
[23]	healthy blood donors	3min, 6min	foot, pulse onset of 1st derivative PW	filtered, not specified
[24]	healthy volunteers	30s, 2min	peak of 1st derivative of PW	manually
[25]	healthy volunteers	1heartbeat	50% peak of PW	manually
[26]	healthy volunteers	60 heartbeats	foot: minimum; peak: maximum	manually
[27]	healthy volunteers and patients	100sec, 400sec	foot of PW	median analysis
[28]	healthy volunteers	1min	PTTa: foot of PW; PTTb: peak of PW; PTTp: 25% of amplitude of PW; PTTq:max slope of PW	not specified
[29]	children	1min	50% point upstroke of PW	not specified
[30]	patients	1heartbeat	not specified	not specified
[31]	not specified	n/a	cross correlation of ECG and derivative PGG	not specified
[32]	patients	5heartbeats, 1min	maximal upslope of derivative PW	not specified
[33]	patients	1min, 5min	foot: signal voltage is 10% of baseline value	not specified
[34]	healthy volunteers	10s	maximum of 1st derivative	not specified
[35]	healthy volunteers	not specified	foot/onset of the PW	not specified
[36]	healthy volunteers and patients	20-30s	foot-foot delay	not specified
[37]	healthy volunteers	2min, 4min	peak of the first derivative of PW	not specified
[38]	healthy volunteers	18s	foot: onset of PW; PTTdp: max derivative point	not specified
[39]	healthy volunteers	1min	onset of PW	not specified
[40]	healthy volunteers	1min	foot of PW	not specified
[41]	healthy volunteers	not specified	50% point on the rising slope of the PPG signal	not specified
[42]	children	not specified	50% point on the rising slope of PW	not specified
[43]	children	>30 heartbeats	upstroke of PW	not specified

[44]	healthy volunteers		25% peak of PW	not specified
[45]	not specified	not specified	5% peak systolic value	not specified
[46]	healthy volunteers	20s	foot of PW	not specified
[47]	children	>30 heartbeats	not specified	not specified
[48]	healthy volunteers	15s	PTT1: peak of 2nd derivative of PW; PTT2: 50% of PW; PTT3: 90% of PW	not specified
[49]	healthy volunteers	2min, 5min	Foot; maximal sloop; peak	not specified
[50]	healthy volunteers	2min	upslope of PW	not specified
[2]	healthy volunteers	60 heartbeats	minimum of PW	not specified
[51]	patients	2min	minimum of PW	not specified
[13]	children	1heartbeat	onset of PW	PTT outside range of 150 to 400ms considered invalid.
[52]	healthy volunteers	1min	foot, onset of the PW	visually
[53]	healthy volunteers and patients	1min	foot/onset of PW	visually
[54]	healthy volunteers	5min	upstroke of PW	visually
[55]	healthy volunteers	15s	foot of PW	visually

Population

The populations described in the studies listed in Table 2.1 consisted of healthy volunteers in 26 studies, of a combination of healthy volunteers and patients in three studies and of only patients in six studies. In seven studies the population consisted of children and in two studies the population was not specified.

Period over which PTT was averaged

In many studies the PTT-values used as the outcome measure were not single-PW PTT-values of all individual PWs, but were average PTT-values over a certain number of heartbeats or a certain period of time. These averaging periods ranged

from 5 heartbeats to 6 minutes. An averaging period of 1 minute was most common (10x). The smaller the number of PTT-values included in the averaging period, the more sensitive the calculated value will be to unsuitable PWs. Yet, in patients having many unsuitable PWs, even PTT-values obtained from long averaging periods may be highly affected by unsuitable PWs.

Definition of PTT used

The PW foot is the reference point most commonly used (19 studies) in PTT-analysis to pinpoint the arrival instance of a PW. However, the PW foot was not always defined identically. In three studies the foot was defined as the minimum of the PW and in three studies the foot was defined as the maximum of the second derivative of the PW. In seven studies the 'onset' of the PW was defined as its foot and six studies did not define what was used as the foot of a PW. In four studies the PW peak was taken as the PW arrival instance, while in eight studies the maximum upslope of the PW was used.

Method of filtering applied to the data

Only seven reports mentioned that unsuitable PWs were eliminated manually or visually, but the criteria were not defined clearly or were not mentioned at all. In the majority of the studies it was unclear whether or not any PWs were eliminated. Some reports mentioned the use of a PW elimination algorithm, but did not specify the applied algorithm. Gil et al. used a filter that eliminated any PTT-values below 150ms or above 400ms before further analysis [13]. Although this filter may eliminate PWs that are so heavily distorted that the calculated PTT becomes unrealistically low or high, it does not remove any nonactual values that are within normal ranges and it may eliminate valid values that simply are unusually low or high.

2.2.2 PW elimination algorithm

In 1937 Hertzman and Spealman [56] were the first to describe the shape of a PW, dividing PWs in two phases: The anacrotic phase consisting of the rising slope of the PW, and the catacrotic phase consisting of the falling slope of the PW. In the catacrotic phase a dicrotic notch is usually seen in subjects with healthy compliant arteries [1]. Common physiological parameters, such as PW-amplitude, PTT and PWV, are generally calculated based on the assumption that a PW has the described shape. Based on these principles, a PW elimination algorithm was formulated that checks whether a PW matches the characteristics of the described predefined shape. The algorithm exists of a list of seven criteria that a PW has to meet to be deemed a suitable PW (see also Figure 2.2):

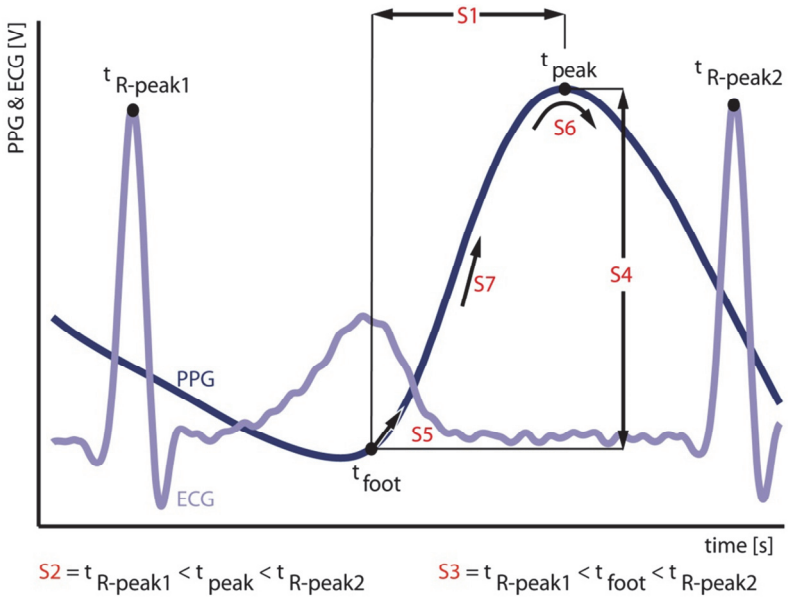

Figure 2.2: Graphical representation of the seven PW elimination criteria of the '7Step PW-Filter'. ECG = Electrocardiogram; PPG = Photoplethysmography. S1: The detected PPG foot should precede the detected PPG peak in time; S2: The detected PPG peak should be in the same heartbeat as the ECG R-peak; S3: The detected PPG foot should be in the same heartbeat as the ECG R-peak; S4:The detected PPG foot should have a lower magnitude than the detected PPG peak; S5: The detected PPG foot must be in an upward slope of the valley of the PW; S6: The PW should be complete; The detected PPG peak should be at a convex maximum of the PW; S7: The steepest rising part of the PW (maximum of its 1st derivative) must be situated between the detected PPG foot and the detected PPG peak

- S1: The detected PPG_{foot} should precede the detected PPG_{peak} in time.
  - $t_{foot} < t_{peak}$
- S2: The detected PPG_{peak} should be in the same heartbeat as the ECG R-peak
  - $t_{R\text{-}peak1} < t_{peak} < t_{R\text{-}peak2}$
- S3: The detected PPG_{foot} should be in the same heartbeat as the ECG R-peak
  - $t_{R\text{-}peak1} < t_{foot} < t_{R\text{-}peak2}$
- S4:The detected PPG_{foot} should have a lower magnitude than the detected PPG_{peak}
  - $PPG_{peak} - PPG_{foot} > 0$
- S5: The detected PPG_{foot} must be in an upward slope of the valley of the PW
  - 1^{st} derivative at $PPG_{foot} > 0$

- S6: The PW should be complete; The detected PPG $_{peak}$ should be at a convex maximum of the PW
  - 2nd derivative at PPG $_{peak}$ < 0
- S7: The steepest rising part of the PW (maximum of its 1st derivative) must be situated between the detected PPG $_{foot}$ and the detected PPG $_{peak}$
  - t $_{foot}$ < t maximum of the 1st derivative < t $_{peak}$

If one or more of the criteria are not met by the PW, that PW is deemed unsuitable and will be eliminated. This PW elimination algorithm will further be referred to as the '7Step PW-Filter'.

2.2.3 PW-analysis

The '7Step PW-Filter' was validated using a dataset consisting of PWs that were collected from the first ten healthy volunteers (7 male, 3 female, ages between 23 and 25 years) from a previous study conducted by the authors (medical ethics committee approval report MEC-2012-489, Erasmus MC, Rotterdam, the Netherlands) [57]. In this study, the PTT was measured using two PPG-sensors, one on each index finger, (TSD200 with the PPG100C amplifier, Biopac Systems, Inc, USA) and three external ECG-leads (ECG100C amplifier, Biopac Systems, Inc, USA).

The three ECG-leads were placed on the subject's right ankle and both wrists. The subject sat in a comfortable position under tranquil conditions and was instructed

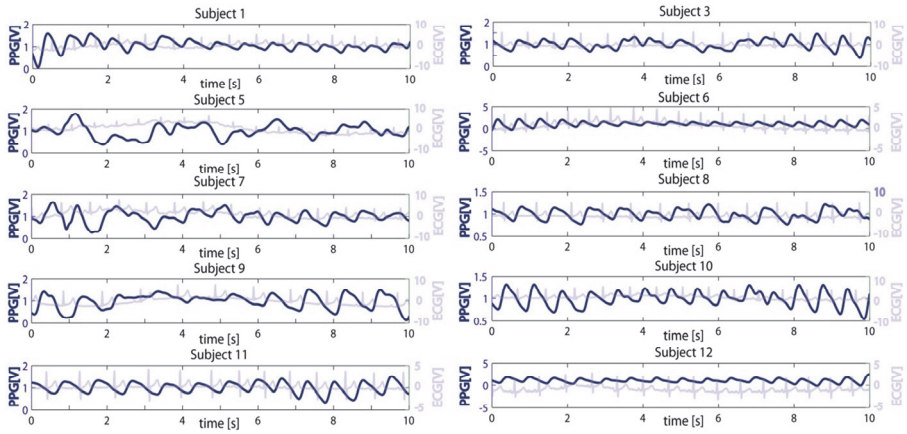

Figure 2.3: Examples of PPG-signals and their corresponding ECG-signal for all ten subjects. Each example shows the first 10 seconds of the baseline measurements on volunteers under tranquil conditions. Subjects 6 and 12 have a PPG-signal without any noticeable artefacts. Subjects 5 and 9 haves many artefacts, rendering it difficult to identify the suitable PWs.

not to talk or move during the measurement. The PWs were measured for 180 or 300 seconds in each subject. The subjects received 3 painful, heat-induced stimuli during the measurements. To give a general impression of the data, Figure 3 shows 10 seconds of the datasets of all subjects. The figures clearly illustrate that it is not always easy to recognise the PWs and their ends or beginnings.

The system used for measuring PTT registered the subject's ECG and PPG signals which were simultaneously converted to digital signals using AcqKnowledge v3.7.3 software (Biopac Systems, Inc, USA) at a sampling frequency of 2 kHz. Matlab R2010a (The MathWorks, Inc) was used for the data analysis. The PPG-signals were filtered with a fourth-order low-pass Butterworth filter with a cut-off frequency of 9 Hz. The PTT was determined by calculating the time between the R-peak of the ECG ($t_{ECG\ R\text{-}peak}(n)$) and the foot of the PW ($t_{PPG\ foot}(n)$):

$$PTT(n) = t_{PPG_{foot}}(n) - t_{ECG_{R-peak}}(n) \tag{2.1}$$

where n is the sequence number of the heartbeats. The R-peaks in the ECG were found using an off-the-shelf Matlab function called 'R-peakdetect' [58]. In order to

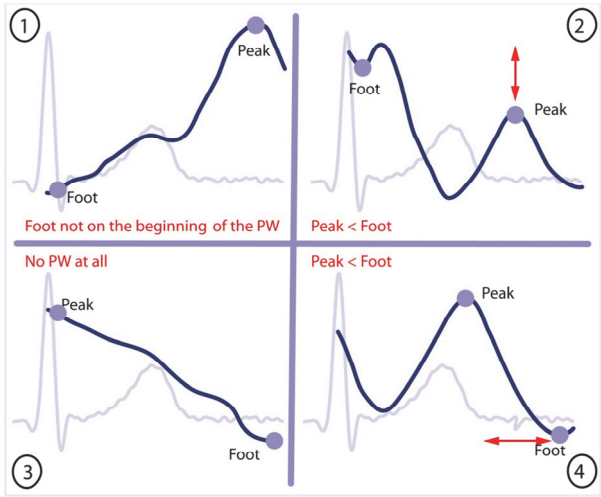

Figure 2.4: Examples of unsuitable PWs. Section 1 shows a detected PW foot that is not on the beginning of the PW but at the beginning of the clipped dataset. This is not correct because the foot has to be at the start of the PW itself and not at the start of the clipped dataset. Section 2 shows a detected PW peak being lower than the detected foot of the same PW. This is not correct because the peak should always be higher than the foot. Section 3 shows a PW that is non-recognisable at all, causing the foot and peak to be incorrectly placed at the extreme values the of the clipped dataset. Section 4 shows a detected PW foot occurring later than the detected peak of the same PW. This is not correct, because the foot of the PW has to precede the peak of the PW.

always use an R-peak and PW that belonged to the same heartbeat, the PWs were digitally clipped from 50ms after the occurrence of the R-peak to 80% of the average interval between two R-peaks (see Figure 2.1). The peak of a PW was determined as the maximum of the PW and was found using an off-the-shelf Matlab function called 'Peakdet' [59]. The foot of a PW was located at the maximum of the second derivative of that PW.

Figure 2.4 shows four examples of unsuitable PWs in which the Matlab detection software placed the foot and/or peak on a wrong location. Figure 2.4A shows a detected PW foot that is not on the beginning of the PW but at the beginning of the clipped dataset. This is not correct because the foot has to be at the start of the PW itself and not at the start of the clipped dataset. Figure 2.4B shows a detected PW peak being lower than the detected foot of the same PW. This is not correct because the peak should always be higher than the foot. Figure 2.4C shows a PW that is not recognisable at all, causing the foot and peak to be incorrectly placed at the extreme values the of the clipped dataset. Figure 2.4D shows a detected PW foot occurring later than the detected peak of the same PW. This is not correct, because the foot of the PW has to precede the peak of the PW.

2.2.4 Validation

To verify whether the '7Step PW-Filter' eliminates only and all of the unsuitable PWs, all PWs of the obtained dataset were put through the '7Step PW-Filter' as well as visually checked by the First Author (M.H.N.V.) and manually marked for elimination if deemed unsuitable (referred to as 'manual elimination' from now on). The literature review (Table 2.1) showed that manual/visual filtering was the most common way of filtering. During manual selection of unsuitable PWs in the current study, it was visually judged whether the detection software in Matlab placed the points of interest on the correct locations on the PWs. If any of those points was judged to be placed wrongly, the PW was marked for elimination.

To analyse the performance of the '7Step PW-Filter' compared to the manual elimination, the outcome of the two methods were considered as a binary classification test. Their sensitivity and specificity were used as statistical measures of performance. For each PW eliminated by the '7Step PW-Filter' the reason for elimination was recorded by registering which of the seven criteria were not met.

To explore the effect of eliminating unsuitable PWs before averaging a calculated outcome variable over a certain period, the mean PTT was calculated after using several distinct averaging periods for subject number five and compared for three

filtering situations: no filtering, filtered by the '7Step PW-Filter' and filtered by manual elimination. This comparison was done for means of the entire dataset in which the individual PTT values were calculated as averages per 60, 30 and 5 heartbeats or taken for each individual heartbeat.

To gain insight into the effect of applying a filter on the PTT-values instead of applying the elimination algorithm on the actual PWs, the filter of Gil et al. (eliminating any PTT-values below 150ms or above 400ms) was applied to the dataset of subject number five. Consecutively, it was checked to what extent the Gil method and the 7Step PW-Filter included and excluded the same data points.

All PTT analyses were done using an Intel Core i7-2640M CPU 2,80GHz, 64-bit operating system with Windows 7 professional Service Pack 1, Microsoft Corporation, Redmond WA.

2.2.5 Statistical Analysis

Three performance measures of the '7Step PW-Filter' were calculated using the manual elimination results as a reference: the sensitivity, the specificity and the overall accuracy. In the context of the current work, the sensitivity is a measure of the '7Step PW-Filter' ability to eliminate unsuitable PWs in accordance with the manual elimination. The specificity is a measure of the '7Step PW-Filter' ability to keep-in suitable PWs in accordance with the manual elimination. The overall accuracy was calculated as the total of the number of true positive PWs plus the number of true negative PWs, divided by the total number of PWs. These three performance measures should ideally be close to 100% under the assumption that the manual elimination results are valid and reliable. The analysis was performed using SPSS version 20.0 (SPSS, Inc., Chicago, IL, USA) and Matlab R2010a (The MathWorks, Inc). The limit for statistical significance was chosen as $p<0.01$.

2.3 Results

The complete dataset consisted of a total of 7746 PWs, obtained from 10 subjects. Manual elimination eliminated 164 PWs (2.1%), based on visual inspection of the PWs. The '7Step PW-Filter' eliminated 209 PWs (2.7%), based on the list of seven criteria. Full processing of the 7746 PWs took about 5 hours for manual elimination and under 5 minutes for the '7Step PW-Filter'. The manual elimination and '7Step PW-Filter' agreed on the elimination of 158 out of all eliminated PWs (which is 2.0% of the total number of PWs, 96% of the manually eliminated PWs and 76% of the PWs eliminated by the '7Step PW-Filter').

Additionally, 6 PWs were manually eliminated while not having been eliminated by the '7Step PW-Filter'. These 6 PWs were manually eliminated because there was no visually recognizable beginning of the PW.

Furthermore, 51 PWs were eliminated by the '7Step PW-Filter' while not having been eliminated manually. Mostly (in 39 instances), these PWs did not meet Criterion S5, (the detected PPG_{foot} must be in an upward slope of the valley of the PW). In eight instances the PW did not meet Criterion S2 (the detected PPG_{peak} should be in the same heartbeat as the ECG R-peak). In one instance the '7Step PW-Filter' eliminated a PW on Criterion S7 (the steepest rising part of the PW should be between the detected PPG $_{foot}$ and the detected PPG_{peak}). One PW was eliminated on Criteria S3 and S5 and two PWs were eliminated on Criteria S5 and S7.

The '7Step PW-Filter' had a sensitivity of 96.3% and a specificity of 99.3%. The overall accuracy of the '7Step PW-Filter' was 99.3% (Table 2.2).

In the dataset of subject number five the '7Step PW-Filter' eliminated 125 PWs,

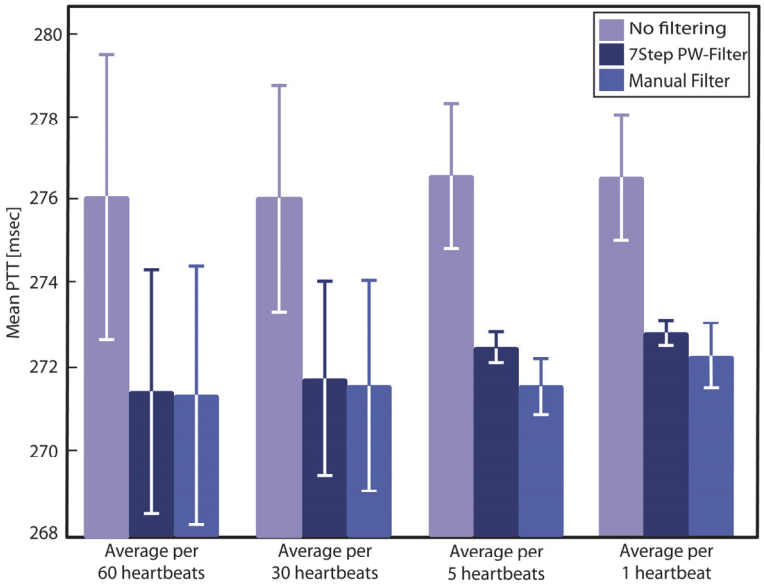

Figure 2.5: Mean PTT values of the dataset of subject number five; no filtering ('No filtering'), after manual elimination of unsuitable PWs by the first author ('Manual Filter') and after applying the'7Step PW-Filter' ('7Step PW-Filter'). The given PTT values are means over the entire dataset in which the individual PTT values were taken as averages per 60, 30 and 5 heartbeats or taken for each individual heartbeat. The whiskers indicate the standard errors of the means.

Table 2.2: Sensitivity and specificity of the manual elimination and the 7Step PW-filter elimination. 'Positive' indicates that a PW was marked as unsuitable and eliminated. 'Negative' indicates that a PW was marked as suitable and kept in the dataset.

	'7Step PW-Filter' outcome positive	**'7Step PW-Filter' outcome negative**
Manual elimination outcome positive	2.0% - 158 PWs	0.1% - 6 PWs
Manual elimination outcome negative	0.7% - 51 PWs	97.2% - 7531 PWs
	Sensitivity	**Specificity**
	96.3%	99.3%

which was 16.4% of the total dataset. Manual elimination resulted in 101 eliminated PWs, which was 13.3% of the total dataset.

Figure 2.5 shows the effect of eliminating unsuitable PWs before averaging a calculated outcome variable over a certain period. The difference between using filtered and unfiltered PPG data can lead to a difference in the calculated average PTT of up to 5ms, which is 1.8% of the original outcome value. The difference between the two filtering methods was less than 0.9 ms. Eliminating unsuitable PWs was over 60 times faster when using the '7Step PW-Filter' (under 5 minutes) than when doing manual elimination (about 5 hours).

Figure 2.6 shows the difference between using unfiltered data, using the Gil method and using the '7Step PW-Filter'. The mean PTT over the entire dataset was comparable for all three methods (no filter: 282 ms, Gil method: 281 ms, 7Step filter: 279 ms). However, the results clearly show that although few suitable PWs fell outside the Gil range, a very large number (91) of unsuitable PWs were included in the analysis when using the Gil method.

2.4 Discussion

The literature study revealed that filtering techniques that are used to eliminate unsuitable PWs are often not described and differ between studies. In fact, most studies do not report whether any or what kind of filtering algorithm was used to eliminate unsuitable PWs. Some studies report using manual techniques to select unsuitable PWs but these techniques are labour intensive, subjective and often not fully described either.

By using seven morphologic criteria to determine the suitability of PWs for PTT analyses, the '7Step PW-Filter' eliminated 158 out of the 164 PWs that were also

eliminated by the manual method. The 6 PWs not eliminated by the '7Step PW-Filter' were eliminated manually because a clear onset of the uprising slope could not be found visually in these 6 PWs. The advantage of the '7Step PW-Filter' is that it objectively determines this onset and determines whether its location fits the characteristics of a suitable PW. Of the 51 PWs that were eliminated by '7Step PW-Filter' while not being eliminated by the manual method 39 PWs were eliminated because the maximum of the second derivative of the PW was not situated on an upward slope. This suggests that visual inspection of the PWs is less reliable because the location of a maximum of a second derivative is very hard to pinpoint by eyeballing.

In order to show the relevance of eliminating unsuitable PWs, a case study on PTT data from a volunteers study was conducted. In that study the mean PTT-values were to be calculated based on finding specific landmarks on PWs and ECG-data. The case study showed that when reporting a mean PTT of a dataset the effect of using or not using elimination of unsuitable PWs can be considerable. PTT-values dropped by 1.5-1.8% when applying either manual elimination or the '7Step PW-Filter' as compared to using unfiltered data. Whether the mean PTT was determined for a range of PTT-values derived from short (5 heartbeats) or long (60 heartbeats) averaging intervals had little effect on the mean PTT.

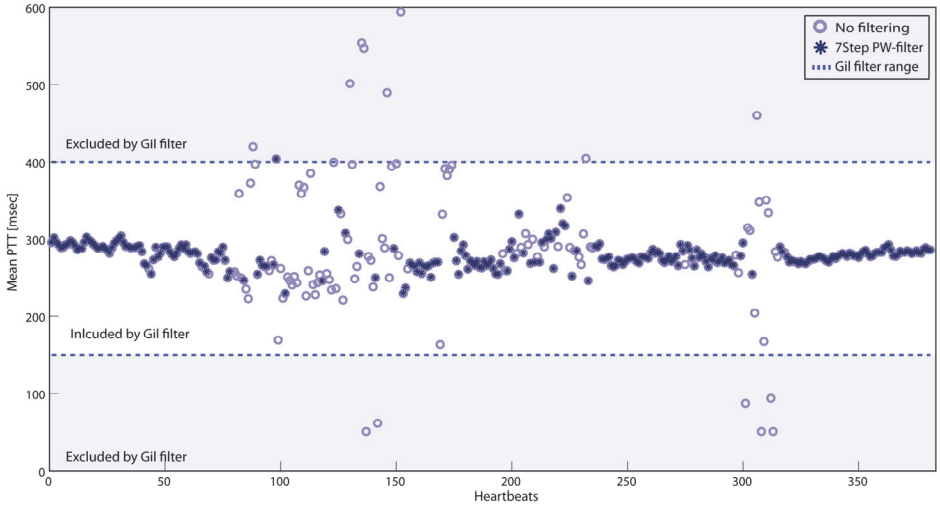

Figure 2.6: Comparison of the '7Step PW-Filter' with the Gil method. The figure shows PTT-values for the dataset without no filtering ('no filtering'), the boundaries set by the Gil method ('Gil filter range') and the PTT-values remaining in the dataset after eliminating unsuitable PWs with the '7Step PW-Filter' ('7Step PW-Filter).

However, the smaller the number of PWs over which the PTT-values were averaged, the more sensitive the calculated mean PTT was to unsuitable PWs. As fast physiological responses or fluctuations can only be measured or monitored properly without averaging over too many PWs, effective and reliable PW elimination algorithms are quintessential for obtaining reliable measurement of fast physiological responses. When measuring changes in PTT, significant results reported in the literature that are deemed clinically relevant amount about 10-20ms [51], which is a change of 3-7% with respect to a common baseline PTT of 300ms, implying that unremoved unsuitable PWs could potentially account for 50% of such results. This clearly indicates that it is essential to dispose of unsuitable PWs, as these can have a considerable effect on clinically relevant outcome values.

As PTT is defined as the time difference between the ECG R-peak heartbeat and a reference point on the PPG signal of the corresponding PW, having proper ECG waves is just as relevant as having suitable PWs. However, several studies have already shown the robustness of various methods for detecting ECG R-peaks [60]. Therefore, this study focused solely on the PPG signal.

Visually selecting unsuitable PWs and removing these manually is highly time consuming. It took about five hours to process the data of only ten subjects. Additionally, the manual elimination may be quite subjective. Although the manual elimination was taken as gold standard, it should be noted that the manual filtering may give varying results, depending on who conducts the filtering. However, in the current study the manual filtering was done by an expert researcher to as much as possible avoid bias in favour of the algorithm, Consequently, for less experienced researchers, large datasets and PWs hard to judge visually, the algorithm potentially offers even larger benefits. The '7Step PW-Filter' offers great time savings compared to manual elimination and can be implemented in many coding languages due to its simple and straight-forward concept.

Gil et al. [13] used a filter that eliminated any PTT-values that were below 150ms or above 400ms before further analysis of the PTT data. However, if the shape of a PW does not show the characteristics that allow calculating a PTT but the PTT value is calculated anyway, this may result in PTT-values that fall within the Gil criteria but are still nonactual data. The comparison between the '7Step PW-Filter' and the Gil method confirmed that although the calculated outcome value (mean PTT in this case) may be only slightly affected by the filtering method used, the Gil method kept a very large number of nonactual PTT-values in the dataset. The '7Step PW-Filter' did remove all unsuitable PWs, thereby preventing nonactual PTT-

values from polluting the filtered dataset. Therefore, the '7Step PW-Filter' should be preferred.

'The '7Step PW-Filter' was validated on healthy volunteers only and with potential sources of motion artefacts in the PWs being avoided. This clearly is quite an ideal situation. In clinical practice, patients may have cardiovascular disease, which affects arterial stiffness and could affect the shape of the PWs. Furthermore, patients may be anxious, in pain, coughing or moving for other reasons, which may also affect and most likely deteriorate the shapes of the PWs. In such situations, experience has shown that the number of unsuitable PWs increases, which makes proper filtering even more important. An extensive quantification of the performance of the '7Step PW-Filter' in such situations has yet to be conducted.

Apart from the artefacts caused by talking and moving, the shapes of the PWs can also be affected by too high contact forces between the subject and the sensor, as was reported by Teng et al. [48, 55] when using reflective PPG-sensors. This effect was also noticed during the current study: when the PPG-sensors were strapped too tightly to the fingers, the blood flow stagnated, causing the PWs to deteriorate both in amplitude and in shape. Therefore, care should be taken to limit or avoid any contact forces when using PPG-sensors. Although this study focused on applying PW elimination for PTT calculations, the advantages of automated elimination of unsuitable PWs will also apply when aiming at other outcome parameters, such as PW-amplitude, heart rate, SpO_2, blood pressure, cardiac output and PWV. For such cases the list of criteria in the '7Step PW-Filter' may have to be adapted.

In order to obtain valid PTT data from PPG measurements, it is quintessential to only use PWs that contain the morphological landmarks on which the definition of PTT is based. The comparison of data-analysis and filtering methods in this study showed that without filtering, the period over which PTT-values are averaged can strongly affect the calculated outcome values. Using unfiltered data may result in deviations in the calculated PTT-values that are close to the orders of magnitude of commonly measured effect sizes in patient and healthy volunteer studies. Compared to manual elimination, using the '7Step PW-Filter' reduces PW elimination times from hours to minutes and helps to increase the validity, reliability and reproducibility of PTT data.

2.5 Reference

1. Allen, J., Photoplethysmography and its application in clinical physiological measurement. Physiol Meas, 2007. 28(3): p. R1-39.
2. Nitzan, M., B. Khanokh, and Y. Slovik, The difference in pulse transit time to the toe and finger measured by photoplethysmography. Physiological Measurement, 2002. 23(1): p. 85-93.
3. Weinman, J. and D. Sapoznikov, Equipment for continuous measurements of pulse wave velocities. Med Biol Eng Comput, 1971. 9(2): p. 125-138.
4. Pitson, D.J., et al., Use of pulse transit time as a measure of inspiratory effort in patients with obstructive sleep apnoea. European Respiratory Journal, 1995. 8(10): p. 1669-1674.
5. Maltz, J.S. and T.F. Budinger, Evaluation of arterial endothelial function using transit times of artificially induced pulses. Physiological Measurement, 2005. 26(3): p. 293-307.
6. Geddes, L.A., et al., Pulse transit time as an indicator of arterial blood pressure. Psychophysiology, 1981. 18(1): p. 71-74.
7. Gizdulich, P., On a non-invasive evaluation of pulse wave velocity in human peripheral arteries. Clinical Physics and Physiological Measurement, 1984. 5(1): p. 33-36.
8. Laurent, S., et al., Expert consensus document on arterial stiffness: methodological issues and clinical applications. Eur Heart J, 2006. 27(21): p. 2588-605.
9. Boutouyrie, P. and S.J. Vermeersch, Determinants of pulse wave velocity in healthy people and in the presence of cardiovascular risk factors: Establishing normal and reference values. European Heart Journal, 2010. 31(19): p. 2338-2350.
10. Blacher, J., et al., Impact of aortic stiffness on survival in end-stage renal disease. Circulation, 1999. 99(18): p. 2434-2439.
11. Laurent, S., et al., Aortic stiffness is an independent predictor of all-cause and cardiovascular mortality in hypertensive patients. Hypertension, 2001. 37(5): p. 1236-1241.
12. Cruickshank, K., et al., Aortic pulse-wave velocity and its relationship to mortality in diabetes and glucose intolerance: An integrated index of vascular function? Circulation, 2002. 106(16): p. 2085-2090.
13. Gil, E., et al., PTT variability for discrimination of sleep apnea related decreases in the amplitude fluctuations of PPG signal in children. IEEE Transactions on Biomedical Engineering, 2010. 57(5): p. 1079-1088.
14. Kortekaas, M.C., et al., Pulse transit time as a quick predictor of a successful axillary brachial plexus block. Acta Anaesthesiol Scand, 2012. 56(10): p. 1228-1233.
15. Foo, J.Y.A., et al., Effects of poorly perfused peripheries on derived transit time parameters of the lower and upper limbs. Biomedizinische Technik, 2008. 53(3): p. 156-159.

16. Foo, J.Y.A. and C.S. Lim, Difference in pulse transit time between populations: A comparison between Caucasian and Chinese children in Australia. Journal of Medical Engineering and Technology, 2008. 32(2): p. 162-166.
17. Foo, J.Y.A. and C.S. Lim, Changes induced in the lower- and upper-limb pulse transit-time ratio during inspiratory resistive breathing. Biomedizinische Technik, 2007. 52(3): p. 248-254.
18. Foo, J.Y.A., Normality of upper and lower peripheral pulse transit time of normotensive and hypertensive children. Journal of Clinical Monitoring and Computing, 2007. 21(4): p. 243-248.
19. Foo, J.Y.A. and C.S. Lim, Dual-channel photoplethysmography to monitor local changes in vascular stiffness. Journal of Clinical Monitoring and Computing, 2006. 20(3): p. 221-227.
20. Foo, J.Y.A., et al., Variability in time delay between two models of pulse oximeters for deriving the photoplethysmographic signals. Physiological Measurement, 2005. 26(4): p. 531-544.
21. Foo, J.Y.A., et al., Motion artefact reduction of the photoplethysmographic signal in pulse transit time measurement. Australasian Physical and Engineering Sciences in Medicine, 2004. 27(4): p. 165-173.
22. Wagner, D.R., et al., Relationship between pulse transit time and blood pressure is impaired in patients with chronic heart failure. Clinical Research in Cardiology, 2010. 99(10): p. 657-664.
23. Middleton, P.M., et al., Changes in left ventricular ejection time and pulse transit time derived from finger photoplethysmogram and electrocardiogram during moderate haemorrhage. Clinical Physiology and Functional Imaging, 2009. 29(3): p. 163-169.
24. Zheng, Y., et al., A clip-free eyeglasses-based wearable monitoring device for measuring photoplethysmograhic signals. Conference proceedings : Annual International Conference of the IEEE Engineering in Medicine and Biology Society IEEE Engineering in Medicine and Biology Society Conference, 2012. 2012: p. 5022-5025.
25. Orini, M., L. Citi, and R. Barbieri, Bivariate point process modeling and joint non-stationary analysis of pulse transit time and heart period. Conference proceedings : Annual International Conference of the IEEE Engineering in Medicine and Biology Society IEEE Engineering in Medicine and Biology Society Conference, 2012. 2012: p. 2831-2834.
26. Allen, J., et al., A prospective comparison of bilateral photoplethysmography versus the ankle-brachial pressure index for detecting and quantifying lower limb peripheral arterial disease. J Vasc Surg, 2008. 47(4): p. 794-802.
27. Allen, J., et al., Chronic fatigue syndrome and impaired peripheral pulse characteristics on orthostasisa new potential diagnostic biomarker. Physiological Measurement, 2012. 33(2): p. 231-241.

28. Li, Y., et al., Characters available in photoplethysmogram for blood pressure estimation: Beyond the pulse transit time. Australasian Physical and Engineering Sciences in Medicine, 2014. 37(2): p. 367-376.
29. Vlahandonis, A., et al., Pulse transit time as a surrogate measure of changes in systolic arterial pressure in children during sleep. Journal of Sleep Research, 2014. 23(4): p. 406-413.
30. Gil, E., et al., Heart rate turbulence analysis based on photoplethysmography. IEEE Transactions on Biomedical Engineering, 2013. 60(11): p. 3149-3155.
31. Winokur, E.S., D.D. He, and C.G. Sodini. A wearable vital signs monitor at the ear for continuous heart rate and Pulse Transit Time measurements. 2012. San Diego, CA.
32. Kim, S.H., et al., Beat-to-beat tracking of systolic blood pressure using noninvasive pulse transit time during anesthesia induction in hypertensive patients. Anesthesia and Analgesia, 2013. 116(1): p. 94-100.
33. Chandran, D.S., et al., Impaired endothelium mediated vascular reactivity in endogenous Cushing's syndrome. Endocrine Journal, 2011. 58(9): p. 789-799.
34. Masè, M., et al., Feasibility of cuff-free measurement of systolic and diastolic arterial blood pressure. J Electrocardiol, 2011. 44(2): p. 201-207.
35. Proença, J., et al. Is Pulse Transit Time a good indicator of blood pressure changes during short physical exercise in a young population? 2010. Buenos Aires.
36. Goswami, D., K. Chaudhuri, and J. Mukherjee, A new two-pulse synthesis model for digital volume pulse signal analysis. Cardiovascular Engineering, 2010. 10(3): p. 109-117.
37. Wong, M.M., et al., Contactless recording of photoplethysmogram on a sleeping bed. Conference proceedings : Annual International Conference of the IEEE Engineering in Medicine and Biology Society IEEE Engineering in Medicine and Biology Society Conference, 2009. 2009: p. 907-910.
38. Yoon, Y., J.H. Cho, and G. Yoon, Non-constrained blood pressure monitoring using ECG and PPG for personal healthcare. Journal of Medical Systems, 2009. 33(4): p. 261-266.
39. Selvaraj, N., et al., Influence of respiratory rate on the variability of blood volume pulse characteristics. Journal of Medical Engineering and Technology, 2009. 33(5): p. 370-375.
40. Zheng, D. and A. Murray, Non-invasive quantification of peripheral arterial volume distensibility and its non-linear relationship with arterial pressure. Journal of Biomechanics, 2009. 42(8): p. 1032-1037.
41. Cox, P., et al. Investigation of photoplethysmogram morphology for the detection of hypovolemic states. 2008.
42. Foo, J.Y.A., S.J. Wilson, and C.S. Lim, Use of the pulse transit time trend to relate tidal breathing and central respiratory events. Proceedings of the Institution of Mechanical Engineers, Part H: Journal of Engineering in Medicine, 2008. 222(6): p. 1005-1011.

43. Foo, J.Y.A., et al., Effect of ethnicity and growth on ratio-based transit time surrogate ankle-brachial index marker from a Chinese children's perception. Acta Cardiologica, 2008. 63(3): p. 369-375.
44. Foo, J.Y.A., Bilateral transit time assessment of upper and lower limbs as a surrogate ankle brachial index marker. Angiology, 2008. 59(3): p. 283-289.
45. McCombie, D.B., et al., Adaptive hydrostatic blood pressure calibration: development of a wearable, autonomous pulse wave velocity blood pressure monitor. Conference proceedings : Annual International Conference of the IEEE Engineering in Medicine and Biology Society IEEE Engineering in Medicine and Biology Society Conference, 2007. 2007: p. 370-373.
46. Teng, X.F. and Y.T. Zhang, An evaluation of a PTT-based method for noninvasive and cuffless estimation of arterial blood pressure. Conference proceedings : Annual International Conference of the IEEE Engineering in Medicine and Biology Society IEEE Engineering in Medicine and Biology Society Conference, 2006. 1: p. 6049-6052.
47. Foo, J.Y.A., et al., Pulse transit time ratio as a potential marker for paediatric crural and brachial blood pressure index. Journal of Human ypertension, 2007. 21(5): p. 415-417.
48. Teng, X.F. and Y.T. Zhang, The effect of applied sensor contact force on pulse transit time. Physiological Measurement, 2006. 27(8): p. 675-684.
49. Zhang, X.Y. and Y.T. Zhang, The effect of local mild cold exposure on pulse transit time. Physiological Measurement, 2006. 27(7): p. 649-660.
50. Payne, R.A., et al., Pulse transit time measured from the ECG: An unreliable marker of beat-to-beat blood pressure. Journal of Applied Physiology, 2006. 100(1): p. 136-141.
51. Babchenko, A., et al., Increase in pulse transit time to the foot after epidural anaesthesia treatment. Medical and Biological Engineering and Computing, 2000. 38(6): p. 674-679.
52. Selvaraj, N., et al., Monitoring of reactive hyperemia using photoplethysmographic pulse amplitude and transit time. Journal of Clinical Monitoring and Computing, 2009. 23(5): p. 315-322.
53. Jago, J.R. and A. Murray, Repeatability of peripheral pulse measurements on ears, fingers and toes using photoelectric plethysmography. Clinical Physics and Physiological Measurement, 1988. 9(4): p. 319-329.
54. Foo, J.Y.A., S.J. Wilson, and P. Wang, Factors that affect pulse wave time transmission in the monitoring of cardiovascular system. Journal of Clinical Monitoring and Computing, 2008. 22(2): p. 141-147.
55. Teng, X.F. and Y.T. Zhang, Theoretical study on the effect of sensor contact force on pulse transit time. IEEE Transactions on Biomedical Engineering, 2007. 54(8): p. 1490-1498.
56. Hertzman, A.B. and C.R. Spealman, Observations on the finger volume pulse recorded photoelectrically Am. J. Physiol. , 1937. 119(119): p. 334–335.

57. van Velzen, M.H.N., et al., Effect of heat-induced pain stimuli on pulse transit time and pulse wave amplitude in healthy volunteers Physiological Measurement, 2015.
58. Clifford, G.D., Rpeakdetect function (ECG toolbox). 2008.
59. Billauer, E., Peakdet. 2012: http://billauer.co.il/peakdet.html. p. Detect peaks in a vector.
60. Rabbani, H., et al., R peak detection in electrocardiogram signal based on an optimal combination of wavelet transform, hilbert transform, and adaptive thresholding. J Med Signals Sens, 2011. 1(2): p. 91-8.

Chapter 3

Small intra-individual variability of the pre-ejection period justifies the use of pulse transit time as approximation of the vascular transit time

Minke C. Kortekaas , Marit H.N. van Velzen, Frank Grüne, Sjoerd P. Niehof, Robert J. Stolker, Frank J.P.M. Huygen

PLOS ONE, September 2018

Vascular transit time (VTT) is the propagation time of a pulse wave through an artery; it is a measure for arterial stiffness. Because reliable non-invasive VTT measurements are difficult, as an alternative we measure pulse transit time (PTT). PTT is defined as the time between the R-wave on electrocardiogram and arrival of the resulting pulse wave in a distal location measured with photoplethysmography (PPG). The time between electrical activation of the ventricles and the resulting pulse wave after opening of the aortic valve is called the pre-ejection period (PEP), a component of PTT. The aim of this study was to estimate the variability of PEP at rest, to establish how accurate PTT is as approximation of VTT. PTT was measured and PEP was assessed with echocardiography (gold standard) in three groups of 20 volunteers: 1) a control group without cardiovascular disease aged <50 years and 2) aged >50 years, and 3) a group with cardiovascular risk factors, defined as arterial hypertension, dyslipidemia, kidney failure and diabetes mellitus. Per group, the mean PEP was: 1) 58.5 ± 13.0 ms, 2) 52.4 ± 11.9 ms, and 3) 57.6 ± 11.6 ms. However, per individual the standard deviation was much smaller, i.e. 1) 2.0-5.9 ms, 2) 2.8-5.1 ms, and 3) 1.6-12.0 ms, respectively. There was no significant difference in the mean PEP of the 3 groups (p=0.236). In conclusion, the intra-individual variability of PEP is small. A change in PTT in a person at rest is most probably the result of a change in VTT rather than of PEP. Thus, PTT at rest is an easy, non-invasive and accurate approximation of VTT for monitoring arterial stiffness.

3.1 Introduction

Pulse transit time (PTT) is the sum of the pre-ejection period (PEP) and the vascular transit time (VTT). After opening of the aortic valve, a pulse pressure wave propagates with a certain speed through the blood vessels from the heart to a distal location; this is called the VTT. If an artery is stiff or has a small diameter (or both), the pulse wave will propagate faster and, subsequently, the VTT decreases. Vice versa, if the diameter of the artery increases, the pulse wave propagation is slower and the VTT increases. Therefore, the VTT is a measure for arterial stiffness. Increased stiffness can be either structural (age and atherosclerosis) or functional due to higher sympathetic activity or elevated blood pressure [1-3]. It is a promising application for e.g. non-invasive continuous and cuffless blood pressure monitoring, which can also be used in children or in ambulatory setting [4-8].

Because reliable non-invasive VTT measurements are difficult, as an alternative we measure the PTT. PTT can be used to assess a successful loco regional block of an extremity [9, 10], to monitor vasomotor tone, and for assessment of autonomic nervous system response [11]. Another non-invasive measurement to estimate the VTT is the pulse wave velocity (PWV). However, determination of the arterial path length is necessary to calculate the PWV and this may create errors in the measurement [12].

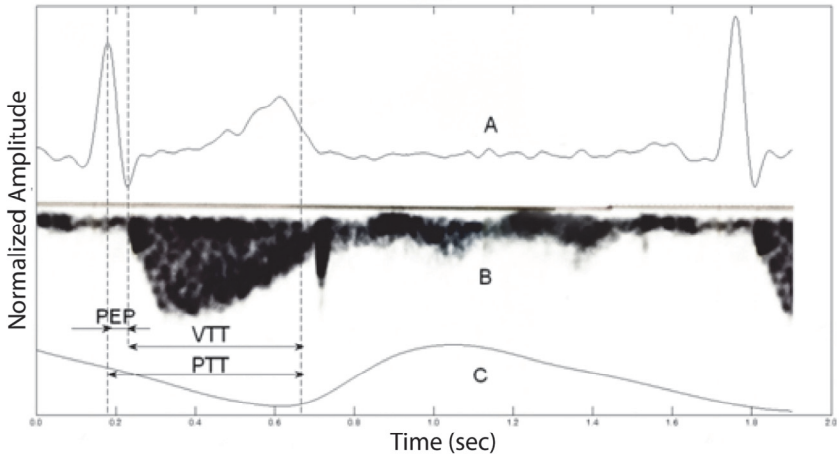

Figure 3.1: A = electrocardiogram (ECG), B = Doppler mode echocardiography signal over the aortic valve, C = photoplethysmographic (PPG) pulse wave; PEP = pre-ejection period, VTT = vascular transit time, PTT = Pulse transit time.

PTT is defined as the time between the R-wave on the electrocardiogram (ECG) and the arrival of the resulting pulse wave measured with photoplethysmography (PPG). The PEP is a component of the PTT measurement (Figure 3.1).

The PEP represents the isovolumetric contraction time of the ventricles of the heart. It is the time between electrical activation of the ventricles (Q-wave) and opening of the aortic valve [13]. The R-wave is commonly used instead of the Q-wave [14]. Identification of R-waves is easier and more reliable than Q-waves. Moreover, Seery et al. showed that PEP can be calculated using the R-wave instead of the Q-wave [15]. PEP can be considered as a measure of left ventricular function, as it reflects changes in the contractility of myocardium, left ventricular end-diastolic volume, and aortic diastolic pressure [13, 16-18]. In patients with diabetic chronic kidney disease, fluid overload is a marker for left ventricular systolic dysfunction and is associated with the ratio of brachial PEP and brachial ejection time [19]. Physical activity, as well as respiration or a stress response, can rapidly change the PEP [20, 21]. Therefore, a change in either PEP and/or VTT can result in a change in the PTT value [22].

Cardiothoracic impedance is a measurement that is often used to acquire data for calculation of the PEP and measured PEP values around 75-134 ms [14, 23, 24]. However, echocardiography is the gold standard for measuring the PEP [13]. Muehlsteff et al. investigated the role of the PEP on PTT [4]; they measured the PEP in a small group of young healthy volunteers with thorax impedance after exercise and found that PEP dominates the PTT variability after exercise. The use of different measuring tools introduces a discrepancy in literature about the magnitude of PEP and its contribution to the PTT.

The aim of this study was to estimate the variability of PEP at rest, to establish how accurate PTT is as an approximation of VTT. Age and cardiovascular risk factors (arterial hypertension, dyslipidemia, kidney failure, and diabetes mellitus) can increase arterial stiffness and, thereby, decrease VTT and possibly influence the PEP. Therefore, to take these factors into account, the PEP was measured in a control group with no medical history of cardiovascular disease aged ≤50 years and aged ≥50 years, and in a group of persons with at least one cardiovascular risk factor.

3.2 Methods

This single-center prospective observational study examined the variability of PEP at rest in 60 volunteers divided into 3 groups (20 per group):

- a control group (group 1) of individuals without a medical history of cardiovascular disease aged under 50 years
- a control group (group 2) aged over 50 years
- a group of individuals with at least one cardiovascular risk factor (group 3), which are defined in the exclusion criteria for the control groups

The study was approved by the Medical Ethical Committee of the Erasmus University Medical Centre in Rotterdam (MEC-2011-213), and was conducted in accordance with the Declaration of Helsinki. The primary endpoints of the study were PEP, VTT and PTT. Volunteers were eligible for inclusion when aged ≥18 years and ≤ 75 years. Exclusion criteria were arrhythmia, tremor, muscle or skeletal injuries in upper limb, hematopoietic disease, and incapacitated subjects. Further exclusion criteria for the control group (groups 1 and 2) were history of cardiovascular or peripheral vascular risk factors; these were defined as arterial hypertension, dyslipidemia, kidney failure, and diabetes mellitus. All participants were informed about the aim of the study and gave written informed consent before being enrolled. None of the eligible volunteers refused inclusion in the trial.

3.2.1 Measurement protocol

All measurements were performed under standardized stable conditions in a quiet temperature- controlled room with dimmed light. First, the participant had a short interview to acquire the data such as weight, height and medication and blood pressure was measured. After that the participant was asked to lie down in a left lateral decubitus position and was connected to the measurement equipment (MP100, Biopac® Systems, Inc. Goleta, USA). ECG electrodes were placed (ECG100C amplifier, Biopac®) to calculate the PTT and for ECG registration during echocardiography. Four PPG sensors (TSD200 and PPG100C amplifier, Biopac®) were placed on the index fingers and big toes for measuring respectively the PTT_{finger} and PTT_{toe}. Data were sampled with 2 kHz using the AcqKnowledge 3.7.3 version software (Biopac®). Per volunteer, the data acquisition took place in 5 to 10 minutes.

3.2.2 Echocardiography

ECG-gated echocardiography was performed at rest in the left lateral decubitus position by an experienced investigator, using a Vivid-i portable ultrasound system (GE, Solingen, Germany). Measurements were performed during 10 consecutive heartbeats, simultaneous with PTT measurements. A continuous wave Doppler registration through the aortic valve was obtained from a standard apical 5-chamber view. The horizontal sweep was set to 200 mm/s for maximum accuracy. PEP was defined as the time measured from the R-wave of the ECG to the start of the ejection phase. The data were synchronized using the matching R-waves of the simultaneously acquired second lead ECG signals from the echocardiography and PTT measurements.

3.2.3 PTT calculations

Data from the AcqKnowledge software were imported into Matlab R2010a® (The MathWorks, Inc., Natick, MA, USA) with the Loadacq syntax for Matlab [25]. In the ECG data, the R-waves were detected using the Rpeakdetect syntax available from the ECGtoolbox [26]. The PPG data were filtered using a fourth-order low-pass Butterworth filter with a cut-off frequency of 9 Hz. For filtering we used a zero-phase digital filtering by processing the input data, PPG, in both the forward and reverse directions. This gives a zero phase delay and is based on a method described by Oppenheim et al. [27]. The signals from the PPG were digitally cut between the R-wave and the next R-wave. Thereafter the pulse waves were selected by a '7Step PW-filter' to filter out the pulse waves that strongly deviated in shape for a suitable pulse wave analysis [28]. PTT was determined by calculating the time between the R-wave of the ECG and the foot of the PPG pulse wave. The foot was determined as the maximum value of the second derivative of the pulse wave [29].

3.2.4 Analyses

We calculated the mean PEP and PTT of the 10 consecutive but not necessary neighboring heartbeats for each participant and of the total group. All data are presented as mean ± standard deviation (SD). Furthermore, to show the magnitude of the contribution of PEP and its variation in the PTT measurements in an individual, the PTT_{Mean} PTT_{SD}, PEP_{Mean} and PEP_{SD} were normalized to a percentage of the PTT_{Mean} by the following formula (see Formula 3.1):

$$PTT_{SD_{\%}} = \frac{PTT_{SD}}{PTT_{Mean}} * 100\% \tag{3.1}$$

A similar calculation was used to determine the $PEP_{Mean\%}$ and $PEP_{SD\%}$. The values of the left and right sensors were compared with the Wilcoxon signed rank test. The difference in PEP and study population characteristics between the 3 groups was tested with ANOVA. To correct for the influence of systolic pressure on PTT the ANCOVE was used. A *p*-value <0.05 was considered statistically significant. Statistical analyses were performed using SPSS version 24 (SPSS Inc., Chicago, USA). Figures were made using GraphPad Prism version 5.00 for Windows (GraphPad Software, San Diego California USA) and Adobe Illustrator (Creative Suits 5 CS5, Adobe Systems Incorporated, San Jose, California, USA).

3.3 Results

The present study included 60 volunteers, divided into 3 groups of 20 participants each. As shown in Table 3.1, the mean age in group 1 is significantly lower than in the other groups. This is mainly caused by the age limit of 50 years in group 1. Also, the BMI was lower in the control group compared to group 2 and 3 and the mean heart rate was higher. The mean systolic blood pressure of group 3 was significantly higher than that of groups 1 and 2 (p=0.048). Of all the participants in group 3, 19 had risk factor arterial hypertension, 13 dyslipidemia, 2 diabetes and 1 kidney failure. The characteristics of the study population are presented in Table 3.1.

In the total group of 60 participants, the mean PEP was 56.2 ± 12.3 ms. In groups 1, 2 and 3 the mean PEP was 58.5 ± 13.0 ms, 52.4 ± 11.9 ms and 57.6 ± 11.6 ms, respectively. The intra-individual SD of the PEP was much smaller, i.e. 2.0-5.9 ms (group 1), 2.8-5.1 ms (group 2) and 1.6-12.0 ms (group 3) (Figure 3.2). There

*Table 3.1: Characteristics of the study population. n=20 per group. Group 1=control group <50 years, group 2=control group >50 years, group 3=participants with a cardiovascular risk factor. Data are presented as mean ± SD or number (%) of participants. MAP=mean arterial pressure. * p<0.05*

Variables	Group 1	Group 2	Group 3
Age, years	27 ± 4	55 ± 4	63 ± 10
Sex (male), no.(%)	9 (45)	10 (50)	10 (50)
Weight [kg]	69 ± 12	78 ± 12	74 ± 12
Height [m]	1.77 ±0 .11	1.75 ± 0.0.9	1.71 ± 0.09
Body Mass Index [kg m^2]	21.8 ± 2.5*	25.5 ± 3.6	25.3 ± 3.2
Blood pressure [mmHg]			
Systolic	131 ± 13	131 ± 17	141 ± 15*
Diastolic	81 ± 10	79 ± 9	81 ± 8
MAP [mmHg]	98 ± 10	97 ± 10	101 ± 9
Heart rate [beats min^{-1}]	79 ± 21*	67 ± 10	68 ± 14

were no missing data in the PEP measurements and no significant difference in the mean PEP of the 3 groups (p=0.235).

For all the PPG measurements of the 3 groups together, 18 sensors showed too many artifacts, modulated waves, for reliable PTT calculation; these measurements were excluded from the analysis, which represents 7.5% of the data (for

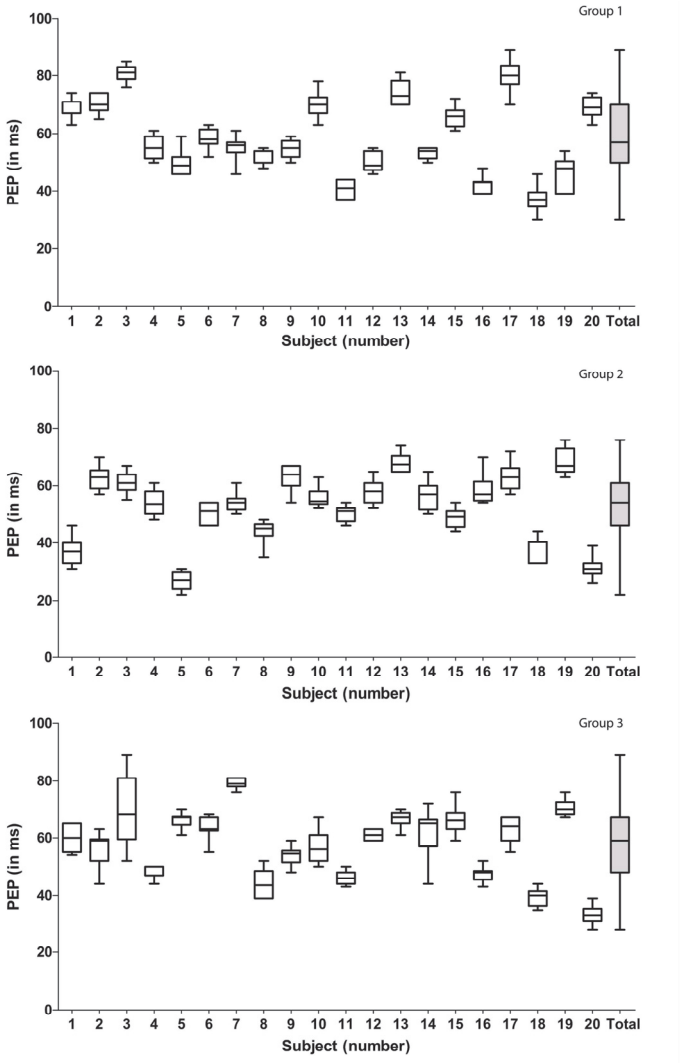

Figure 3.2: Box plots of the pre-ejection period (PEP) of 10 consecutive heartbeats of each group. The boxes represent the median with interquartile range. The whiskers represent the minimum and maximum value.

Table 3.2: Data on normalized PTT and PEP variability.

Subjects	**Normalized PTT [%] (PTT_{Mean} [ms])**	**PTT_{SD} [%] (PTT_{SD} [ms])**	**PEP_{Mean}**	**PEP_{SD}**
1	100 (305)	1.6 (5)	22.4	1.1
2	100 (272)	2.6 (7)	25.8	1.1
3	100 (285)	2.5 (7)	28.3	0.9
4	100 (299)	1.7 (5)	18.5	1.3
5	100 (309)	1.9 (6)	16.1	1.3
6	100 (268)	1.1 (3)	21.8	1.3
7	100 (266)	1.9 (5)	20.7	1.5
8	100 (286)	1.0 (3)	17.9	0.8
9	100 (230)	1.7 (4)	23.8	1.3
10	100 (270)	1.9 (5)	25.9	1.5
11	100 (272)	1.1 (3)	14.9	1.3
12	100 (274)	0.7 (2)	18.3	1.3
13	100 (247)	4.5 (11)	29.9	1.7
14	100 (271)	3.3 (9)	19.6	0.7
15	100 (292)	1.0 (3)	22.5	1.2
16	100 (240)	5.8 (14)	17.5	1.3
17	100 (330)	2.7 (9)	24.2	1.7
18	100 (294)	2.0 (6)	12.7	1.5
19	100 (276)	5.4 (15)	16.7	2.1
20	100 (315)	3.8 (23)	22	1.2
Mean Group	**100**	**2.4**	**21.0**	**1.3**

specification see Figure 3.3, 3.4 and 3.5). Pulse waves were only excluded from analyses when they did not pass the '7Step PW-filter'.

In the normalized data of group 1, the $PEP_{Mean\%}$ contribution to the $PTT_{Mean\%}$ of the left hand was significantly different compared to the right hand (p=0.004) (Table 3.2 and 3.3) (Figure 3.3). This result is still significant after applying the Bonferroni correction for multiple testing, p<0.008. In groups 2 and 3 there was no significant difference between the left and right measurements (Figure 3.4 and 3.5). Between the groups was no significant difference in the contribution of $PEP_{Mean\%}$ to the $PTT_{Mean\%}$, neither after correction for SBP.

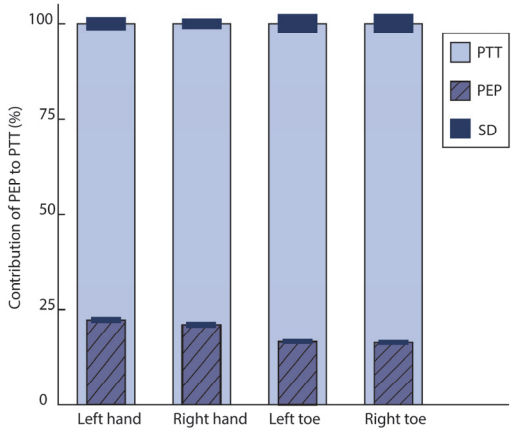

Figure 3.3: Contribution of the PEP (mean and SD) to the PTT for each sensor of group 1 (control group aged <50 years). All values are normalized to a percentage (%) of the mean PTT (which is 100%) of the specific sensor. PTTMean% of left hand (n=19) 100%±3.1%, PTTMean% of right hand (n=20): 100%±2.4% (p=0.004). Contribution of PEPMean% for PTT of left versus right hand 22.2%±1.3% versus 21.0%±1.3%. PTTMean% of left big toe (n=18) 100%±4.7%, PTTMean% right big toe (n=17) 100%±4.8%. Contribution of PEPMean% for left big toe versus right big toe 16.5%±1.0% versus 16.3%±1.0%.

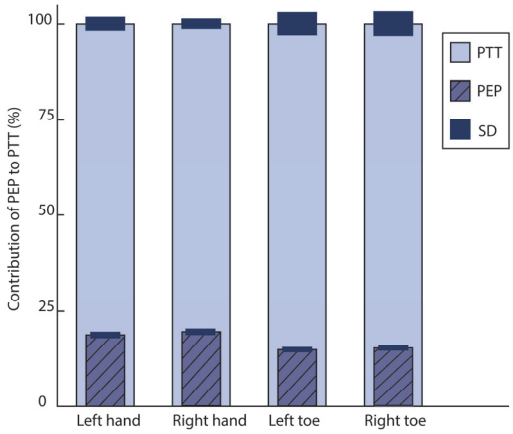

Figure 3.4: Contribution of the PEP (mean and SD) to the PTT for each sensor of group 2 (control group aged >50 years). All values are normalized to a percentage (%) of the mean PTT (which is 100%) of the specific sensor. PTTMean% of left hand (n=19) 100%±3.5%, PTT of right hand (n=20) 100%±2.6%. Contribution of PEPMean% for PTT of left versus right hand PEP 18.7%±1.4% versus PEP 19.4%±1.4%. PTTMean% of left big toe (n=18) 100%±5.9%, PTTMean% right big toe (n=17) PTT 100%±6.3%. Contribution of PEPMean% for left big toe versus right big toe 4.8%±1.1% versus 5.1%±1.1%.

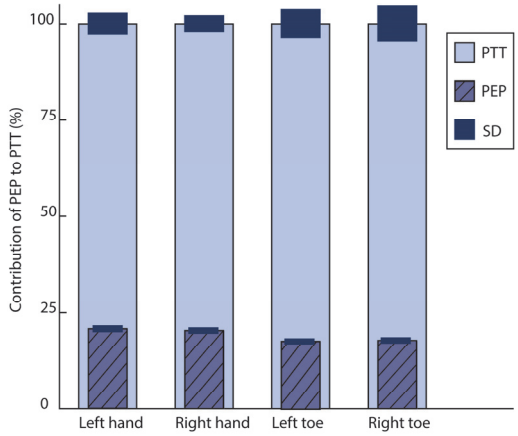

Figure 3.5: Columns represent the contribution of the PEP (mean and SD) to the PTT for each sensor of group 3 (participants with a cardiovascular risk factor). All values are normalized to a percentage (%) of the mean PTT (which is 100%) of the specific sensor. PTTMean% of left hand (n=19) 100%±5.5%, PTT of right hand (n=20) 100%±4.2%. Contribution of PEPMean% for PTT of left versus right hand 20.7%±1.5% versus 20.3%±1.4%. PTTMean% of left big toe (n=15) 100%±7.3%, PTTMean% right big toe (n=14) 100%±9.1%. Contribution of PEPMean% for left big toe versus right big toe 17.6%±1.3% versus 17.7%±1.4%.

3.4 Discussion

This study aimed to determine the variability of PEP at rest and its contribution to PTT in order to assess the accuracy of measuring VTT with PTT. Since it is difficult to measure PEP with echocardiography during exercise, we measured the PEP at rest only. The absolute value of the variability and SD of the PEP between individuals at rest was large when compared with the variability in one participant, However, in the normalized data, the SD of the PEP is only approximately 1.0-1.5% of the PTT. In an earlier study, we found an increase of the PTT of 17 ms after a successful axillary block from 259 ms to 276 ms [30]. This change is larger than can be expected to be caused by a variation of PEP alone.

This study has some limitations. The participants of this study did not refrain of caffeine, neither for physical activity for 48 hours. This might have an effect on the measurements. Nonetheless, in the study of Kohler et al caffeine had no significant effect on the PEP compared to the baseline measurements [31]. However, after exercise, the hemodynamic stress response is reduced and causes an significant increase in PEP [32]. Moreover, we did not control for the estrogenic phase of the participants. In this study 50% of the participants is female and the female participants in group 2 and 3 are above 50 years old and most likely

*Table 3.3: Normalized PTT and PEP variability per group. Mean values per group, n=20 per group. Group 1=control group participants aged <50 years, group 2=control group participants aged >50 years, group 3=participants with a cardiovascular risk factor. Values are normalized as percentage (%) of the PTT sensor. * = p<0.05*

Subjects	Normalized PTT [%] (PTT_{Mean} [ms])	PTT_{SD} [%] (PTT_{SD} [ms])	PEP_{Mean}	PEP_{SD}
Group 1				
Left hand	100 (267)*	3.1 (8)	22.2	1.3
Right hand	100 (280)*	2.4 (7)	21.0	1.3
Left foot	100 (369)	4.7 (17)	16.5	1.0
Right foot	100 (375)	4.8 (18)	16.3	1.0
Group 2				
Left hand	100 (276)	3.5 (12)	18.7	1.4
Right hand	100 (275)	2.6 (7)	19.4	1.4
Left foot	100 (359)	5.9 (21)	14.8	1.1
Right foot	100 (350)	6.3 (20)	15.1	1.1
Group 3				
Left hand	100 (280)	5.5 (16)	20.7	1.5
Right hand	100 (284)	4.2 (12)	20.3	1.4
Left foot	100 (339)	7.3 (22)	17.6	1.3
Right foot	100 (336)	9.1 (25)	17.7	1.4

postmenopausal. Farinatti et al showed in their study that the PEP was similar across age groups in men and women [33].

Furthermore, the PTT was measured bilaterally and the difference between the blocked arm and the contralateral arm was calculated. Other studies have shown that PTT difference is a method to exclude the effect of PEP and can be used to monitor arterial distensibility or pulse wave velocity changes [34]. Therefore, the increase in PTT in the present study is most probably a result of the vascular component of the PTT, the VTT.

Furthermore, in group 1, the contribution of the PEP to the PTT_{finger} was 22.3% and 21.0% for the left and right hand, respectively; this was a significant difference between the left and right hand. This can be explained by the difference in PTT of the left and right hand. In our earlier study, we found no difference between the PTT of the left and right hand in a person at rest in supine position [30]. For an optimal apical 5-chamber view with echocardiography, a left lateral decubitus position was required with the left hand positioned above their head. PTT is related to the position of the arms [35, 36]. Moreover, this position can introduce a different curvature of the artery to the arm. Therefore, the left lateral decubitus position is a possible explanation for this difference in PTT and, subsequently, the contribution to PTT. However, there was no significant

difference between the left and right hand in groups 2 and 3.The contribution of the PEP to the PTT_{toe} was smaller compared to the PTT_{finger}. This difference can be explained by the length of the arterial pathway to the toes and a subsequently longer VTT (and PTT). In this study, the mean PEP of all 3 groups was 56.2 ± 12.3 ms; this differs from the values found in other studies. The main reason for this is the diverse acquisition techniques used and/or an estimation of PEP made by measuring the left ventricular ejection time [17]. Johansson et al. investigated the use of PTT for respiration rate monitoring; PTT varies with respiration. The authors investigated whether measuring the individual components of the PTT (PEP and VTT) could improve their respiration detection [21]. The PEP was measured with phonocardiography, by using the sound of the closing valves. For technical reasons, they used the first heart sound (S1) which represents the closing of the mitral valve, instead of measuring the opening of the aortic valve. However, after the mitral valve closes (S1) and the isovolumetric contraction starts, the ventricular pressure will rise. When the ventricular pressure is high enough, the aortic valve opens and the ejection of blood to the aorta starts. Therefore, using phonography will introduce an inaccuracy in the measurement. They found a mean PEP at rest of 30.1 ms with a SD of 8.0 ms. Furthermore, the PEP and VTT varied synchronously during respiration; focusing on these components did not improve their respiration detection.

In most of the studies, the PEP was measured with cardiothoracic impedance, which measures the change in blood volume in the thorax, which is primarily caused by the blood flow in the aorta. The advantage of cardiothoracic impedance is that it does not require specially trained personnel and can be measured in every body position and also during movements. It is an indirect measurement and is less accurate than a direct measurement and gold standard echocardiography [37], which was used in the present study. Furthermore, these measurements were performed in three different groups. Age and cardiovascular risk factors such as hypertension and atherosclerosis are important factors for PTT. They influence the stiffness of arteries and can change the contribution of PEP to the PTT. However, our measurements showed no significant difference in the PEP between the groups; moreover, the $PEP_{SD\%}$ was very small (between 1.0 and 1.5).

3.5 Conclusion

In conclusion, the contribution of PEP to the PTT measured at the finger tips at rest is approximately 20%. Therefore, the VTT is represented by the remaining

80% of the PTT. Since the PEP variability within an individual at rest is small ($PEP_{SD\%}$1.0-1.5% of the PTT value), its contribution to a change in PTT is also small. Therefore, PTT is an attractive method to non-invasively monitor arterial stiffness at rest. Furthermore, unlike methods such as Doppler ultrasound, it does not need specially trained personnel. ECG and PPG (pulse oximeter) are already available in hospitals and software implementation in the monitors is needed to enable PTT calculation. Therefore, PTT at rest is an easy, non-invasive, low-priced measurement, and accurate approximation of VTT for monitoring arterial stiffness.

3.6 Acknowledgments

Special thanks to Mariska Nieuwenhoff and Erik Jan Bakker for their help during the first inclusions.

3.7 Reference

1. Nitzan, M., B. Khanokh, and Y. Slovik, The difference in pulse transit time to the toe and finger measured by photoplethysmography. Physiol Meas, 2002. 23(1): p. 85-93.
2. Suurland, J., et al., Infant Parasympathetic and Sympathetic Activity during Baseline, Stress and Recovery: Interactions with Prenatal Adversity Predict Physical Aggression in Toddlerhood. J Abnorm Child Psychol, 2017.
3. Wang, A., et al., The product of resting heart rate times blood pressure is associated with high brachial-ankle pulse wave velocity. PLoS One, 2014. 9(9): p. e107852.
4. Muehlsteff, J., X.L. Aubert, and M. Schuett, Cuffless estimation of systolic blood pressure for short effort bicycle tests: the prominent role of the pre-ejection period. Conf Proc IEEE Eng Med Biol Soc, 2006. 1: p. 5088-92.
5. Zhang, G., et al., Pulse arrival time is not an adequate surrogate for pulse transit time as a marker of blood pressure. J Appl Physiol, 2011. 111(6): p. 1681-6.
6. Yang, C., et al., Novel blood pressure estimation method using single photoplethysmography feature. Conf Proc IEEE Eng Med Biol Soc, 2017. 2017: p. 1712-1715.
7. Ibrahim, B., V. Nathan, and R. Jafari, Exploration and validation of alternate sensing methods for wearable continuous pulse transit time measurement using optical and bioimpedance modalities. Conf Proc IEEE Eng Med Biol Soc, 2017. 2017: p. 2051-2055.
8. Bhattacharya, T., et al., Robust motion artefact resistant circuit for calculation of Mean Arterial Pressure from pulse transit time. Conf Proc IEEE Eng Med Biol Soc, 2017. 2017: p. 3553-3556.

9. Babchenko, A., et al., Increase in pulse transit time to the foot after epidural anaesthesia treatment. Med Biol Eng Comput, 2000. 38(6): p. 674-9.
10. Kortekaas, M.C., et al., Pulse transit time as a quick predictor of a successful axillary brachial plexus block. Acta Anaesthesiol Scand, 2012. 56(10): p. 1228-33.
11. Foo, J.Y. and C.S. Lim, Pulse transit time as an indirect marker for variations in cardiovascular related reactivity. Technol Health Care, 2006. 14(2): p. 97-108.
12. Lehmann, E.D., K.D. Hopkins, and R.G. Gosling, Comment on: Assessment of arterial distensibility by automatic pulse wave velocity measurement. Hypertension, 1996. 27(5): p. 1188-91.
13. Paiva, R.P., et al., Assessing PEP and LVET from heart sounds: algorithms and evaluation. Conf Proc IEEE Eng Med Biol Soc, 2009. 2009: p. 3129-33.
14. Buxi, D., et al., Comparison of the impedance cardiogram with continuous wave radar using body-contact antennas. Conf Proc IEEE Eng Med Biol Soc, 2017. 2017: p. 693-696.
15. Seery, M.D., et al., Preejection period can be calculated using R peak instead of Q. Psychophysiology, 2016. 53(8): p. 1232-40.
16. Etemadi, M., et al., Non-invasive assessment of cardiac contractility on a weighing scale. Conf Proc IEEE Eng Med Biol Soc, 2009. 2009: p. 6773-6.
17. Paiva, R.P., et al., Beat-to-beat systolic time-interval measurement from heart sounds and ECG. Physiol Meas, 2012. 33(2): p. 177-94.
18. Noda, K., et al., Comparison of the measured pre-ejection periods and left ventricular ejection times between echocardiography and impedance cardiography for optimizing cardiac resynchronization therapy. J Arrhythm, 2017. 33(2): p. 130-133.
19. Tsai, Y.C., et al., Fluid overload, pulse wave velocity, and ratio of brachial pre-ejection period to ejection time in diabetic and non-diabetic chronic kidney disease. PLoS One, 2014. 9(11): p. e111000.
20. Wong, M.Y., et al., The effects of pre-ejection period on post-exercise systolic blood pressure estimation using the pulse arrival time technique. Eur J Appl Physiol, 2011. 111(1): p. 135-44.
21. Johansson, A., et al., Pulse wave transit time for monitoring respiration rate. Med Biol Eng Comput, 2006. 44(6): p. 471-8.
22. Pollak, M.H. and P.A. Obrist, Aortic-radial pulse transit time and ECG Q-wave to radial pulse wave interval as indices of beat-by-beat blood pressure change. Psychophysiology, 1983. 20(1): p. 21-8.
23. Chan, G.S., et al., Change in pulse transit time and pre-ejection period during head-up tilt-induced progressive central hypovolaemia. J Clin Monit Comput, 2007. 21(5): p. 283-93.
24. Fiskum, C., et al., Cardiac complexity and emotional dysregulation in children. Int J Psychophysiol, 2017. 121: p. 38-45.

25. Moldovan, M. Matlab central, file exchange (online). 2003 22 October 2008 4 November 2008]; Available from: http://www.mathworks.com/matlabcentral/fileexchange/4061-loadacq.
26. Clifford, G.D. Rpeakdetect syntax (ECG toolbox). 2008 16 November 2008]; Massachusetts Institute of Technology]. Available from: http://www.mit.edu/~gari/CODE/.
27. Oppenheim, A.V. and R.W. Schafer, Discrete-Time Signal Processing. 1989: Prentice-Hall. 284-285.
28. van Velzen, M.H., et al., Increasing accuracy of pulse transit time measurements by automated elimination of distorted photoplethysmography waves. Med Biol Eng Comput, 2017.
29. Elgendi, M., et al., Frequency analysis of photoplethysmogram and its derivatives. Comput Methods Programs Biomed, 2015. 122(3): p. 503-12.
30. Kortekaas, M.C., et al., Comparison of bilateral pulse arrival time before and after induced vasodilation by axillary block. Physiol Meas, 2012. 33(12): p. 1993-2002.
31. Kohler, M., A. Pavy, and C. van den Heuvel, The effects of chewing versus caffeine on alertness, cognitive performance and cardiac autonomic activity during sleep deprivation. J Sleep Res, 2006. 15(4): p. 358-68.
32. Brownley, K.A., et al., Sympathoadrenergic mechanisms in reduced hemodynamic stress responses after exercise. Med Sci Sports Exerc, 2003. 35(6): p. 978-86.
33. Farinatti, P., et al., Cardiorespiratory responses and myocardial function within incremental exercise in healthy unmedicated older vs. young men and women. Aging Clin Exp Res, 2018. 30(4): p. 341-349.
34. Foo, J.Y. and C.S. Lim, Dual-channel photoplethysmography to monitor local changes in vascular stiffness. J Clin Monit Comput, 2006. 20(3): p. 221-7.
35. Zheng, D. and A. Murray, Non-invasive quantification of peripheral arterial volume distensibility and its non-linear relationship with arterial pressure. J Biomech, 2009. 42(8): p. 1032-7.
36. Foo, J.Y., et al., Pulse transit time changes observed with different limb positions. Physiol Meas, 2005. 26(6): p. 1093-102.
37. Carvalho, P., et al., Comparison of systolic time interval measurement modalities for portable devices. Conf Proc IEEE Eng Med Biol Soc, 2010. 2010: p. 606-9.

Chapter 4

Pulse transit time as a quick predictor of a successful axillary brachial plexus block

Minke C. Kortekaas, Sjoerd P. Niehof, Marit H.N. van Velzen, Eilish M. Galvin, Frank J.P.M. Huyghen, Robert Jan Stolker

Acta Anaesthesiologica Scandinavia, June 2012

It can take up to 30 min to determine whether or not axillary block has been successful. Pulse transit time (PTT) is the time between the R-wave on electrocardiography (ECG) and the arrival of the resulting pressure pulse wave in the fingertip measured with photoplethysmography. It provides information about arterial resistance. Axillary block affects vasomotor tone causing loss of sympathetic vasoconstriction resulting in an increased PTT. Early objective assessment of a block can improve efficacy of operating room time and minimize patient's fear of possible conversion to general anesthesia. This study explores whether PTT can objectively, reliably and quickly predict a successful axillary block. Forty patients undergoing hand surgery under axillary block were included. A three-lead ECG and photoplethysmographic sensors were placed on both index fingers. Measurements were made from 2 min before until 30 min after induction of the block or less if the patient was transferred for operation. Afterwards, PTT was calculated as the time between the R-wave on ECG and a reference point on the photoplethysmogram. To assess the change in PTT caused by the block, the PTT difference between the control and blocked arm was calculated. Sensitivity and specificity of PTT difference were calculated using receiver operating characteristic analysis. In a successful block, the mean PTT difference significantly increased after 3 min by 12 (standard error of the mean 3.9) ms, sensitivity 87% and specificity 71% (area under the curve 0.87, P=0.004). PTT is a reliable, quick and objective method to assess whether axillary block is going to be successful or not.

4.1 Introduction

Patients scheduled for upper-limb surgery have a number of options regarding anesthesia techniques. Two such options are general anesthesia and a brachial plexus block, both of which have their own advantages and disadvantages. For example, patients undergoing locoregional anesthesia have less opioid-related side-effects (e.g. nausea and drowsiness) after surgery, but the block placement can be time consuming. On the other hand, general anesthesia is fast and can be a solution for patients who fear locoregional techniques or being awake during surgery.

The success rate of a locoregional block depends on several factors, including the anatomy of the patient, available technology (e.g. electrostimulation or ultrasound) and the skills of the anesthesiologist. Since the introduction of ultrasound guided regional anesthesia success rates have improved [1], however ultrasound is not always available. After injection of the local anesthetic, it can take up to 30 min or more to determine if the block is successful.

Multiple tools are available to assess a block, the most common being a pinprick or loss of cold sensation with an icepack [2], as well as skin temperature and peripheral flow index [3, 4]. In case of a partial or failed block, a supplemental regional block can be performed, or the local anesthesia technique can be converted to general anesthesia. However, this can be at the expense of additional (costly) operating room time.

Locoregional blocks affect the sensory function (pain impulses are blocked) and somatic motor function, as well as the sympathetic nerves resulting in relaxation of the arterial wall muscle, vasodilatation, and increased blood flow [5, 6]. The compliance (C) is a measure of the elasticity of the arteries and is defined as

$$C = \frac{\Delta V}{\Delta P} \tag{4.1}$$

where ΔV is the change in arterial volume and ΔP the change in blood pressure[7]. A change in compliance can be measured with pulse wave velocity [8] and with the pulse transit time (PTT). Babchenko et al. [6] measured an increase in PTT to the feet after epidural anesthesia.

Quick objective assessment of an axillary block can improve the efficacy of total operating room time by reducing the time to surgical incision and by minimizing

patients' uncertainty about a possible conversion to general anesthesia. Therefore, this study explores whether PTT can be used to objectively, reliably and quickly predict whether an axillary block is going to be successful.

4.2 Method

4.2.1 Study population

The trial protocol was approved by the Medical Ethics Committee of Erasmus University Center Rotterdam (MEC-2008-249), and this single-center observational study was conducted in accordance with the Declaration of Helsinki. All participants gave informed and written consent. ASA I-II patients (age 18–80 years) scheduled for elective unilateral upper limb surgery under axillary block were included. Exclusion criteria were diseases which can influence the vascular system (e.g. diabetes, Raynaud's), cardiac disease, use of anti-hypertensive therapy, essential tremor in the upper extremity, neuropathy, malformation at the measurement sites, allergy for local anesthetic agents, or skin infection at the site of needle insertion.

4.2.2 Protocol

After arrival of the patient at the holding, an intravenous catheter was inserted and standard monitoring electrocardiography (ECG) and non-invasive blood pressure was applied. To measure the PTT three external ECG leads were placed (ECG100C amplifier, Biopac®, Goleta, U.S.A.), and photoplethysmography (PPG) sensors (TSD200 and PPG100C amplifier, Biopac®) were attached to the index finger of both hands. Data were sampled with 2 kHz with AcqKnowledge version 3.7.3 software (Biopac®). Afterwards the recorded data were analysed in Matlab R2008b® (The MathWorks, Inc., Natick, Massachusetts, U.S.A.).

The PTT was measured to establish the baseline for approximately 2 min with the patient lying supine in bed. The patient was asked not to move during this measurement. The arm was abducted to a 90° angle to apply the block. A needle connected to a nerve stimulator was inserted and set to deliver 1mA current (50 mm insulated needle, Stimuplex B Braun, Melsungen, Germany). The nerves of the brachial plexus were identified with nerve stimulation techniques. Once an appropriate single nerve response was obtained of at least the nerve supplying the planned surgical site (hand twitch at a current of 0.2-0.5 mA), the local anesthetic was administered. The majority of the patients had the median, radial and ulnar nerve stimulated and injected separately. The local anesthetics that were used (at

choice of the individual anesthesiologist) are ropivacaine, mepivacaine, lidocaine, and prilocaine. If any sedatives, propofol or midazolam were given during the procedure, this was documented.

After the first injected bolus of local anesthetic (t=0), the PTT was measured on both arms for intra-subject comparison between the arms. Measurements were continued for 30 min after induction of the axillary block, or less if the anesthesiologist assessed the block with an ice pack as a complete sensory block and the patient was transferred to the operating room. A successful block was defined as a complete sensory block of the median, ulnar, and radial nerve, tested with ice pack and surgical forceps, where neither extra analgesics, nor supplemental local regional techniques were required at the time of surgical incision.

4.2.3 Pulse wave analysis

Data from the AcqKnowledge software were directly imported into Matlab with the Loadacq syntax for Matlab. ECG data were analysed with the Rpeakdetect syntax available from the ECGtoolbox [9]. PPG-data were filtered with a fourth-order low-pass Butterworth filter with a cut-off frequency of 20 Hz. The signals from the PPG-sensors were digitally cut between the R-wave and the next R-wave.

To reduce artefacts of the PPG-signal we filtered the data with the following algorithm. Each pulse wave was compared to an average pulse wave of 10 subsequent pulse waves ±1 standard deviation. When 25% or more of the current pulse wave was outside this window, then the pulse wave was filtered out. The PTT was calculated for the remaining pulse waves. For each minute after injection of the local anesthetic, we fitted a mean pulse wave and identified 3 previously agreed reference points on this mean pulse wave, i.e. the foot, point of maximum steepness of the upstroke pulse wave (first derivative), and the peak (Figure 4.1).

PTT was determined by calculating the time between the R-wave of the ECG and two different reference points on the pressure pulse wave: the foot, and first derivative. The 'foot' was determined by the maximum value of the second derivative of the pulse wave. The 'first derivative' was determined by taking the maximum of the first derivative of the upstroke pulse wave. The 'peak' was the maximum value of the pulse wave and was only used to determine the amplitude of the pulse wave. The amplitude of a pulse wave is determined by calculating the voltage difference between the reference points foot and peak.

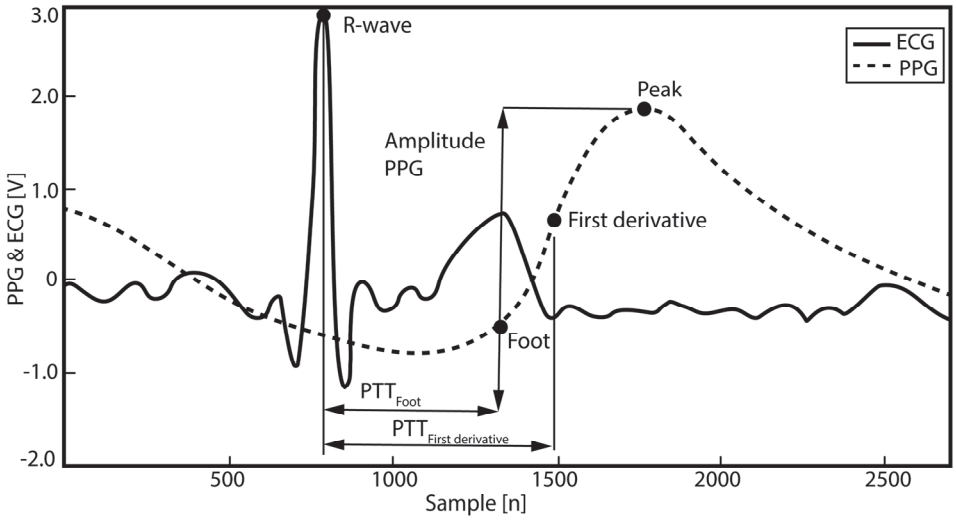

Figure 4.1 Graphical representation of calculation of the pulse transit time (PTT). ECG = electrocardiogram; PPG = photoplethysmogram. Data were measured with a sampling rate of 2 kHz.

The aim was to investigate the effect of the axillary block on PTT. Therefore, the calculated PTTs with standard error of the mean (SEM) from the baseline measurements were subtracted from the PTT values after an axillary block for both arms

$$\Delta PTT_{tx} = PTT_{tx} - PTT_{Baseline} \tag{4.2}$$

The PTT_{tx} was determined for each minute after the first injected bolus of local anesthetic (t=0), where x is in minutes. Subsequently, we calculated the difference (PTT_{difftx}) between the blocked arm ($PTT_{blocktx}$) and the contralateral arm ($PTT_{contralateraltx}$)

$$PTT_{difftx} = \Delta PTT_{blocktx} - \Delta PTT_{contralateraltx} \tag{4.3}$$

Similarly, the difference between the amplitude of the pulse waves was calculated. We tested the PTT and amplitude of the pulse waves against the above described definition of a successful axillary block.

4.2.4 Statistical analysis

Patient characteristics were calculated as mean and standard deviation. To find the most optimal combination of sensitivity and specificity of PTT in a successful axillary block a receiver operating characteristic (ROC) analysis was used. After injection of the local anesthetic, the PTT_{difftx} of the subsequent 10 min was tested.

Table 4.1: Characteristics of the study population. N = 37, data are presented as mean ± SD or number (%) of patients. ASA = American Society of Anesthesiologists

Variable	
Age [years]	43 ± 15
Sex (female), no. (%)	17 (46)
Weight [kg]	76 ± 14
Height [m]	1.76 ± 0.11
Body mass index [kg/m²]	24.6 ± 3.8
ASA status, no. (%)	
I	23 (62)
II	14 (38)
Blood pressure [mmHg]	
Systolic	136 ± 20
Diastolic	80 ± 12
Smoker, no. (%)	12 (32)
Success rate, no. (%)	27 (73)

A *p*-value <0.05 was considered statistically significant. The coordinates on the ROC curve were selected on a combination of the highest sensitivity with specificity higher than 70%. Statistical analyses were performed with SPSS version 18 (SPSS Inc. Chicago, Illinois).

4.3 Results

A total of 40 patients were included. Because data from 3 patients contained too many artefacts they were excluded from the analyses. The overall success rate of the axillary blocks was 73%. Table 4.1 presents the characteristics of the study group (n=37).

The first significant increase in PTT difference for the reference point 'foot' was reached 3 min after injection of the local anesthetic (t=3) with a sensitivity of 78%, a specificity of 71% and an area under the curve (AUC) of 0.77 (p=0.031) (Figure 4.2). In a successful axillary block the mean increase in PTT was 12 (SEM 6.9) ms. At 10 min after injection (t=10) this had improved to a sensitivity of 91% and a specificity of 86% (AUC=0.88, p=0.003).

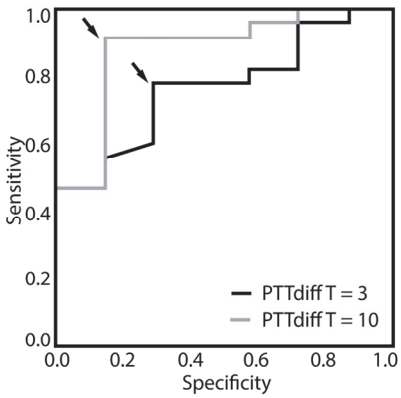

Figure 4.2 Receiver operating characteristic of pulse transit time (PTT) difference between both arms of reference point 'foot' at 3 min (t=3) and at 10 min (t=10) after axillary block. The arrows indicate the selected coordinates of the ROC curve. At t=3 sensitivity 78%, specificity 71% and AUC=0.77 (p=0.031). At t=10 sensitivity 91%, specificity 86% and AUC=0.88 (p=0.003).

Also for the 'first derivative' reference point on the pulse wave, at t=3 the PTT difference showed a significant increase of 12 (SEM 3.9) ms, with a sensitivity of 87% and a specificity of 71% (AUC 0.87, p=0.004) (Figure 4.3). At t=10 this had remained stable with the same sensitivity and specificity (AUC 0.85, p=0.005). At t=3 the amplitude difference of the pulse waves had increased, with a sensitivity of 74% and a specificity of 71% (AUC 0.81, p=0.013). At t=10 the sensitivity had increased to 96%, with a specificity of 71% (AUC=0.91, p=0.001).

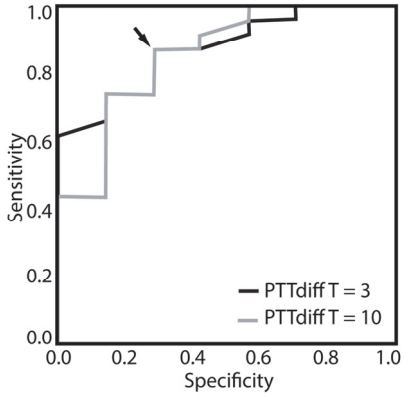

Figure 4.3 Receiver operating characteristic of pulse transit time (PTT) difference between both arms of reference point 'first derivative' at 3 min (t=3) and at 10 min (t=10) after axillary block. The arrow indicates the selected coordinates of the ROC curve. At t=3 sensitivity 87%, specificity 71% and AUC 0.87 (p=0.004). At t=10 sensitivity 87%, specificity 71% and AUC 0.85 (p=0.005).

For all these results the ROC analyses of only the contralateral arm (with baseline correction) showed no significant change after axillary block.

4.4 Discussion

From these results we can conclude that PTT can objectively predict a successful axillary block with a high sensitivity and specificity after only 3 min. Clinically, it is impossible to do this at such an early stage with sensory test such as ice pack, pinprick, skin temperature and peripheral flow index [2-4]. Although peripheral flow index and PTT are both measurements that use photoplethysmography, the main difference is that peripheral flow index is a local measure unlike the PTT. Peripheral flow index measures the ratio of the pulsatile to nonpulsatile component of the plethysmogram of the local digital blood flow [4]. A possible limitation of this study is the measurement of PTT on the index finger only, which is innervated by the median nerve. However, we were able to predict a successful complete sensory axillary block, as defined in the methods, by only measuring the index finger. Placement of additional PPG-sensors on the thumb and little finger, innervated by respectively the radial and ulnar nerve, or additionally measuring peripheral flow index on these sites, could solve this limitation. Then it would be possible to determine if there is a difference in PTT between the different innervation areas in a partial block. However, it may be questioned whether this additional measurements are necessary as we were able to make a reliable prediction after measuring the index finger only. This may indicate once more that PTT is more an overall measurement. We defined a failing block as a partial sensory block in which only one or two of the nerves were blocked. However, this is clinically irrelevant if there is no pain sensation in the operated area.

In this observational study design the PTT measurement was standardized, however the choice of local anesthetic and injected volume depended on the duration of the surgery and was made by the individual anesthesiologist. Therefore different local anesthetics were used with different onset times. In the majority of the patients, ropivacaine with mepivacaine 30-40 ml was used. A standardized technique allowing only a standardized dose of a specific fast onset local anesthetic could shorten the time until prediction further. However, in routine everyday anesthesia, it is usual to use a variety of different local anesthetics, as we have done in this study.

By calculating the difference between the blocked arm and the contralateral arm, we ruled out factors which influence the vascular tone of the total body. For

example, temperature change and systemic medication that influence vasomotor tone (e.g. propofol or midazolam), as well as a change in the pre-ejection period, can affect the PTT [10]. Therefore, in our calculations a change in PTT will be caused by a change in arterial resistance due to the axillary block.

In our measurements we take into account that a change in the position of the blocked arm might influence the PTT [11]. After insertion of the block, the arm was restored to a resting position lateral to the body. This movement can cause artefacts in the PPG-signals. Moreover, a different arm position can change the angle and thereby the resistance of the arterial pathway to the hand. Therefore the pulse wave form and resulting PTT can change. However, our t=1 measurement started immediately after the first bolus of local anesthetic was injected. Since the anesthesiologist stimulated and injected local anesthetic to multiple nerves of the brachial plexus separately, this takes several minutes. Therefore, it is most likely that the arm was moved after the significant change in PTT found at t=3, and the PTT change can therefore be attributed to the axillary block.

In the present study we used a fixed protocol to filter the artefact of the measured data. Therefore, the analyses are more standardized and objective compared with subjective selection of the pulse waves by a researcher; in turn, this effectively removes artefacts caused by e.g. movements or non-invasive blood pressure measurement. However, this filter also removes pulse waves that increase very rapidly and differ from the average pulse wave by ±1 standard deviation; this may erroneously identify pulse waves as artefacts and cause loss of relevant data. Consequently, extreme values in the data are filtered out and this can result in a 'regression toward the mean phenomenon' with a decrease in statistical significance, sensitivity and specificity.

In our results the coordinate on the ROC curve with the highest sensitivity and a specificity of at least 70% were selected. The sensitivity indicates the probability of correctly identifying a successful axillary block, while specificity indicates the probability of correctly identifying failed axillary blocks. When a successful axillary block can be predicted quickly, patients with a successful axillary block can be transported from the holding to the operating room and prepared for operation. This saves time waiting for the onset of loss of pain sensation, where after the patient will be transported to the operating room. Therefore this improves the efficacy of operating room time. This is especially of value in a university hospital with a residency training setting were the block procedures can be more time

consuming. Moreover, the 73% success rate may be low, but is realistic in this setting [12]. However the use of ultrasound may improve the results, the problem of early recognition of failed blocks the problem of early recognition of failed blocks remains [1]. Even in a setting with higher success rates, early identification of failed axillary blocks is important and could potentially save time.

The ultimate goal is to implement software to calculate PTT in the commonly used anesthesia monitors, enabling PTT measurement with a standard ECG and a standard pulse oximeter. This would allow PTT to be a widely available measurement tool, which is easy to use, non-invasive, and a safe and quick method of objectively assessing axillary blocks.

4.5 References

1. McCartney, C.J., L. Lin, and U. Shastri, Evidence basis for the use of ultrasound for upper-extremity blocks. Reg Anesth Pain Med, 2010. 35(2 Suppl): p. S10-5.
2. Curatolo, M., S. Petersen-Felix, and L. Arendt-Nielsen, Sensory assessment of regional analgesia in humans: a review of methods and applications. Anesthesiology, 2000. 93(6): p. 1517-30.
3. Galvin, E.M., et al., Thermographic temperature measurement compared with pinprick and cold sensation in predicting the effectiveness of regional blocks. Anesth Analg, 2006. 102(2): p. 598-604.
4. Galvin, E.M., et al., Peripheral flow index is a reliable and early indicator of regional block success. Anesth Analg, 2006. 103(1): p. 239-43, table of contents.
5. Sorensen, J., et al., Laser Doppler perfusion imager (LDPI)--for the assessment of skin blood flow changes following sympathetic blocks. Acta Anaesthesiol Scand, 1996. 40(9): p. 1145-8.
6. Babchenko, A., et al., Increase in pulse transit time to the foot after epidural anaesthesia treatment. Med Biol Eng Comput, 2000. 38(6): p. 674-9.
7. O'Rourke, M.F., et al., Clinical applications of arterial stiffness; definitions and reference values. Am J Hypertens, 2002. 15(5): p. 426-444.
8. Bramwell J.C., H.A.V., The Velocity of the Pulse Wave in Man. Proc. Royal Society of London. SerieB, Containing Papers of a Biological Character, 1922. 93(652): p. 298-306.
9. Clifford, G.D., Rpeakdetect function (ECG toolbox). 2008.
10. Muehlsteff, J., X.L. Aubert, and M. Schuett, Cuffless estimation of systolic blood pressure for short effort bicycle tests: the prominent role of the pre-ejection period. Conf Proc IEEE Eng Med Biol Soc, 2006. 1: p. 5088-92.

11. Zheng, D. and A. Murray, Non-invasive quantification of peripheral arterial volume distensibility and its non-linear relationship with arterial pressure. J Biomech, 2009. 42(8): p. 1032-7.
12. Luyet, C., et al., Different Learning Curves for Axillary Brachial Plexus vBlock: Ultrasound Guidance versus Nerve Stimulation. Anesthesiol Res Pract, 2010. 2010: p. 309462.

Chapter 5

Effect of heat-induced pain stimuli on pulse transit time and pulse wave amplitude in healthy volunteers

Marit H.N. van Velzen, Arjo J. Loeve, Minke C. Kortekaas,
Sjoerd P. Niehof, Egbert G. Mik

Physiological Measurement, January 2016

Pain is commonly assessed subjectively by interpretations of patient behaviour and/or reports from patients. When this is impossible the availability of a quantitative objective pain assessment tool based on objective physiological parameters would greatly benefit clinical practice and research beside the standard self-report tests. Vasoconstriction is one of the physiological responses to pain. The aim of this study was to investigate whether pulse transit time (PTT) and pulse wave amplitude (PWA) decrease in response to this vasoconstriction when caused by heat-induced pain. The PTT and PWA were measured in healthy volunteers, on both index fingers using photoplethysmography and electrocardiogram. Each subject received 3 heat-induced pain stimuli using a Temperature-Sensory Analyzer thermode block to apply a controlled, increasing temperature from 32.0°C to 50.0°C to the skin. After reaching 50.0°C, the thermode was immediately cooled down to 32.0°C. The study population was divided in to 2 groups with a different time-interval between the stimuli, 20s or 60s. The results showed a significant (p<0.05) decrease of both PTT and PWA on the stimulated and contralateral side. Moreover, there was no significant effect between the stimulated and contralateral side. No significant effect of applying multiple successive stimuli was found. The time-interval of 20s was too short to allow PTT and PWA to return to baseline values and should exceed 40s in future studies. Heat-induced pain causes a decrease of PTT and PWA. Consequently, it is expected that, in the future, PTT and PWA may be applied as objective indicators of pain, either beside the standard self-report test, or when self-report testing is impossible.

5.1 Introduction

According to the definition of the International Association for the Study of Pain, pain is "an unpleasant sensory and emotional experience associated with actual or potential tissue damage, or described in terms of such damage" [1]. The clinical tests used most commonly to rate pain are the Numeric Rating Score (NRS) and the Visual Analog Scale (VAS) [2, 3]. These tests are based on self-reporting. Since pain is a subjective phenomenon, these self-report tests are generally accepted gold standard for the assessment of presence of pain. However, self-report is difficult or even impossible by intubated or sedated patients, intellectually disabled patients, and neonates and infants. There is an ongoing search for more objective methods for detection of pain, for example based on heart rate variability [4], skin conductance [5] and photoplethysmography (PPG) [6]. The availability of a quantitative objective pain assessment tool based on objective physiological parameters would greatly benefit clinical practice and research beside the standard self-report tests.

Vasoconstriction is one of the physiological responses of the body to pain, causing a decrease in compliance and vessel diameter [7, 8]. The compliance is a measure of the elasticity of the arteries [9] and can be determined using Doppler ultrasound [10]. However, limited availability and the requirement of an experienced operator are disadvantages of Doppler ultrasound. Alternatively, the compliance may easily be measured using PPG [11, 12]. PPG is a widely available non-invasive optical technique that uses infrared light and a photodiode to visualize the pressure pulse e waves (PWs) in the vessels by measuring the volumetric changes of pulsating blood and thus the expansion and contraction of the vessels. PPG enables continuous measurement of the PWs [13, 14] and is routinely used in everyday medicine for measuring among others, heart rate and oxygen saturation (SpO_2).

During vasoconstriction the arterial stiffness increases, which causes an increase in pulse wave velocity [15]. Consequently, the propagation time of a PW going from the heart to the peripheral arteries (generally called Pulse Transit Time, PTT) should decrease due to pain-induced vasoconstriction [16]. The PTT is commonly used for the assessment of arterial stiffness, for monitoring sympathetic activity in sleep apnoea patients [17], measuring endothelial function [18] and as an indicator for arterial blood pressure [19]. The Pulse Wave Amplitude (PWA) is a measure of the difference between the foot and peak of one single PW.

Previous reports described the effect of cold exposure on PTT or studied local warming/heating in the upper extremities [20-22]. To the best of our knowledge, there are no reports about the effect of heat-induced pain on PTT. Grönroos et al. found a centrally mediated autonomic (sympathetic) vasoconstriction response to painful peripheral stimulation on healthy human volunteers [7]. Therefore, it is hypothesised that PTT and PWA decrease by a central mechanism in response to heat-induced pain, allowing these effects to be measured at the contralateral side as well.

The goal of this study was to test whether PTT and PWA decrease in response to heat-induced pain stimuli and whether these could provide an objective binary indicator of pain, either beside the gold standard self-report, or when self-report is impossible. It was not the purpose of this study to relate the level (expressed in VAS and/or NRS) of pain to the change of PTT and/or PWA. Obviously the goal to develop an objective pain indicator is highly ambitious because pain is a complex phenomenon involving both (patho-)physiological and psychological mechanisms. Therefore, the experience of pain is likely to remain subjective, at least partly.

5.2 Method

5.2.1 Study population

This study was approved by the Medical Ethics Committee of Erasmus University Medical Center Rotterdam (MEC-2012-489). Twenty healthy volunteers, 18-35 years old, without any known history of atherosclerosis associated diseases, (such as diabetes mellitus, hypertension, coronary artery disease, stroke, renal disorder) or injuries at the upper limbs were included in this study after obtaining written informed consent from the subject.

5.2.2 Protocol

The PTT consists of 2 components, the isometric contraction time (pre-ejection period, PEP), and the PW propagation-time through the vessel. The PEP is known to vary with cardiac preload and heart rate [23, 24]. Therefore, all measurements were conducted in a quiet room under tranquil conditions at a room temperature of 22.5°C (SD 0.5°C). The subject sat on a chair with both hands resting on a table. To minimize any influences of a varying PEP or cardiac output during the measurement, the subject was instructed not to talk or move during the measurement.

Defrin et al. found that at a threshold of 42.8°C (SD 3.4°C) humans experience thermal heat as pain [25]. In the current study each stimulus consisted of a temperature rise, starting at '*start(i)*' at 32.0°C rising with a speed of 1.0°C/s and stopping at '*stop(i)*' at 50.0°C (where *i ={1..3})* indicates the sequence number of the stimulus). As such, the applied stimulus gets well above 46.2°C (mean plus SD of the sensory determinant), which should thus be sufficient to assure pain at the end of the stimulus. When the maximum temperature was reached, the temperature of the thermode was programmed to immediately drop back from 50.0°C to the starting temperature of 32.0°C with 10.0°C/s. Consequently, a relatively short pain stimulus was experienced by the subjects.

Before the start of the first stimulus the baseline of PTT and PWA at rest were measured for 60s, in order to determine the range of the normal fluctuations. The baseline variations were calculated as standard deviation expressed as a percentage of the mean PTT and PWA over these 60s. The PTT and PWA were determined beat-to-beat during the entire measurement (Figure 5.1-ABCD). The system used for measuring the PTT, PWA and heart rate consisted of a measurement device and analysis software. The measurement device contained two PPG-sensors (TSD200 with the PPG100C amplifier, Biopac Systems, Inc, USA), positioned on each index finger, and three external ECG-leads (ECG100C amplifier, Biopac Systems, Inc, USA). The three ECG-leads were placed on the subject's wrists and right ankle. The PPG- and ECG-signals were simultaneously converted to digital signals using AcqKnowledge version 3.7.3 software (Biopac Systems, Inc, USA), at a sampling frequency of 2kHz.

Kortekaas et al. found no significant difference in PTT on left and right side baselines, but did not investigate, whether pain responses in the PTT or PWA differed between the stimulated and contralateral sides [26]. Therefore, in the current study the PWs were measured on the left side, where the heat-induced pain stimulus was applied, as well as on the contralateral side (right side) to determine whether PTT and PWA changed due to centrally mediated vasoconstriction.

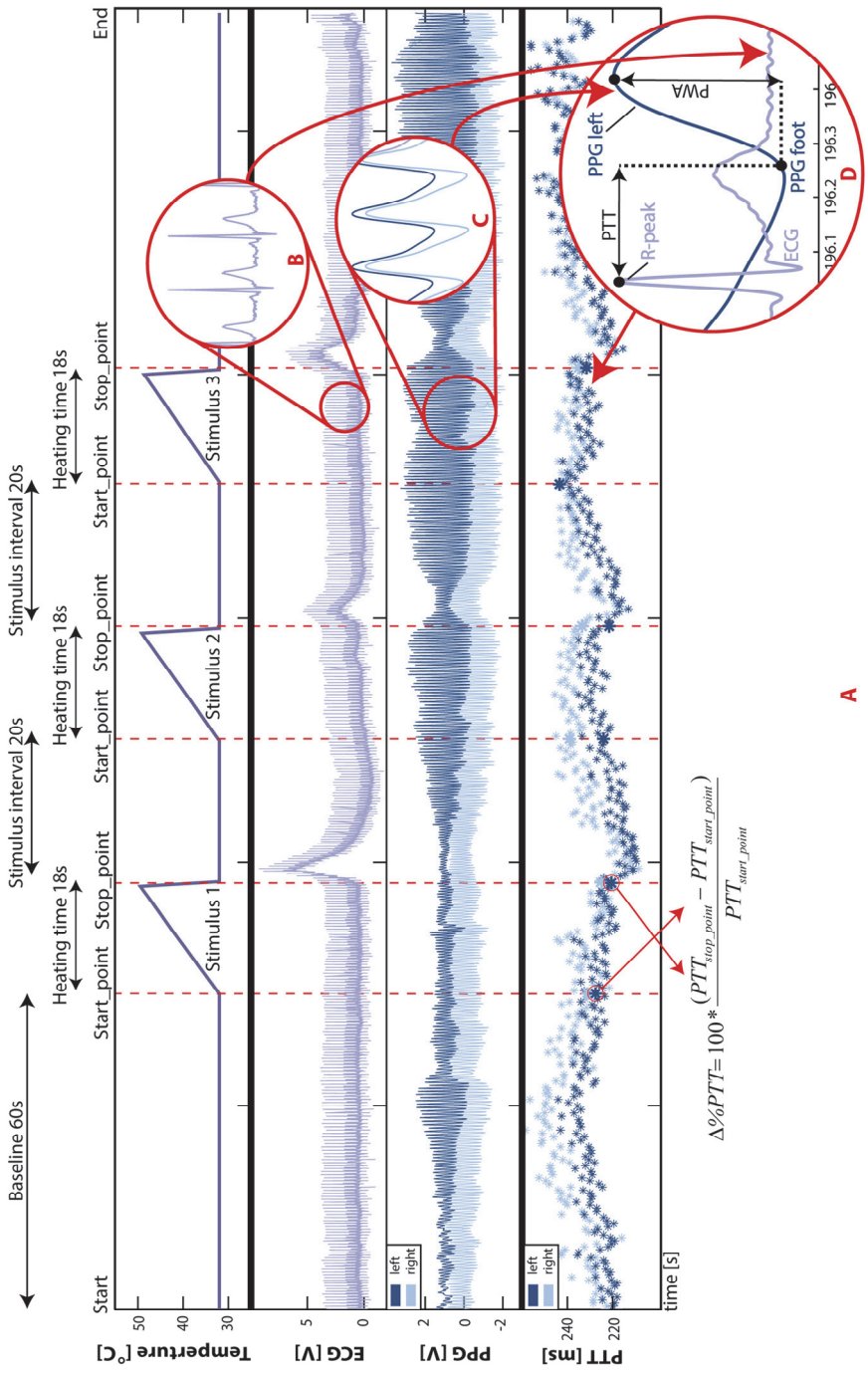

Figure 5.1: Explanation of method and parameters. A = Graphical presentation of the method and Pulse Transit Time (PTT) and Pulse Wave Amplitude (PWA) calculation, B = Electrocardiogram (ECG), C = Photoplethysmography (PPG) and D = Visual presentation of the calculation of the PTT and the PWA.

To check whether the heat stimulus was indeed experienced as painful, the subject was asked to indicate how painful the stimulus was at the maximum temperature by giving an NRS-pain score for the amount of pain experienced. Each subject was told in advance that he/she would receive a painful heat stimulus rising up to 50.0°C. If the stimulus would become too painful, the subject could terminate the heat stimulus by pressing a button with the left foot, therefore causing the temperature to immediately drop to the base temperature of 32.0°C. In order to minimise any potential fear for the pain, the stimulus was applied 3 times.

To determine the influence of the duration of the time-interval between successive heat-induced pain stimuli, the study population was randomized into 2 groups (equal gender distribution) with different time-intervals between the heat stimuli; a time-interval of 20s ('20s') and a time-interval of 60s ('60s'). Because the conditions before and during the first stimulus were identical in both interval groups, an additional dataset was made by combining the '20s' and '60s' groups data for the first stimulus ('All Subjects'-group) for statistical reasons. The randomization was performed by blindly taking a ticket prescribing the time-interval to be used from a closed envelope for each subject.

5.2.3 Pulse wave analysis

The PPG-signals were filtered with a fourth-order low-pass Butterworth filter with a cut-off frequency of 9Hz using Matlab R2010a (The MathWorks, Inc., Matick, MA, USA). The PTT was calculated as the time period between the time instance $t_{ECG\ R\text{-}peak}(n)$ of the occurrence of the R-peak of the ECG and the time instance $t_{PPG\ foot}(n)$ of the arrival of the foot of the PW measured by PPG on the fingertip (Figure 5.1D):

$$PTT\ (n) = t_{PPG_{\ foot}}\ (n) - t_{ECG_{\ R-peak}}\ (n) \tag{5.1}$$

where n is the sequence number of the heartbeats. To find the foot of the PW, the maximum of the second derivative of each PW was taken as PPG_{foot} [26-28]. In some articles the foot of the PW is taken as the minimum value of PPG occurring before the peak [29]. However, in practice, the shape of PWs is often quite irregular, showing multiple local minima before the peak. Therefore, finding the foot of the PW at the maximum of the second derivative proved to be much more robust and less sensitive for noise.

Besides the foot of the PW (PPG_{foot}) there are two other common used reference points: the peak of the PW and the maximum of the first derivative of the PW [20].

The arrival time of the peak of the PW depends on the steepness of the slope of the PW, other than the arrival time of the foot of the PW. Using the peak of the PW, the PTT may change disproportionally if the steepness of the slope or the shape of the PW in general is affected by a change in vascular stiffness. The amplitude of the PW and steepness of the slope are related to age and arterial stiffness, i.e. in young adults the amplitude and steepness of the slope are steeper [30]. In our opinion, PPG_{foot} is the most natural and accurate point to use for measuring the arrival time of the PW as it is least affected by factors that influence the shape of the PW. Therefore, PPG-$_{foot}$ was used as reference for determining the change in PW arrival time during the experiment.

The R-peaks in the ECG were found using an off-the-shelf Matlab function called 'R-peakdetect' [31]. The PWA was determined by subtracting the signal strength difference of PPG_{foot} from the peak of the PW (PPG_{peak}). The PPG_{peak} was found using an off-the-shelf Matlab function called 'Peakdet'([32].

As sensitive PPG-sensors were used, artefact signals sometimes distorted the shapes of the PWs in a way that these PWs were rendered unsuitable for further analysis. Therefore, a '7Step PW-filter' was implemented in the data analysis to filter out any PWs that strongly deviated in shape from an undistorted PW. The '7Step PW-filter' was described in Chapter 2.

Thereafter the pulse waves were selected by a 'to filter out the pulse waves that strongly deviated in shape for a suitable pulse wave analysis.

To find any decrease in PTT due to a heat-induced pain stimulus, the relative difference ($\Delta_{\%}PTT$) between the instantaneous PTT at the last heartbeat before starting ($PTT_{start(i)}$) and the instantaneous PTT at the first heartbeat after ending ($PTT_{stop(i)}$) the I^{th} stimulus was determined:

$$\Delta_{\%}PTT(i) = 100 * \frac{(PTT_{stop(i)} - PTT_{start(i)})}{PTT_{start(i)}} \tag{5.2}$$

A similar calculation was used to determine the relative changes of PWA ($\Delta_{\%}PWA$) and heart rate ($\Delta_{\%}heart\ rate$). Some subjects had a distorted PW at *stop(i)* of some stimuli because they moved or talked. In these cases, the first available, recognisable and undistorted PW before *stop(i)* was used in order not to overestimate any potential effects. Please note that these $\Delta_{\%}$ values do not

represent any variance or variation over time, but are simply the difference between a variable's instantaneous values at *start(i)* and at *stop(i).*

At first analysis the raw data showed a continuing decrease of PTT and PWA after the *stop(i)*, suggesting a prolonged effect of the stimuli beyond *stop(i)*. Therefore, the data were interpolated over time using Matlab function 'Piecewise cubic Hermite interpolation' to compare the data between subjects and analyse whether the PTT and PWA decreased similarly over time in the 20 subjects. The data were mapped on a 0.1s resolution time axis ranging from the *start(i)* of a stimulus to the end of the time-interval after *stop(i).* For each dataset the minimum PTT and PWA after the *stop(i)* and the time of the occurrence of these minima were determined.

5.2.4 Statistical analysis

A linear model Generalized Estimating Equations (GEE) test (Pearson chi-square) was used to test for any effects of the heat-induced pain on PTT, PWA and heart rate. Four factors were considered in the GEE: the time-interval (20s and 60s), the measurement instance (*start(i)* versus *stop(i)*), the measurement side (stimulated and contralateral), and the stimulus number (1 to 3). The analysis was performed using SPSS version 20.0 (SPSS, Inc., Chicago, IL, USA) and Matlab. The significance level adopted was $p<0.05$.

5.3 Results

Twenty subjects were included at random, divided in 2 groups of 10 subjects.

Table 5.1: Characteristics of the study population. There were no statistically significant differences between the groups.

Variable	'20s' Group Mean ± SD	'60s' Group Mean ± SD
Gender [m/f]	5 / 5	5 / 5
Age [years]	28 ± 4	25 ± 5
Weight [kg]	69 ± 13	75 ± 13
Height [m]	1.73 ± 0.09	1.79 ± 0.12
Body mass index [kg/m²]	22.7 ± 3.1	23.3 ± 3.0
Blood pressure [mmHg]		
Systolic	125 ± 13	124 ± 15
Diastolic	78 ± 10	77 ± 12
Heart rate [bpm]	77 ± 15	69 ± 13
Smoker, yes [%]	0 (0)	1 (10)

Table 5.2: Baseline fluctuations. The fluctuation in PTT (Pulse Transit Time), PWA (Pulse Wave Amplitude) and heart rate during the baseline measurements. N=20

Baseline fluctuation	SD (%) Left [Mean ± SD]	SD (%) Right [Mean ± SD]	Pearson Correlation of left and right
PTT	2.71 ± 1.04	2.44 ± 0.81	0.867
PWA	32.76 ± 14.95	29.37 ± 13.78	0.654
heart rate	7.34 ± 2.64		

Table 5.1 presents the characteristic of the groups. The fluctuation of the PTT, PWA, and heart rate during the baseline measurements are listed in table 5.2.

The algorithm used to remove distorted, unusable PWs, filtered out 0.34% (median with Q_1 = 0% and Q_3 = 2.51%) of the PWs. A distorted PW at *stop(i)* was observed in 4 subjects and exclusively in the first stimulus. In the worst case, the PW at the 3rd heartbeat before the *stop(i)* had to be used.

Table 5.3 lists the results of the GEE test. There was a significant effect of the

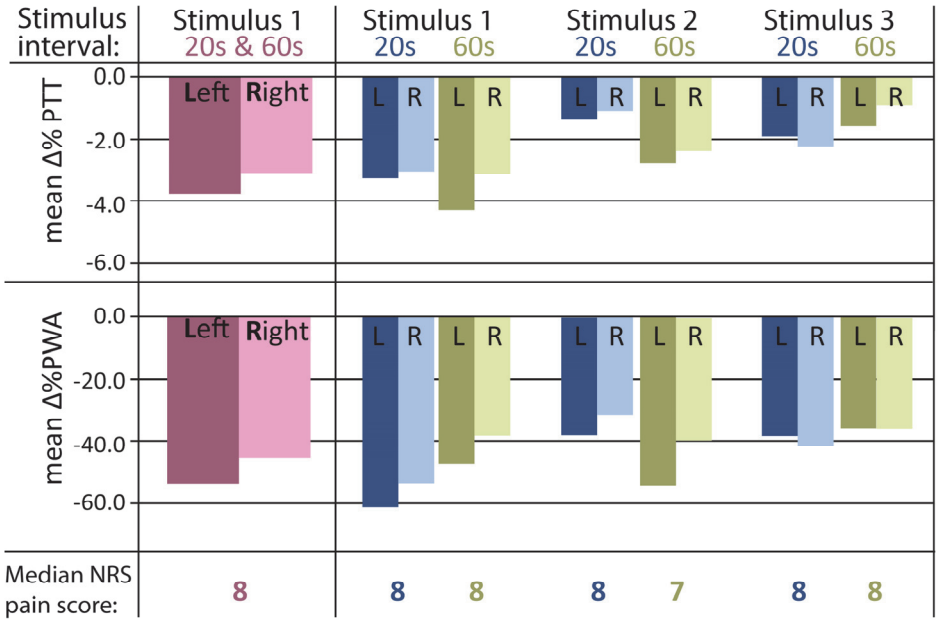

Figure 5.2: The decrease of PTT (Pulse Transit Time) and PWA (Pulse Wave Amplitude) in response to the three heat-induced pain stimuli. The '20s' and '60s' group names correspond with the time-interval between the stimuli. The standard deviations are given in Table 5.4.

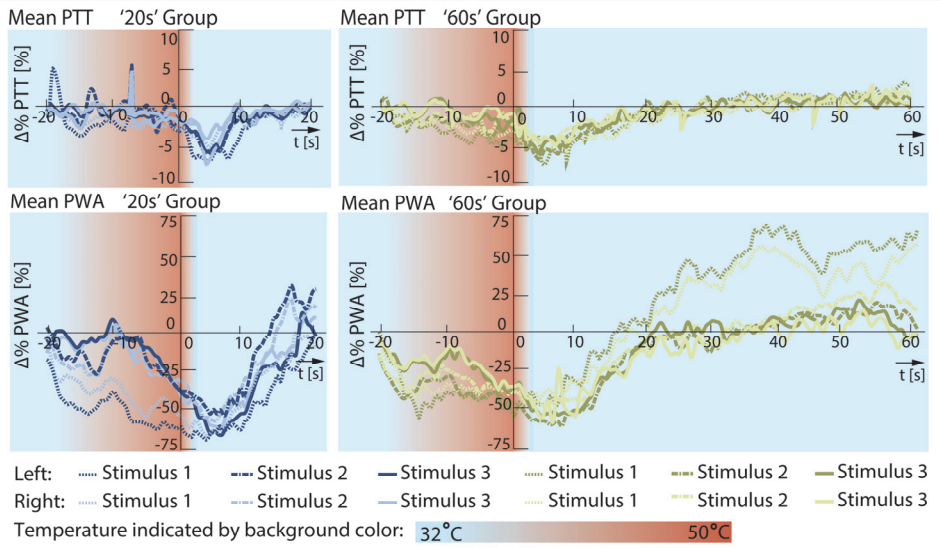

Figure 5.3: Mean PTT ($\Delta_{\%}$PTT) and PWA ($\Delta_{\%}$PWA) during the heat-induced pain stimuli interpolated and mapped onto a time axis. The mean PTT (Pulse Transit Time) and PWA (Pulse Wave Amplitude) for each heat-induced pain stimulus, for the left and right side. Shown from the start(i) of each stimulus to the start(i) of the next stimulus or till the end of the measurement in case of stimulus 3 data. One may notice that the time delays presented in Table 5.5 do not seem to correspond with the minima shown in Figure 5.3. However, the time delays in Table 5.5 are means of the individuals time delays whereas the minimum in a line in Figure 5.3 is a minimum of the mean of all data.

measurement instance for all of the measured physiological responses, indicating that the values at *stop(i)* differed significantly from those at *start(i).* There was no significant effect of the time-interval, of the stimulus number, or the measurement side for any of the measured physiological responses.

The algorithm used to remove distorted, unusable PWs, filtered out 0.34% (median with Q_1 = 0% and Q_3 = 2.51%) of the PWs. A distorted PW at

Table 5.3: The Generalized Estimating Equations Test of Model Effects. PTT=Pulse Transit Time, PWA=Pulse Wave Amplitude. The $\Delta_{\%}$ changes for PTT, PWA and heart rate were used for the GEE model. Bold type p-values indicate statistically significant effects.

	$\Delta_{\%}$PTT ***p*-value**	**$\Delta_{\%}$PWA** ***p*-value**	**$\Delta_{\%}$heart rate** ***p*-value**
Time-interval	0.717	0.815	0.835
Measurement side	0.717	0.105	
start(i)* versus *stop(i)	**0.000**	**0.000**	**0.001**
Stimulus number	0.065	0.306	0.154

stop(i) was observed in 4 subjects and exclusively in the first stimulus. In the worst case, the PW at the 3rd heartbeat before the *stop(i)* had to be used.

Table 5.3 lists the results of the GEE test. There was a significant effect of the measurement instance for all of the measured physiological responses, indicating that the values at *stop(i)* differed significantly from those at *start(i).* There was no significant effect of the time-interval, of the stimulus number, or the measurement side for any of the measured physiological responses.

Table 5.4 and Figure 5.2 show the $\Delta_{\%}$PTT, $\Delta_{\%}$PWA, $\Delta_{\%}$heart rate and NRS-pain score for each stim ulus. The data of the third stimulus for one subject (in '60s' group) were lost due to technical reasons and could not be analysed.

All three stimuli were scored as equally painful within each subject. The stimuli were stopped by the subjects four times prior to reaching 50.0°C: by two subjects during the first stimulus at 49.3°C (NRS-score 7) and 49.7°C (NRS-score 8), respectively, and by one subject during the first and second stimulus at 49.4°C (NRS-score 9) and 49.3°C (NRS-score 9), respectively. Whenever the stimulus was stopped before reaching 50.0°C, vasoconstriction was still observed during the heat-induced pain stimuli as a reduced PWA.

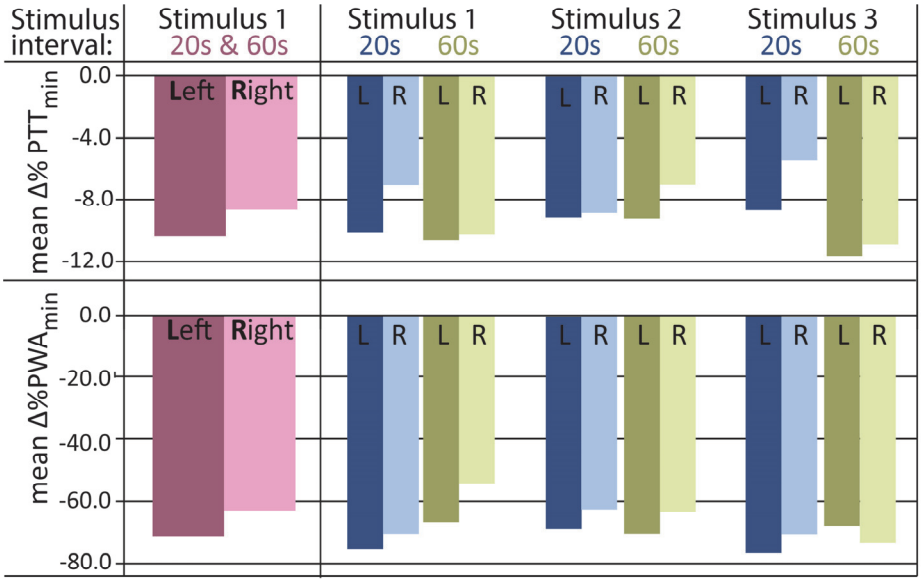

Figure 5.4: The maximum decrease of PTT (Pulse Transit Time) and PWA (Pulse Wave Amplitude) in response to the three heat-induced pain stimuli. The '20s' and '60s' group names correspond with the time-interval between the stimuli. The standard deviations are given in Table 5.5.

Table 5.4: The changes after heat-induced pain stimuli for PTT, PWA and heart rate. Left is the stimulated side and right is the contralateral side. PTT = Pulse Transit Time, PWV = Pulse Wave Amplitude, N = number of subjects. IQR = interquartile range. Stimuli 2 and 3 for the '20s'group should not be considered representative due to possible residual effects of the preceding stimuli 1 and 2, respectively.

			Stimulus 1			Stimulus 2		Stimulus 3	
			'All subjects' (N=20)	'20s' Group (N=10)	'60s' Group (N=10)	'20s' Group (N=10)	'60s' Group (N=10)	'20s' Group (N=10)	'60s' Group (N=9)
Left	$\Delta_{\%}$PTT	Average [%]	-3.8	-3.3	-4.3	-1.3	-2.8	-1.9	-1.6
		SD [%]	5.0	5.2	4.9	8.7	3.4	4.3	4.3
	$\Delta_{\%}$PWA	Average [%]	-54.1	-61.1	-47.1	-37.6	-54.7	-38.5	-36.0
		SD [%]	33.5	20.0	43.3	30.3	12.7	47.7	39.1
Right	$\Delta_{\%}$PTT	Average [%]	-3.1	-3.1	-3.2	-1.1	-2.4	-2.2	-0.9
		SD [%]	3.4	3.4	3.7	2.0	3.9	2.2	1.9
	$\Delta_{\%}$PWA	Average [%]	-45.8	-53.4	-38.2	-31.5	-39.2	-41.4	-35.6
		SD [%]	36.0	31.1	40.6	22.2	26.1	37.0	30.6
$\Delta_{\%}$heart rate		Average [%]	13.9	13.9	13.8	9.2	8.7	4.6	9.2
		SD [%]	17.4	20.2	15.2	19.3	10.4	17.8	12.0
Pain score stimuli		Median	8	8	8	8	7	8	8
		[IQR]	1	3	1	3	2	3	2

Table 5.5: Minimum PTT and PWA and their times of occurrence. Measured PWA and their corresponding times for the maximum decrease after the stimuli. Left is the stimulated side and right is the contralateral side. PTT_{min}=Pulse Transit Time at maximum decrease after stop(i), PWA_{min}=PulseWave Amplitude at maximum decrease after stop(i), i = number of stimuli. N=number of subjects. Stimuli 2 and 3 for the '20s'group should not be considered representative due to possible residua effects of the preceding stimuli 1 and 2, respectively.

			Stimulus 1			Stimulus 2		Stimulus 3	
			'All subjects' (N=20)	'20s' Group (N=10)	'60s' Group (N=10)	'20s' Group (N=10)	'60s' Group (N=10)	'20s' Group (N=10)	'60s' Group (N=9)
Left	$\Delta_{\%}PTT_{min}$	Average [%]	-10.4	-10.2	-10.6	-9.1	-9.2	-8.7	-11.7
		SD [%]	4.9	3.7	6.2	3.7	3.2	3.0	8.7
	Time delay	Average [s]	9.1	5.7	12.5	6.9	12.2	6.3	11.0
		SD [s]	10.2	2.4	13.7	4.4	10.3	3.1	13.5
	$\Delta_{\%}PWA_{min}$	Average [%]	-71.3	-75.6	-67.0	-69.1	-70.7	-76.8	-67.9
		SD [%]	22.7	15.7	28.4	22.9	15.1	17.2	32.45
	Time delay	Average [s]	5.2	5.1	5.4	5.0	8.5	5.4	8.4
		SD [s]	3.2	3.6	2.9	2.8	9.4	4.0	7.3
Right	$\Delta_{\%}PTT_{min}$	Average [%]	-8.6	-7.0	-10.2	-8.9	-7.00	-5.5	-10.9
		SD [%]	4.5	2.8	5.5	11.4	3.2	2.8	8.1
	Time delay	Average [s]	9.4	7.7	11.1	5.8	11.6	5.5	11.0
		SD [s]	10.9	5.7	14.5	3,3	12.1	3.0	13.5
	$\Delta_{\%}PWA_{min}$	Average [%]	-62.7	-71.0	-54.4	-63.0	-63.6	-70.6	-73.7
		SD [%]	31,5	25.9	35.7	19.1	29.6	18.0	21.7
	Time delay	Average [s]	6.3	5.5	7.1	4.8	16.5	6.3	18.2
		SD [s]	4.2	4.4	4.0	2.2	14.3	4.1	20.2

The data consistently showed that PTT and PWA continued to decrease after the *stop(i)* (Figure 5.1 shows a typical example). Figure 5.3 shows the time-interpolated PTT-data and PWA-data. It was noticed that the PTT and PWA generally had not returned to the baseline or a new stable value within 20s after the *stop(i)*. The values for the minimum PTT and PWA ($\Delta_{\%}PTT_{min}$ and $\Delta_{\%}PWA_{min}$) after the *stop(i)* and their corresponding instances of occurrence are listed in Table 5.5 and show in Figure 5.4.

5.4 Discussion

This study is the first to demonstrate a decrease of PTT and PWA in response to heat-induced pain stimuli in healthy volunteers, who experienced equal pain scores in all stimuli. The effect on PTT is small but significant immediately after a stimulus and increases largely within several seconds after the stimulus. The effect on PTT may be different when another kind of pain stimulus is induced, such as pinprick or compression and therefore should be studied and compared to heat-pain. The data showed no significant effect of the measurement side on the PTT or PWA change due to heat-induced pain stimuli, suggesting that the PTT and PWA responses are centrally mediated. This suggests that the PTT and PWA are reliable parameters of pain-induced alterations of vasotonus and can be measured on a contralateral extremity in situations in which it is impossible or undesirable to measure directly on the affected extremity. Such measurement side independency of PTT and PWA has been demonstrated for baseline measurements as well [26]. The data showed no significant effect of the stimulus number on PTT, PWA or heart rate. This agrees with the consistently equal NRS-pain scores, which further suggest that no habituation or adaptation occurred to the pain stimuli during the successive measurements. The decrease of the PTT and PWA suggests these parameters potentially can be used as objective indicators of pain beside the gold standard self-report, or when the self-report is impossible.

For calculating the change in PTT, PWA and heart rate before and after the stimuli, it was decided to calculate these changes over the first single values before and after the stimuli instead of averaging several values before and after the stimuli. A drawback of this simple approach might be that the calculated changes may be easily affected by stochastic variations, requiring larger sample sizes. However, because the data consistently showed that PTT and PWA continued to decrease after the *stop(i),* the chance of inadvertently suggesting too large effects by averaging several values before and after the stimulus would have been

considerable. Nevertheless, even when using the chosen, simple calculation, a significant effect of heat-induced pain stimuli on PTT, PWA and heart rate was still detected. However, the chosen approach might also be a reason why the effect is rather small for PTT directly at the *stop(i).* When including measuring points till a few seconds after *stop(i)* the change in PTT can reach up to 10.4%. For the same reasons, i.e. to prevent inadvertently overestimating any effect of the stimuli due to a distorted PW at *stop(i),* it was decided to use the first available, recognisable and undistorted PW before the *stop(i)* as opposed to after the *stop(i)*.

Few studies show that PTT reflects blood pressure quite well [19, 33]. As PTT is related to blood pressure and other factor, such as cardiac output, it might have been beneficial to measure blood pressure and/or cardiac output simultaneously with PTT. However, blood pressure and cardiac output were assumed to be kept constant due to the quiet and stable conditions in which the subjects were during the measurements. Furthermore, simultaneous measurement of blood pressure and cardiac output was not pragmatic as the required sensors would have affected the PPG measurements. Additionally, in this study, the point of interest specifically was whether the change in vasoconstriction during heat induced pain stimuli can be detected. PTT and PWA were measured, as these parameters are straightforward measures of vasoconstriction and thus the arterial stiffness. Furthermore, PTT and PWA are widely used in clinical practice and can be easily measured continuously during interventions. In this study, a continuous measure that may be related to pain was found.

In the '60s' group PTT, PWA and heart rate returned to the baseline, or a new stable value, within about 40s after the *stop(i)*. This return to the (new) baseline was incomplete in the '20s' group. Therefore, it was concluded that even through the GEE showed no effect of the stimulus number, the responses measured for stimuli 2 and 3 in the '20s' group should not be considered to be representative as these could also include a partial effect of preceding stimuli. If the time-interval is chosen too short, the effects on the measured physiological parameters may diminish, which may specifically occur when there already was a maximal response of the vessels. In order to exclude any effects of earlier stimuli, using a time-interval of at least about 40s is advised.

As the heart rate significantly increased together with PTT, the results are inconclusive whether the $\Delta_{\%}$PTT was caused only by a change of PW propagation-time through the vessel or (also) by a changed PEP. It would be worthwhile to measure PEP using cardiothoracic impedance or echocardiography

[34, 35]. An decreased PEP could indicate stress and if stress occurred during the measurements it would be difficult to distinguish whether the $\Delta_{\%}$PTT and $\Delta_{\%}$PWA were caused by the actual pain stimuli or by the stress caused by anticipation on the pain stimuli. However, the fear for pain was limited in this study by clearly and carefully explaining the experiment to the subjects. Furthermore, the subjects sat in a comfortable position under tranquil conditions. So the stimuli are unlikely to have caused anxiety due to sudden application beyond control of the subjects. The temperature of the thermode block rose very slowly. For each stimulus it took 18s for the temperature to rise from 32.0 to 50.0°C and the subjects could stop the heat-induced pain stimuli at any desired moment. Therefore, it is expected that the measured effects were not caused by any anticipation stress but by the subjects' reactions on the actual pain stimuli. To distinguish the vasoconstriction-reactions due to pain from reactions due to stress, metrics like the bispectral index or blood pressure could be used [36, 37]. An approach to assess the effect of stress during a stimulus could be to apply a placebo stimulus, during which the same procedure as during the real stimulus will be performed, but without heating the thermode block.

PPG signals are influenced by and are highly dependent on heart rate, arteriosclerosis, use of anaesthetics and neurological diseases [38]. Hence, the usability of the absolute values of PTT and PWA in patients are at best questionable. The main reason is that the vessel compliance plays a major role in the change of PTT and PWA development. For this reason the *relative* change in PTT and PWA was used. To exclude the influence of some of the abovementioned factors, for this study only young healthy volunteers were included. However, factors like gender, age and Quetelet index are important determinants of the compliance, and thus of PTT and PWA [39]. Additionally, physiological responses may depend on the type of pain stimulus applied. As this study focussed on heat-induced pain in young, healthy adults, it remains unclear whether the results may be generalised for all populations and all types of pain stimuli.

The utilized PPG-sensors were quite sensitive for motion and positioning disturbances. This sensitivity to disturbances poses a potential limitation on the usability. Although the algorithm used to eliminate distorted PWs functioned well, the availability of a more robust PPG-sensor would greatly benefit measuring PWs in awake and moving patients. Obviously, this is less relevant when measuring PWs in patients under general anesthesia.

Having a heat-induced pain stimulus with a fixed NRS-pain score was preferred over a stimulus with a constant end temperature. However, our pilot study showed a high variation of end temperatures when the volunteers were asked to end the heat-induced pain stimulus when pain started to occur (range 37.2°C – 50.0°C). Therefore, a fixed end temperature of 50°C was chosen for this study. The results show that the median NRS-pain score of all the stimuli at the *stop(i)* of heat-induced pain stimuli was 8 with an interquartile range of 2. This indicates that pain was present and that it was experienced as similarly painful by all subjects at 50°C. Never the less, the study outcome was not the level of pain, but the possibility to measure pain in an objective way.

Surprisingly, the decrease of the PTT and PWA consistently continued for a about 9.4s and 6.2s, respectively, after each *stop(i)*. These delayed PTT and PWA responses could partly be caused by the method used to apply the pain stimuli. Therefore, we investigated the course of the skin temperature in time with a thermography camera (ThermaCAM SC2000; FLIR Systems, Berchem, Belgium) after applying a heat-induced pain stimulus and quickly removing the thermode block. The thermode block temperature was 50.0°C when the stimulation stopped, while the skin temperature under the thermode block was 47.7°C. Due to this few degrees temperature difference between the thermode block and the skin there will be some residual heating of the skin during up to the first 0.3s of the rapid cooling of the thermode block. Only as soon as the thermode block is colder than the skin, the skin will be actively cooled down. However, since the measured delays in PTT and PWA responses were much larger, it is unlikely that these delays were caused entirely by the residual temperature difference between the thermode block and the skin. Therefore, the delayed response may more likely be caused by residual heat present in the skin. The discharge of residual heat after a stimulus is limited by the vasoconstriction still present due the same heat, which could contribute to the persistence of the physiological responses to the heat-induced pain stimuli after the *stop(i)*.

5.5 Conclusion

The results of this study suggest that PTT and PWA decrease centrally in response to heat-induced pain stimuli. PTT and PWA can be measured non-invasively and objectively by using standard ECG and PPG equipment generally available in hospitals. To limit cross-dependencies, time-intervals between successive stimuli should exceed 40s. Further research is required to investigate whether and how

the relation between pain (levels) and PTT and PWA responses can be quantified. A preferred next step is to adapt commonly used ECG/PPG monitors to also show PTT and PWA. This could make PTT and PWA widely available, objective indicators of pain, either beside the gold standard self-report, or when the self-report is impossible.

5.6 Acknowledgments

The authors thank Prof. dr. ir. H. Boersma for his expert statistical help.

5.7 References

1. Merskey, H. and N. Bogduk, Classification of Chronic Pain, Second Edition, IASP Task Force on Taxonomy. 1994, Seattle: IASP Press.
2. Price, D.D., et al., A comparison of pain measurement characteristics of mechanical visual analogue and simple numerical rating scales. Pain, 1994. 56(2): p. 217-226.
3. Price, D.D., et al., The validation of visual analogue scales as ratio scale measures for chronic and experimental pain. Pain, 1983. 17(1): p. 45-56.
4. Oberlander, T. and J.P. Saul, Methodological considerations for the use of heart rate variability as a measure of pain reactivity in vulnerable infants. Clin Perinatol, 2002. 29(3): p. 427-443.
5. Valkenburg, A.J., et al., Skin conductance peaks could result from changes in vital parameters unrelated to pain. Pediatric Research, 2012. 71(4): p. 375-379.
6. Hamunen, K., et al., Effect of pain on autonomic nervous system indices derived from photoplethysmography in healthy volunteers. Br. J. Anaesth, 2012. 108(5): p. 838-844.
7. Grönroos, M., H. Naukkarinen, and A. Pertovaara, Capsaicin-induced central facilitation of a sympathetic vasoconstrictor response to painful stimulation in humans. Neuroscience Letters, 1994. 182(2): p. 163-166.
8. Gunnar Wallin, B., Neural control of human skin blood flow. Journal of the Autonomic Nervous System, 1990. 30(SUPPL.): p. S185-S190.
9. O'Rourke, M.F., et al., Clinical applications of arterial stiffness; definitions and reference values. Am J Hypertens, 2002. 15(5): p. 426-444.
10. Lehmann, E.D., K.D. Hopkins, and R.G. Gosling, Aortic compliance measurements using Doppler ultrasound: In vivo biochemical correlates. Ultrasound med biol, 1993. 19(9): p. 683-710.
11. Lopez-Beltran, E.A., et al., Non-invasive studies of peripheral vascular compliance using a non-occluding photoplethysmographic method. Med Biol Eng Comput, 1998. 36(6): p. 748-53.
12. Allen, J., Photoplethysmography and its application in clinical physiological measurement. Physiol Meas, 2007. 28(3): p. R1-39.

13. Nitzan, M., B. Khanokh, and Y. Slovik, The difference in pulse transit time to the toe and finger measured by photoplethysmography. Physiol Meas, 2002. 23(1): p. 85-93.
14. Weinman, J. and D. Sapoznikov, Equipment for continuous measurements of pulse wave velocities. Med Biol Eng Comput, 1971. 9(2): p. 125-138.
15. Nichols, W.W., et al., Effects of arterial stiffness, pulse wave velocity, and wave reflections on the central aortic pressure waveform. Journal of Clinical Hypertension, 2008. 10(4): p. 295-303.
16. Bramwell, J.C. and A.V. Hill, *Velocity of transmission of the pulse-wave. And elasticity of arteries*. Lancet, 1922. 199(5149): p. 891-892.
17. Pitson, D.J., et al., Use of pulse transit time as a measure of inspiratory effort in patients with obstructive sleep apnoea. European Respiratory Journal, 1995. 8(10): p. 1669-1674.
18. Maltz, J.S. and T.F. Budinger, Evaluation of arterial endothelial function using transit times of artificially induced pulses. Physiological Measurement, 2005. 26(3): p. 293-307.
19. Geddes, L.A., M.H. Voelz, and C.F. Babbs, Pulse transit time as an indicator of arterial blood pressure. Psychophysiology, 1981. 18(1): p. 71-74.
20. Xin-Yu, Z. and Z. Yuan-Ting, The effect of local mild cold exposure on pulse transit time. Physiol Meas, 2006. 27(7): p. 649.
21. Bergersen, T.K., M. Eriksen, and L. Walloe, Effect of local warming on hand and finger artery blood velocities. Am J Physiol-Reg I, 1995. 26(2 38-2): p. R325-R330.
22. Hirata, K., et al., Local thermal sensation and finger vasoconstriction in the locally heated hand. Eur J Appl Physiol, 1988. 58(1-2): p. 92-6.
23. Weissler, A.M., W.S. Harris, and C.D. Schoenfeld, Systolic time intervals in heart failure in man. Circulation, 1968. 37(2): p. 149-159.
24. Newlin, D.B. and R.W. Levenson, Pre-ejection period: Measuring beta-adrenergic influences upon the heart. Psychophysiology, 1979. 16(6): p. 546-553.
25. Defrin, R., et al., Sensory determinants of thermal pain. Brain, 2002. 125(Pt 3): p. 501-10.
26. Kortekaas, M.C., et al., Comparison of bilateral pulse arrival time before and after induced vasodilation by axillary block. Physiol Meas, 2012. 33(12): p. 1993-2002.
27. Kortekaas, M.C., et al., Pulse transit time as a quick predictor of a successful axillary brachial plexus block. Acta Anaesthesiol Scand, 2012. 56(10): p. 1228-1233.
28. Teng, X.F. and Y.T. Zhang, The effect of applied sensor contact force on pulse transit time. Physiological Measurement, 2006. 27(8): p. 675-684.
29. Allen, J., et al., A prospective comparison of bilateral photoplethysmography versus the ankle-brachial pressure index for detecting and quantifying lower limb peripheral arterial disease. J Vasc Surg, 2008. 47(4): p. 794-802.

30. Zahedi, E., et al., Analysis of the effect of ageing on rising edge characteristics of the photoplethysmogram using a modified windkessel model. Cardiovascular Engineering, 2007. 7(4): p. 172-181.
31. Clifford, G.D., Rpeakdetect function (ECG toolbox). 2008.
32. Billauer, E., Peakdet. 2012, E. Billauer: http://billauer.co.il/peakdet.html. p. Detect peaks in a vector.
33. Naschitz, J.E., et al., Pulse transit time by r-wave-gated infrared photoplethysmography: Review of the literature and personal experience. Journal of Clinical Monitoring and Computing, 2004. 18(5-6): p. 333-342.
34. Paiva, R.P., et al., Assessing PEP and LVET from heart sounds: algorithms and evaluation. Conference proceedings : Annual International Conference of the IEEE Engineering in Medicine and Biology Society IEEE Engineering in Medicine and Biology Society Conference, 2009. 2009: p. 3129-3133.
35. Chan, G.S.H., et al., Change in pulse transit time and pre-ejection period during head-up tilt-induced progressive central hypovolaemia. J Clin Monitor Comp, 2007. 21(5): p. 283-293.
36. Sigl, J.C. and N.G. Chamoun, An introduction to bispectral analysis for the electroencephalogram. J Clin Monitor Comp, 1994. 10(6): p. 392-404.
37. Hjortskov, N., C. Hye-Knudsen, and N. Fallentin, Lumbar position sense acuity during an electrical shock stressor. BMC Musculoskeletal Disorders, 2005. 6.
38. Elgendi, M., On the analysis of fingertip photoplethysmogram signals. Current Cardiology Reviews, 2012. 8(1): p. 14-25.
39. Allen, J. and A. Murray, Age-related changes in the characteristics of the photoplethysmographic pulse shape at various body sites. Physiol Meas, 2003. 24(2): p. 297-307.

Development & Validation

Part II

Chapter 6

Design and functional testing of a novel blood pulse wave velocity sensor

Marit H.N. van Velzen & Arjo J. Loeve, Egbert G. Mik, Sjoerd P. Niehof

Journal of Medical Devices, October 2017

The Multi Photodiode Array (MPA) is a novel transmission photoplethysmography sensor to measure pulse wave velocity (PWV) in the finger. To validate the MPA a setup was built to generate a red laser dot traveling over the MPA with known and constant scanning velocities. These scanning velocities were chosen to include speeds at least twice as high as those found in the normal range of PWV in healthy populations, and were set at 12.9, 25.8, 36.0 or 46.7 m/s. The aim of this study was to verify the functionality of the MPA: performing local non-invasive PWV measurements. To illustrate the applicability of the MPA in clinical practice, an in vivo pilot study was conducted using the flow mediated dilation technique. The in vitro accuracy of the MPA was ± 0.2%, 0.3%, 0.5% and 0.6% at the applied scanning velocities. The MPA can measure PWVs with a maximum deviation of 3.0%. The in vivo pilot study showed a PWV before the flow mediated dilation of 1.1 ± 0.2 m/s. These results suggest that this novel MPA can reliably and accurately measure PWV within clinically relevant ranges and even well beyond.

6.1 Introduction

Globally, cardiovascular diseases (CVDs) are the number one cause of death. Smoking, unhealthy diet, physical inactivity and excessive use of alcohol are the most important behavioural risk factors for CVDs. As an effect, individuals may develop hypertension, diabetes, heart failure or atherosclerosis, most of which are related to a change in arterial stiffness. Arterial stiffness is most commonly used to express the viscoelastic property of the arterial wall, which is expressed the relationship between change in pressure and change in volume[1]. Therefore, arterial stiffness, or its inverse the arterial compliance, is a reliable prognostic indicator of cardiovascular morbidity and mortality in the adult population [2-4]. The effect of increased arterial stiffness is a decreased propagation time of pressure pulse waves (PWs) through the vessels and thus an increase of the pulse wave velocity (PWV) [5, 6]. The arterial stiffness of a blood vessel is important because the elastic wall of the arteries attenuate the systolic pressure wave of each heartbeat. The potential energy stored in the vessel walls is used to continue to propel the blood during the diastole between successive heartbeats [1].

To determine arterial stiffness, the gold standard is to measure the PWV, because the speed with which the PWs travel through the blood is directly related to the incremental elastic modulus $E_{inc,}$ vessel wall thickness h_{vessel} and vessel radius r_{vessel} by the Moens-Korteweg equation (with ρ_{blood} the density of blood) [7]:

$$PWV = \sqrt{\frac{E_{inc} \cdot h}{2r \cdot \rho}} \tag{6.1}$$

The PWV is measured as an average speed of a PW between two locations on the body. Note that the PWV is not the speed of blood, but the speed of the pressure pulse traveling through the moving blood (comparable to a sound wave). The PWV can be measured both invasively and non-invasively and is highly reproducible [8]. In clinical practice, the PWV is generally determined as an average velocity over the carotid-femoral trajectory or the brachial-ankle trajectory. Depending on age, in healthy subjects the PWV is about 6-10 m/s over the carotid-femoral trajectory. In cardiovascular risk patients the PWV can be as high as 20 m/s over the same trajectory [6, 9, 10], so two to three times as high as in healthy subjects.

Several non-invasive techniques to measure PWV are clinically available, e.g. Doppler ultrasound [11], tonometric (SphygmoCor), oscillometric (Arteriograph)

and piezoelectronic (Complior) techniques [12]. To the best of our knowledge, only one group has reported on relatively peripheral PWV, providing the average PWV over the trajectory between the wrist and finger [13], using the Hall-effect and photoplethysmography (PPG) The drawback of these methods is that they require two separate devices. Limitations of these techniques include the difficulty of accurately placing the sensors, and the discrepancy between the distance between the sensors and the actual path length traveled by the PW. Moreover, these methods are not always comfortable for the patient, e.g., the use of the blood-pressure cuff arteriography technique is inconvenient. Furthermore, Doppler ultrasound requires an experienced operator to conduct the measurements. Clinical practice would benefit from a device that can reliably measure the PWV over a short, accurately known distance, using a simple technique that is already familiar to clinicians. The measurement preferably should not require an experienced operator, should allow continuous monitoring, should not cause the patient discomfort and should potentially be easily added to available clinical monitoring systems.

We designed a device, further called the Multi Photodiode Array (MPA), for peripheral, non-invasive PWV measurements along a trajectory of 12.0 mm, without having the drawbacks of the currently available alternatives. The MPA will guide enable comfortable measurements with a single, simple device without requiring highly trained operators.

The working principle of the MPA is based on photoplethysmography (PPG). A widely used non-invasive optical technique, to measure volumetric expansion and contraction of vessels (Figure 6.1) [14].

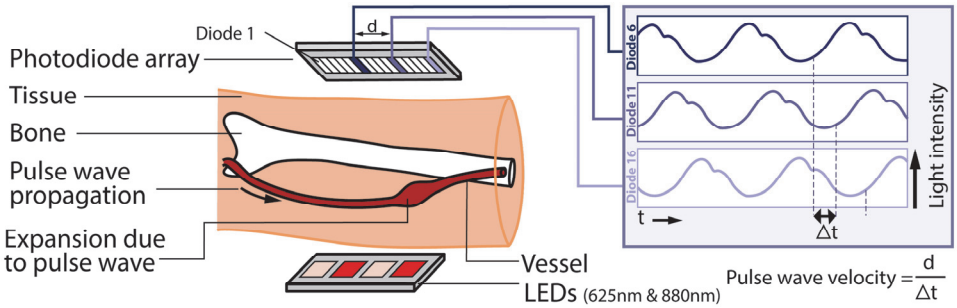

Figure 6.1. Schematic overview of the multi photodiode array (MPA) and calculation of the pulse wave velocity.

The maximum volumetric expansion at any point along a vessel occurs when the peak of a PW passes that point. Thus, the peripheral PWV can be calculated using the time differences between the detection of the PW peaks at successive points along the vessel spaced a known distance apart. It is not yet known to what extent this peripheral PWV measured in, for example, a finger correlates with PWVs elsewhere in the vascular system. However, to investigate this, it should first be validated whether the MPA can be used to properly measure peripheral PWV. If this proves to be feasible and if there is good correlation with conventional measuring techniques, using the MPA for determining the PWV would open the road to fast and simple PWV-based diagnostics that do not put any burden on patients. Furthermore, with some small alterations of the design, the MPA could also be used for reflective measurements, making it suitable for non-invasive measurement of PWVs for, e.g., the carotid arteries. The aim of this study was to verify the functionality of the MPA. More specifically, to determine whether the MPA accurately measures the velocity of light pulses traveling over it.

6.2 Materials and methods

6.2.1 Multi Photodiode Array

The MPA is a transmission PPG-sensor for measuring the PWV, for example, in the finger by measuring light transmission at multiple points along a short trajectory. The PPG-sensor element is a Si PIN S8558 photodiode array (Hamamatsu Photonics, Hamamatsu, Japan) with 16 high-sensitivity photodiodes, with a peak sensitivity wavelength of 960 nm, positioned in a single row. Each photodiode has an active area of 0.7 x 2.0 mm. An array with more than 2 photodiodes was chosen because this enabled assessing which combination of the number of photodiodes and the distances between them would provide the most accurate PWV measurements. The array of 16 photodiodes was chosen rather arbitrarily because of its availability and because it enabled achieving the study goals. The light source of the MPA consists of two red (620 nm) and two infrared LEDs (880 nm). These two wavelengths are known to provide very good signal transmission through the finger and to the photodiode array [15]. All 16 analogue signals from the photodiode array are converted to digital signals through a NI-USB 6229 Multifunction Data Acquisition system and LabVIEW 2010 software (both: National Instruments, Austin, TX, USA). The data acquisition-system has a 250 kHz sampling rate and 32 analog, 16-bit input channels.

Figure 6.2: Overview of the validation setup. A long exposure was used to visualize the motion cycle of the laser beam, MPA= multi photodiode array.

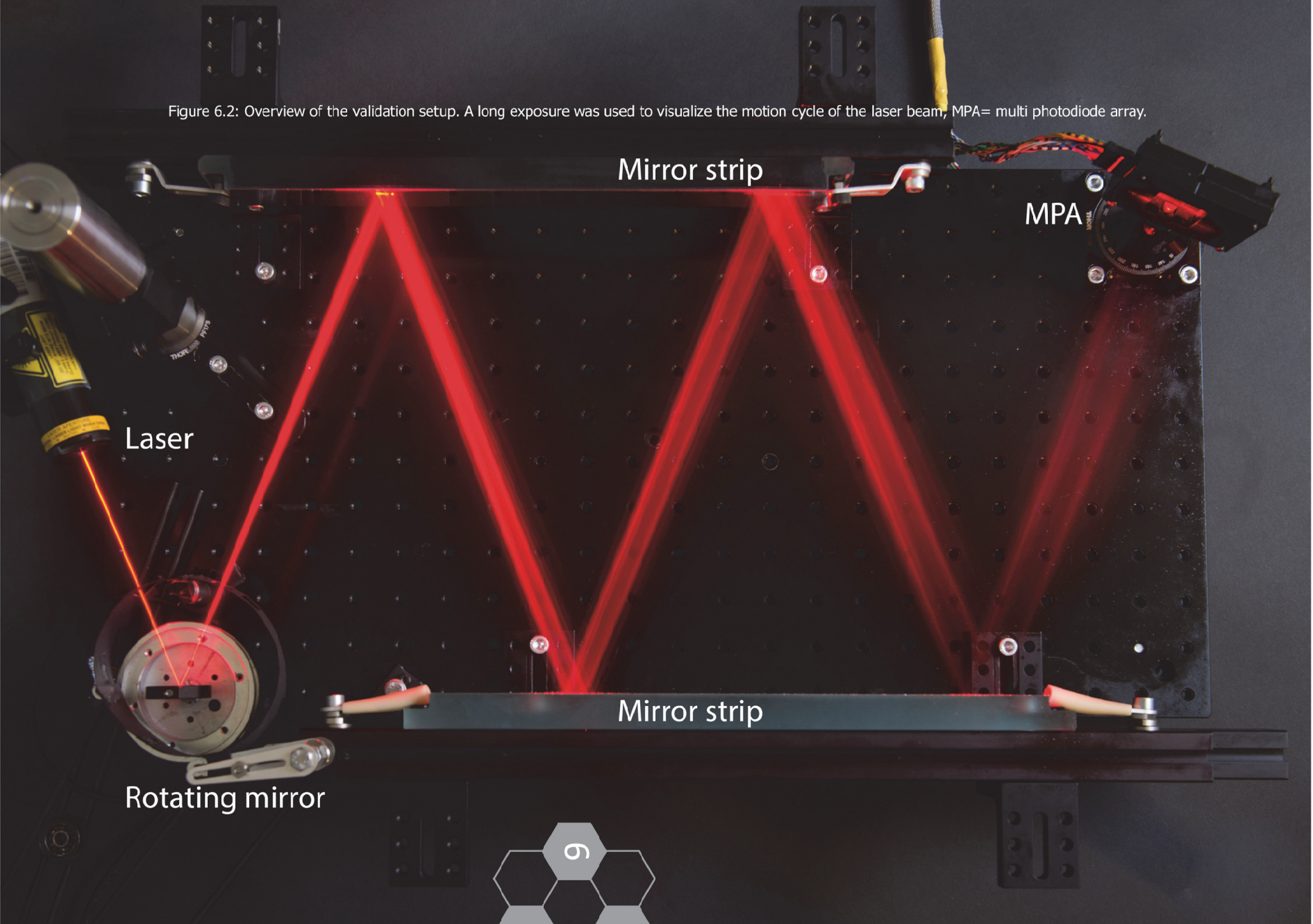

6.2.2 Validation setup and protocol

To functionally validate the MPA a setup (Figure 6.2) was built in which a laser dot periodically scanned over the MPA with a known and constant scanning velocity. A linearly polarized laboratory Helium Neon Laser with a power of 0.5 mW (25-LHP-213, Melles Griot, Carlsbad, CA, USA) provided a continuous 632.8 nm wavelength red laser light dot with a 0.46 mm beam diameter ($1/e^2$). This laser was chosen for its wavelength, as it resembles the spectrum transmission through the finger when using commercial PPG sensors. The laser dot was made to scan over the MPA using a rotating mirror, which was actuated using a stepper motor to deliver various velocities of the light dot scanning over the MPA.

Four different scanning velocities were used with 24 scans (24 full mirror rotations) for each scanning velocity. These scanning velocities were chosen to include speeds over twice as high as the normal range of PWVs found in healthy populations over the carotid-femoral trajectory to ensure including values that can be expected when measuring locally on the carotid artery and to explore the full potential of the MPA, and were chosen to be 12.9, 25.8, 36.0 or 46.7 m/s. These scanning velocities were pre-set by setting the motor actuating the mirror to a matching rotational speed Ω using the relation:

$$\Omega = \frac{v_{set}}{2\pi \cdot r_{path}} \tag{6.2}$$

where v_{set} is the desired scanning velocity and r_{path} is the distance between the mirror center and the MPA (Figure 6.3). In order to achieve a constant scanning velocity over the entire MPA, it was necessary to have a large r_{path} of 1390 mm (Figure 6.3).

To avoid requiring a very large space for the setup for increasing r_{path}, the laser beam was made to zigzag five times between two mirror strips before reaching the MPA (Figure 6.2). As a result, the resulting laser dot speed variation across the MPA was only about 0.0001%.

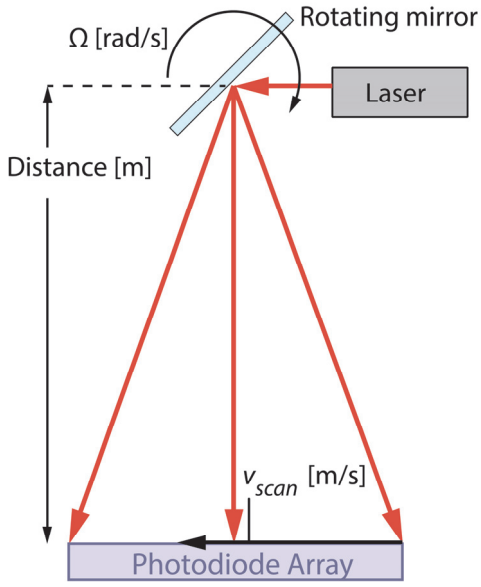

Figure 6.3. Schematic overview of the validation setup in which v_{input} is the input velocity, and Ω the angular velocity. The distance between the mirror and the photodiode array is expressed in meters.

The MPA was placed in a holder that allowed precise horizontal, vertical and rotational positioning and orienting. A mask with a (1.00 ± 0.05 mm) high slot was placed over the entire width of the MPA to limit the amount of light exciting the photodiodes. As a result of the laser dot scanning over the MPA, the photodiodes consecutively received a light pulse of sinusoidally-varying intensity with a clearly defined peak.

The actually delivered scanning velocity (v_{scan} [m/s]) at the MPA depends on the accuracy of the set Ω and r_{path}. Therefore, v_{scan} was continuously verified for each mirror rotation by measuring the time period t between the successive peaks received in the signal measured at photodiode 1 in the MPA:

$$v_{scan} = \frac{2\pi * r_{path}}{t} \tag{6.3}$$

The peaks of the photodiode 1 signals were detected using an off-the-shelf Matlab (The MathWorks, Inc., Matick, MA, USA) function called 'Peakdet' [16].

In order not to overestimate the accuracy of the MPA, the four most relevant

Table 6.1: Scanning velocities and measured pulse velocity [m/s] (averaged over 24 scans for each velocity).

Scanning Velocity [Mean ± SD]	Protocol 1 Measured Pulse Velocity [Mean ± SD]	Protocol 1 Measured Pulse Velocity [Mean ± SD]
12.9 ± 0.02	13.1 ± 0.16	13.2 ± 0.28
25.8 ± 0.06	25.9 ± 0.14	26.0 ± 0.52
36.0 ± 0.04	36.0 ± 0.11	36.8 ± 0.78
46.7 ± 0.09	46.7 ± 0.19	48.1 ± 1.23

tolerances (T1-T4) in the validation setup and the MPA were determined and taken into account: Firstly, the scanning velocity tolerance of the validation setup as determined by:

- T1; the accuracy of the distance between the rotating mirror and the MPA
- T2; the accuracy of the speed of the rotating mirror

Secondly, the accuracy of the measured pulse velocity by the MPA as determined by:

- T3; the tolerance of the distances between the successive photodiodes
- T4; the accuracy of the detection of the peaks of the light pulses received by the photodiodes which is mainly determined by the data acquisition sampling frequency (SF)

These tolerances were determined using manufacturers' specifications of the components and the of measurement equipment used.

Because of the multiplexing in the data acquisition system, the actual sampling frequencies with which the MPA-data were gathered depended on the number of photodiodes that were read out. To verify the functioning of the MPA at different SFs and inter-diode distances, all scanning velocities were applied 24 times with each of the three protocols:

- Protocol 1: using 2 photodiodes (no. 1 and 16) at a SF of 125 kHz
- Protocol 2: using 4 photodiodes (no. 1, 6, 11 and 16) at SF of 62.5 kHz
- Protocol 3: using all 16 photodiodes at a SF of 15.6 kHz.

Figure 6.4 shows an example of the signals measured when the laser dot makes a single scan over the MPA and Protocol 2 is used.

6.2.3 Data analysis

After obtaining the MPA data, Matlab R2010a was used for the data analysis and to calculate the velocity of the laser dot ('measured pulse velocity') from the signals received by the MPA. The measured pulse velocity was calculated as the distance between a pair of photodiodes divided by the time difference between the peaks detected on the signals measured by these photodiodes. The peaks were detected using an off-the-shelf Matlab function called 'Peakdet' [16].

For each protocol, this was done for each combination of any two of the photodiodes used. That way, any eventual misalignments of the MPA with respect

to the laser dot travel path potentially causing slight laser dot speed variations over the MPA, and any influences of the geometrical tolerance on the distance between the sensor's photodiodes (2%) were averaged out. Finally, the average measured pulse velocity was calculated by averaging all the measured pulse velocities from all combinations of two photodiodes for all 24 scans.

The data obtained with Protocol 2 showed that the SF of 62.5 kHz was too low to accurately measure the highest simulated PWV of 45.0 m/s. Therefore, these data were interpolated over time using the Matlab function 'v5cubic interpolation'. The v5cubic interpolation function determines the interpolated value at a point based on a shape-preserving piecewise cubic interpolation of the values at neighbouring points. This results in a more accurate approximation of the wave peaks because it takes the shape of the wave into account.

For Protocol 3 the SF of 15.6 kHz was too low to fit any proper curve through the data samples for any of the applied scanning velocities. Therefore, the datasets for Protocol 3 were excluded from further analysis. For Protocols 1 and 2 it was verified whether the measured pulse velocities matched the applied scanning velocities.

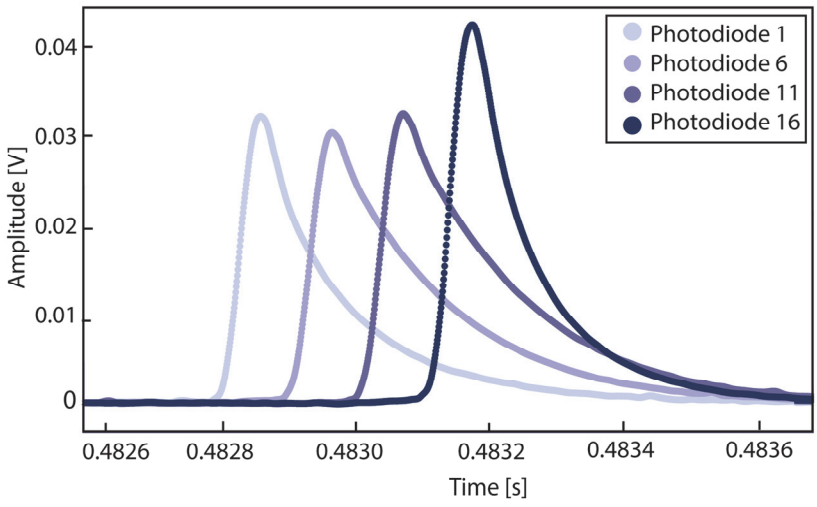

Figure 6.4: Example of light pulse detection with the multi photodiode array using four photodiodes.

6.2.4 In vivo pilot study

To illustrate the applicability of the MPA in practice, an *in vivo* pilot measurement was conducted on the right finger of the first author (M.H.N.V.) as a healthy volunteer, using the flow-mediated dilation (FMD) technique [17] which provokes the release of nitric oxide, resulting in vasodilation, causing the pulse wave amplitude (PWA) to increase after release of the blood-pressure cuff and causing the PWV to decrease The Medical Ethics Committee Erasmus MC of Rotterdam, the Netherlands confirmed that the rules laid down in the Medical Research Involving Human Subjects Act (also known by its Dutch abbreviation WMO), do not apply for this in vivo pilot study. Therefore, the study was allowed without further review by the MEC board. The MPA was placed on the right finger and set to use Protocol 1. The healthy volunteer was sitting on a chair with both hands resting on a table, in a quiet room under tranquil conditions and without talking or moving during the measurement. First, the PWV was measured for 1 minute to obtain a baseline. Next, the blood-pressure cuff, placed around the upper arm, was inflated to 150 mmHg pressure to block the blood flow to the lower arm. After 5 minutes, the blood-pressure cuff was instantly released. During this entire process, the PWV was measured. After releasing the blood-pressure cuff, the PWV and PWA were measured for 5 minutes and averaged over each 30 s.

6.3 Results

6.3.1 Functional validation

The validation setup has a scanning velocity tolerance which is determined by:

- T1; the accuracy of the distance between the rotating mirror and the MPA
- T2; the accuracy of the speed of the rotating mirror.

The tolerance of the distance between the rotating mirror and the MPA was determined to be 1% (using a solid aluminium breadboard with a tolerance of 0.25 mm between the mounting holes). For the peak detection, the accuracy was ± 1 sample for the two lowest scanning velocities and ± 2 samples for the two highest scanning velocities. T1 and T2 together lead to uncertainties in the scanning velocities of ± 0.5 m/s for two lowest scanning velocities and ± 1.1 m/s for two highest scanning velocities. Table 6.1 shows the mean ± SD of the scanning velocities.

The measured pulse velocity tolerance by the MPA as determined by:

- T3; the tolerance of the distances between the successive photodiodes
- T4; the accuracy of the detection of the peaks of the light pulses received by the photodiodes.

The tolerance specified by the manufacturer for the distance between photodiodes 1 and 16 was ± 0.25 mm over the full distance of 12.0 mm. Therefore, the uncertainties in the measured pulse velocities caused by T3 and T4 are ± 0.2%, 0.3 %, 0.5 % and 0.6 % for the successive measured pulse velocities. Table 6.1 shows the mean ± SD of the measured pulse velocities using Protocols 1 and 2.

Figure 6.5 shows the relative difference between the scanning velocity and the measured pulse velocity and their variation. The maximum differences was 3.0 % when using the four photodiodes by the highest scanning velocity. For using two photodiodes, Protocol 1, the maximum differences was 1.7 %. Both reported accuracies are including the additional potential deviations caused by the system

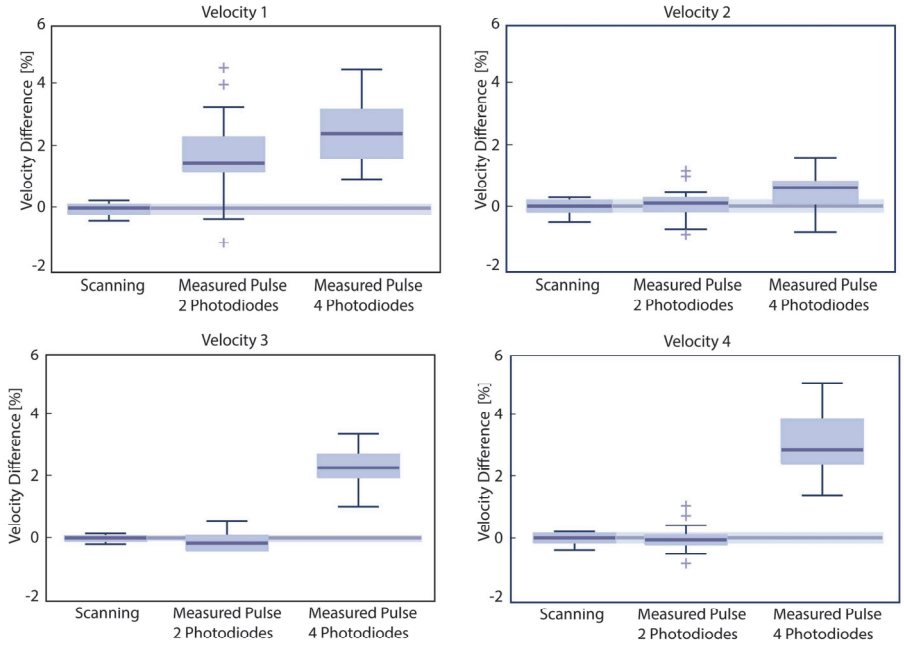

Figure 6.5: Boxplot of the relative differences between the set-scanning velocities (taken as the zero reference) and the measured pulse velocities (for 2 and 4 photodiodes). The line in the middle of each box is the sample median. The tops and bottoms of each "box" are the 25th and 75th percentiles of the samples, respectively. The whiskers are drawn from the ends of the interquartile ranges to the furthest observations excluding outliers.

tolerances.

6.3.2. In vivo pilot study

Figure 6.6 shows the PWV and the PWA averaged over each 30 seconds as measured for each heartbeat before and after the FMD test. After release of the blood-pressure cuff the PWA increased, which agrees with the Guidelines for the Ultrasound Assessment of Endothelial-Dependent Flow-Mediated Vasodilation of the Brachial Artery [17]. The PWV measured between photodiodes 1 and 16 before inflating the blood-pressure cuff was 1.1 ± 0.2 m/s during this 1 min baseline. The PWV was higher after releasing the blood-pressure cuff and then decreased over time.

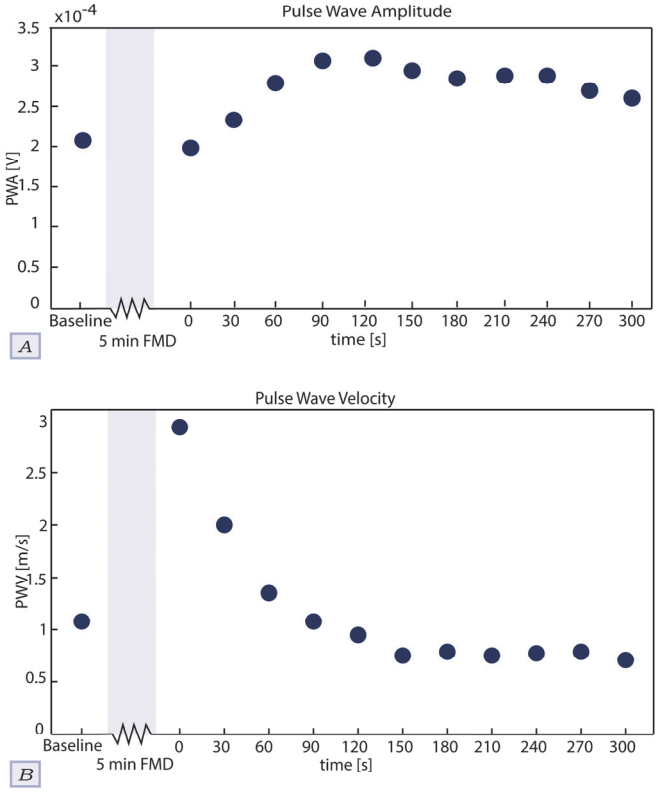

Figure 6.6: (A) pulse wave amplitude and (B) pulse wave velocity (PWV) before and after flow-mediated dilation (FMD) in a healthy volunteer. First a baseline of 1 min was measured (leftmost dot). Each dot indicates the average over each 30 sec. The dot at 0 s indicates the value at the moment the cuff is released immediately after the 5 min of FMD.

6.4 Discussion

To the best of our knowledge, this study is the first to demonstrate measuring the PWV based on photoplethysmography with a single photodiode array. The validation setup used enabled assessing the maximum technical accuracy for measuring pulse speeds in the range of naturally occurring pressure pulse wave velocities and beyond.

6.4.1 Scanning velocity

The scanning velocities used to validate the functionality of the MPA were relatively high compared to commonly reported average PWVs in healthy subjects or patients. However, these velocities were chosen in order to assure that proper PWV measurements can also be obtained even in patients— who often have with exceptionally high PWVs— and to explore the full potential of the designed sensor, both for application in the primarily intended transmission measurements on the extremities as well as in future reflective measurements on, e.g., the carotid artery. Furthermore, the measurement inaccuracies increase with increasing PWV, which is why the chosen velocities provide a very strong worst-case validation. Despite the tolerances causing uncertainties in the applied scanning velocities, the validation setup proved to be sufficiently accurate for our purposes.

6.4.2 Measured pulse velocity

At all scanning velocities, the MPA accuracy proved to be more than adequate to provide reliable results. In the MPA, any inaccuracies in the measured pulse velocity could in principle be caused by:

a) the tolerance on the distances between the photodiodes, which is a systematic error because the inter-diode distances never change;
b) the response time of the MPA photodiodes, which was unlikely to be a source of inaccuracy because the amplitudes were comparable for all measured velocities;
c) and the sampling frequency, of which the relative effect size depends on the pulse velocity to be measured.

One may notice in Figure 6.4 that the amplitude of the response of photodiode 16 was higher than that of the other photodiodes. No explanation for this systematic deviation could be found, but it could have been induced by a small irregularity in the laser-cut mask in front of the MPA, which might have caused reflections or slightly more light to pass the mask. However, irrespective of the cause of the

amplitude variation, such systematic response amplitude variations between the different diodes do not affect the speed calculations, as these do not change the location of the amplitude peaks on the time axis.

The MPA showed to enable accurate measurement of PWVs up to 45 m/s when using two photodiodes (spaced 12.0 mm apart) at 125 kHz. When using four photodiodes (spaced 4 mm apart) at 62.5 kHz the MPA can accurately measure PWVs up to 25.0 m/s without the need for interpolation and up to 45.0 m/s with interpolation. In clinical practice, the PWV is unlikely to exceed 20.0 m/s [6, 9, 10]. Therefore, the MPA is sufficiently accurate for clinical use when using four photodiodes. Having four photodiodes instead of two can be of potential value when local artefacts disturb the PW shapes and inhibit proper detection of the PW peaks, something often observed in clinical practice. In such cases, the velocity measurements can be made more robust by ignoring any diodes that return disturbed PW signals and averaging the velocities measured over several sections of the array. Furthermore, using more than two photodiodes allows to investigate whether there is a change in PWV over a short trajectory; this could potentially be useful to determine the presence of arthrosclerosis in a specific area.

When sampling all 16 photodiodes, the MPA could not accurately measure the PWV for any of the applied scanning velocities. The sampling frequency (which is multiplexed over all channels) was too low to accurately provide the true peak location, even after interpolation. The 16 photodiodes array was selected because of its availability, but having 2 photodiodes suffices for measuring the PWV and with 4 photodiodes the robustness of the PWV measurements can be increased. However, having a plurality of photodiodes could potentially maximize the robustness of the velocity measurements in patients demonstrating high rates of disturbed PWs. Obviously, the MPA performance with 16 photodiodes could be improved by using higher sampling frequencies, but that would require costlier equipment. A way to improve the measurements while using low sampling frequencies could be to determine the time differences of the pulse waves arriving at the different diodes using cross-correlation instead of peak detection. However, the current study focused on the use of peak detection because this is a simple approach that can applied easily in many software packages and analysis tools. Additionally, peak detection requires little computational power compared to using cross-correlation methods, making it more suitable for fast, real-time measurements.

The pulse velocities measured using two or four photodiodes had deviations of at most 3.0 % compared to the corresponding scanning velocities. In an in vivo study, Boutouyrie et al. measured PWVs to differ between healthy volunteers (Optimal) and patients with CVD (Grade II/III HT) by more than 25% (for ages ≤ 30 years a mean PWV of 6.0 m/s versus 7.6 m/s) [6]. Implying once more that, when using two or four diodes, the MPA can reliably measure clinically realistic PWV values with sufficiently high accuracy to detect clinically relevant PWV variations. The applicability of the MPA could be even further increased by adapting it to enable reflective PPG measurements. This would allow measuring PWVs on locations that can be approached from a single side only, such as the carotid artery.

6.4.3 In vivo pilot

To further test the clinical applicability of the MPA, an in vivo pilot study was conducted on author M.H.N.V. These results were similar to those reported by Nam et al. [13], i.e. around 0.8 m/s. Furthermore, the response of the PWA to the FMD agrees with that described in the guidelines for FMD measurement [17]. It is known that the PWA increases during FMD. Assuming other parameters (e.g. cardiac output, heart rate) to be constant throughout the experiment, the PWV should decrease after FMD; our pilot results were in line with this expectation.

It is not yet known to what extent the peripheral PWV measured in a finger correlates with conventional techniques of measuring the PWV in the aortic. To investigate this, the functionality of the MPA first had to be verified, as was done in this research. The correlation between conventional PWV measurements and peripheral PWV is currently being investigated. If there is good correlation, this novel way of measuring the PWV will open the road to fast and simple PWV-based diagnostics with minimal burden on patients.

6.5 Conclusion

The results of this study indicate that the novel photoplethysmography-based MPA can accurately and reliably measure PWV within clinically relevant ranges, and even well beyond. Some important advantages of the MPA as compared to other PWV measuring systems are that the MPA is easy-to-use, non-invasive and objective. Using the MPA will not require trained staff or costly equipment, and allows continuous monitoring. In addition, the MPA eliminates the need for any other measurement systems, such as ECG, for measuring PWVs.

Further research is required to investigate whether the PWVs measured with the MPA on the fingers can be used as an index for evaluation of aortic stiffness as a factor of cardiovascular risk [9]. A subsequent step is to examine the reproducibility and variance of the PWV in healthy volunteers and cardiovascular risk patients when applying measurements over short trajectories, instead of the currently used measurements over larger distances.

6.6 Acknowledgments

The authors thank the colleagues in the department of Experimental Medical Instrumentation (Erasmus University Medical Center, Rotterdam, the Netherlands) for manufacturing the MPA and for their assistance with the MPA design; Mr. Rob Lutjeboer (Department of Precision and Microsystems Engineering, Delft University of Technology, Delft, the Netherlands) for providing optical components for the test setup; and the department of Minimally Invasive Surgery and Interventional Techniques and Mr. Reinier van Antwerpen (Delft University of Technology, Delft, the Netherlands) for providing laboratory space and the test setup.

6.7 References

1. Quinn, U., L.A. Tomlinson, and J.R. Cockcroft, Arterial stiffness. JRSM Cardiovasc Dis, 2012. 1(6).
2. Blacher, J., et al., Impact of aortic stiffness on survival in end-stage renal disease. Circulation, 1999. 99(18): p. 2434-2439.
3. Laurent, S., et al., Aortic stiffness is an independent predictor of all-cause and cardiovascular mortality in hypertensive patients. Hypertension, 2001. 37(5): p. 1236-1241.
4. Cruickshank, K., et al., Aortic pulse-wave velocity and its relationship to mortality in diabetes and glucose intolerance: An integrated index of vascular function? Circulation, 2002. 106(16): p. 2085-2090.
5. Laurent, S., et al., Expert consensus document on arterial stiffness: methodological issues and clinical applications. Eur Heart J, 2006. 27(21): p. 2588-605.
6. Boutouyrie, P. and S.J. Vermeersch, Determinants of pulse wave velocity in healthy people and in the presence of cardiovascular risk factors: Establishing normal and reference values. European Heart Journal, 2010. 31(19): p. 2338-2350.
7. Bramwell, J.C. and A.V. Hill, The Velocity of the Pulse Wave in Man. Proceedings of the Royal Society of London Series B, Containing Papers of a Biological Character, 1922. 93(652): p. 298-306.

8. Wilkinson, I.B., et al., Reproducibility of pulse wave velocity and augmentation index measured by pulse wave analysis. Journal of Hypertension, 1998. 16(12 SUPPL.): p. 2079-2084.
9. Mancia, G., et al., 2013 ESH/ESC guidelines for the management of arterial hypertension: The Task Force for the management of arterial hypertension of the European Society of Hypertension (ESH) and of the European Society of Cardiology (ESC). European Heart Journal, 2013. 34(28): p. 2159-2219.
10. Meaume, S., et al., Aortic pulse wave velocity predicts cardiovascular mortality in subjects >70 years of age. Arteriosclerosis, Thrombosis, and Vascular Biology, 2001. 21(12): p. 2046-2050.
11. Lehmann, E.D., et al., Non-invasive Doppler ultrasound technique for the in vivo assessment of aortic compliance. Journal of Biomedical Engineering, 1992. 14(3): p. 250-256.
12. Jatoi, N.A., et al., Assessment of arterial stiffness in hypertension: Comparison of oscillometric (Arteriograph), piezoelectronic (Complior) and tonometric (SphygmoCor) techniques. Journal of Hypertension, 2009. 27(11): p. 2186-2191.
13. Nam, D.H., et al., Measurement of spatial pulse wave velocity by using a clip-type pulsimeter equipped with a Hall sensor and photoplethysmography. Sensors (Basel, Switzerland), 2013. 13(4): p. 4714-4723.
14. Allen, J., Photoplethysmography and its application in clinical physiological measurement. Physiol Meas, 2007. 28(3): p. R1-39.
15. Millikan, G.A., The oximeter, an instrument for measuring continuously the oxygen saturation of arterial blood in man. Review of Scientific Instruments, 1942. 13(10): p. 434-444.
16. Billauer, E., Peakdet. 2012: http://billauer.co.il/peakdet.html. p. Detect peaks in a vector.
17. Corretti, M.C., et al., Guidelines for the ultrasound assessment of endothelial-dependent flow-mediated vasodilation of the brachial artery: A report of the international brachial artery reactivity task force. Journal of the American College of Cardiology, 2002. 39(2): p. 257-265.

Chapter 7

Comparison between pulse wave velocities measured using Complior or measured using Biopac

Marit H.N. van Velzen, Robert J. Stolker, Arjo J. Loeve,
Sjoerd P. Niehof, Egbert G. Mik

Journal of Clinical Monitoring and Computing, May 2018

Arterial stiffness is a reliable prognostic parameter for cardiovascular diseases. The effect of change in arterial stiffness can be measured by the change of the pulse wave velocity (PWV). The Complior system is widely used to measure PWV between the carotid and radial arteries by means of piezoelectric clips placed around the neck and the wrist. The Biopac system is an easier to use alternative that uses ECG and simple optical sensors to measure the PWV between the heart and the fingertips, and thus extends a bit more to the peripheral vasculature compared to the Complior system. The goal of this study was to test under various conditions to what extent these systems provide comparable and correlating values. 25 Healthy volunteers, 20 30 years old, were measured in 4 sequential position:, sitting, lying, standing and sitting. The results showed that the Biopac system measured consistently and significantly lower PWV values than the Complior system, for all positions. Correlation values and Bland-Altman plots showed that despite the difference in PWV magnitudes obtained by the two systems the measurements did agree well. Which implies that as long as the difference in PWV magnitudes are taken into account, either system could be used to measure PWV changes over time. However, when basing diagnosis on absolute PWV values, one should be very much aware of how the PWV was measured and with what system.

7.1 Introduction

Arterial stiffness is a reliable prognostic parameter for cardiovascular morbidity and mortality in adults. In particular, this is the case in patients with renal disease, diabetes mellitus or hypertension and in elderly patients [1-4]. Cardiovascular disease (CVD) is worldwide the number one cause of death. Smoking, unhealthy diet, physical inactivity and harmful use of alcohol are the most important behavioural risk factors of CVD. These behavioural risks may lead to hypertension, diabetes, obesity, heart failure, or atherosclerosis. Most of these phenomena are related to an increase in arterial stiffness.

Arterial stiffness is a measure of the capability of an artery to expand and contract in response to local blood pressure changes and is the inverse of arterial compliance. The compliance, and therefore the volume change in response to a blood pressure change, in a stiff vessel is reduced compared to a healthy vessel. The effect of reduced compliance is a decreased propagation time of pressure pulse waves (PWs) through the vessels and thus an increase of the velocity of the PW. The relationship between this pulse wave velocity (PWV) and the compliance of the vessel wall is described in the Moens-Korteweg equation [5]:

$$PWV = \sqrt{\frac{E_{inc} \cdot h}{2r \cdot \rho}} \tag{7.1}$$

where E_{inc} is the incremental elastic modulus, h is the wall thickness, and r the radius of the vessel. The symbol ρ represents the density of blood.

PWV measurements are widely used as an index of arterial stiffness [6] and for the evaluation of cardiovascular risk. PWV measurements are generally simple, accurate and highly reproducible [7, 8]. In clinical practice, several invasive and non-invasive measurement systems are readily available to measure PWV. Two of such systems, equally often used in clinical practice by the Erasmus Medical Centre in Rotterdam, the Netherlands, are the Complior (Alam Medical, Vincennes, France), using piezoelectric sensors [9], and the Biopac (Biopac Systems, Inc, USA), using a photoplethysmography (PPG) sensor and ECG. These systems are used to non-invasively measure PWV in big arteries over long trajectories.

The Complior system is used to measure PWV between the carotid and radial arteries by means of piezoelectric clips placed around the neck and the wrist. The Biopac system is an easier-to-use alternative to the Complior system, but it

measures the PWV between the heart and the fingertips, and thus extends a bit more to the peripheral vasculature. One may expect the two systems to show good agreement, because the majority of the trajectory (sternoclavicular joint to wrist) of the arterial trajectories over which the Biopac and Complior systems measure PWV are identical. However, the trajectory for the Biopac additionally includes the wrist-fingertip vasculature. Furthermore, the Biopac includes the heart-sternoclavicular trajectory, whereas with the Complior the sternoclavicular-carotid trajectory is taken as an approximation for the heart-sternoclavicular trajectory.

While both systems are supposed to measure or approximate a PWV value for the more or less the same trajectory from the heart to the hand, the potentially differing physiological responses of the carotid and the peripheral arteries may cause different PWV measurement outcomes. The baroreceptor reflex is one of the body's homeostatic mechanisms that helps to maintain blood pressure at nearly constant levels [10] by detecting blood pressure using the baroreceptors located in the walls of the carotid arteries. If one suddenly rises from a lying position, gravity pulls the blood in the direction of the legs, which could endanger the blood flow to the brain. As a response, the baroreceptor reflex causes the peripheral veins to be squeezed and the carotid arteries to be widened to aid the blood flow to the brain. Therefore one may expect that depending on the measurement situations the PWV change measured with the Complior system will oppose the PWV measured with the Biopac system if the baroreceptor reflex is invoked.

So while both systems are aimed at providing a similar measure of vascular condition and while the trajectories over which they measure PWV largely overlap, there are various reasons why it is unclear whether they will provide similar measurement outcomes. To the best of our knowledge, there are no reports about the agreement between PWV values measured using the Complior system or the Biopac system. Yet, in clinical practice it is crucial to know whether using different devices for the same purpose provides the same outcome. One would never accept it if measuring a heart rate using ECG versus using a pulse oximeter on the finger would provide a 30 bpm difference. Therefore, the goal of this health technology assessment was to test under various conditions to what extent these systems provide comparable values and to what extent these values correlate.

7.2 Method

7.2.1 Study population

Twenty-five healthy volunteers, 20-30 years old, without any known history of atherosclerosis associated diseases (such as diabetes mellitus, hypertension, coronary artery disease, stroke, renal disorder), or injuries at the upper limbs were included in this study after obtaining written informed consent from the subject. This study was approved by the medical ethics committee of Erasmus University Medical Center Rotterdam, the Netherlands (MEC-2012-139).

7.2.2 Protocol

The transit time of a PW traveling from within the heart to easily accessible locations, such as the extremities or the neck, consists of 2 components: the PW propagation-time from the heart through the artery to the PW measurement location, and the isometric contraction time of the heart (pre-ejection period, PEP). The PEP is known to vary with cardiac preload and heart rate [11-13]. Therefore, all measurements were conducted in a quiet room under tranquil conditions at a room temperature of 22.4°C (SD 0.5°C). To further minimize any influences of a varying PEP or cardiac output during the measurement, the subjects were instructed not to talk or move during the measurement for each position. Because caffeine, tobacco and alcohol influence the heart rate and cardiac output, all subjects were asked to not take any caffeine, tobacco or alcohol for at least 3 hours prior to the experiment.

The measurements were conducted 4 times for each subject, each time in a different body position. In the first position, the subject sat on a chair with both hands resting on a table. In the second position, the subject lied on a bed with both arms and hands resting along his/her body. In the third position, the subject stood upright with both hands hanging down along his/her body. The fourth position was the same as the first position, to check if the PWV-value was reproducible.

Before the start of each measurement in each position the subject was kept at rest for 60s in the requested position. The PWV values were recorded with both of the tested systems simultaneously during the entire measurement, which lasted up to 60s.

7.2.3 Pulse wave velocity analysis

The PWV was measured between the carotid and radial arteries using the Complior system (Alam Medical, Vincennes, France) and between the carotid artery and the left index finger tip using ECG and PPG (described below). The Complior system measures the PWV using piezoelectric sensors. For measuring the PWs on the carotid artery, a clip containing a piezoelectric sensor was placed on the left side of the neck. For measuring the PWs on the radial artery, a clip containing a piezoelectric sensor was placed on the left wrist (see Figure 7.1). Both sensor signals were recorded by the ”Complior SP” software. The distance between the sensors, measured in a straight line from the sternoclavicular joint to the styloid process of the radius, was used to approximate the arterial distance travelled by the PWs. Using the ‘’Complior SP” software, the foot of the PW measured at both locations was used to calculate the mean PWV once per 5 s.

The system used for measuring the PWV between the carotid artery and the left index finger tip consisted of a measuring device and analysis software. The measurement device contained one PPG-sensor (TSD200 with the PPG100C amplifier, Biopac Systems, Inc, Goleta, USA), positioned on the left index finger, and three external ECG-leads (ECG100C amplifier, Biopac Systems, Inc, Goleta, USA) (see Figure 7.1). The three ECG-leads were placed on the subject’s both wrists and right ankle. The PPG- and ECG-signals were simultaneously converted to digital signals using AcqKnowledge version 3.7.3 software (Biopac Systems, Inc, Goleta, USA), at a sampling frequency of 2 kHz. The PPG-signal was filtered with a

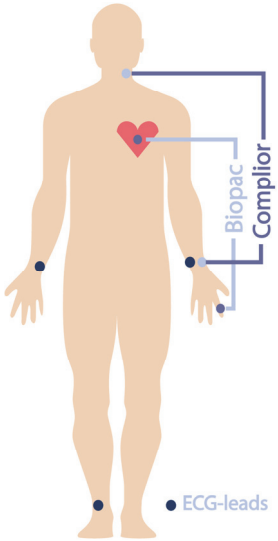

Figure 7.1: Schematic view of placement of the both measurement systems.

fourth-order low pass Butterworth filter with a cut-off frequency of 9 Hz using Matlab R2010a (The MathWorks, Inc., Matick, MA, USA). The PWV was determined by dividing the distance between the PPG-sensor on the left index finger and the sternoclavicular joint *(d)* by the calculated time-difference between the time instance of the R-peak of the ECG ($t_{ECG\ R\text{-}peak}(n)$) and the foot of the PW measured at the left index finger tip ($t_{PPG\ foot}(n)$):

$$PWV_{Biopac}(n) = \frac{d}{t_{PPG_{foot}}(n) - t_{ECG_{R-peak}}(n)} \tag{7.2}$$

where *n* is the sequence number of the heartbeats. The R-peaks in the ECG were found using the off-the-shelf Matlab function 'R-peakdetect' [14]. The maximum of the second derivative of each PW was taken as the foot of the PW (PPG_{foot}) and the corresponding time was indicated as $t_{PPG\ foot}(n)$ *[15].* The utilized PPG-sensor was quite sensitive for motion and positioning artefacts, which sometimes distorted the shapes of the PWs in a way that they were rendered unsuitable for further analysis. Therefore, a custom-made Matlab algorithm, called '7Step PW-Filter', was implemented in the data analysis to filter out any PWs that strongly deviated in shape from a suitable PW [16]. If more than 50% of the PWs were filtered out for being too distorted, the data-set was excluded from further analysis.

7.2.4 Statistical analysis

The mean PWVs +/- standard deviation (SD) over 60s were calculated for each measurement technique for each body position. The Shapiro-Wilk test was used to check if the data was normally distributed. PWV values obtained using the Complior and Biopac system were compared using a paired samples t-test and a Bland-Altman plot was used to analyse the agreement between the two different PWV measurement techniques. Correlation between both sitting positions (Position 1 and Position 4) were analysed using a Pearson Correlation test. A significance level of *p*-value < 0.05 was used. A repeated measurement ANOVA with Greenhouse-Geisser correction and a post hoc test with Bonferroni correction was used to test for any effects of the repeated measurements. All 7statistical analyses were performed using SPSS version 22.0 (SPSS, Inc., Chicago, IL, USA).

7.3 Results

Twenty-five subjects, (11 male, 14 female) were included in this study. The data of one male and one female subject were excluded from the analysis because there

Table 7.1: Characteristics of the study population. Values are means ± SD or number (%) of participants

Variable	[n =23]
Gender (male), no. (%)	10 (43.5)
Age [years]	25 ± 3
Weight [kg]	72 ± 9
Height [m]	1.77 ± 0.08
Body mass index [kg/m²]	23.03 ± 2.72
Blood pressure [mmHg]	
Systolic	127 ± 11
Diastolic	80 ± 9
Heart rate [bpm]	77 ± 14
Smoker (yes), no. (%)	2 (8.33)
Distance from sternoclavicular to wrist [cm]	69 ± 3
Distance from wrist to fingertip [cm]	17 ± 1

was too much noise in the signals to obtain any usable PWs. Table 7.1 presents the characteristic of the remaining study population. For positions 1, 2 and 4 (sitting 1, lying, sitting 2)the '7Step PW-Filter' filtered out none of the PWs. For Position 3 (standing) there were 8 datasets with over 50% unsuitable PWs, which were therefore excluded from further analysis. In the remaining 15 datasets, the median percentage of unsuitable PWs that were filtered out was 2.2% (Q_1 = 0% and Q_3 = 36.6%).

The means and SDs for the $PWV_{complior}$ and PWV_{biopac} for the 4 different positions are listed in Table 7.2, as well as the results of the paired samples *t*-test. Significant differences were found for each position between $PWV_{complior}$ and PWV_{biopac}.

Table 7.2: Mean and standard deviation of the PWV

Position	$PWV_{complior}$ [m/s]	PWV_{biopac} [m/s]	Paired sampled t-test
Sitting 1	10.2 ± 1.4	3.0 ± 0.2	$t(21) = -24.442$, $p < 0.001$
Lying	9.3 ± 1.6	3.1 ± 0.2	$t(19) = -18.654$, $p < 0.001$
Standing	9.8 ± 2.2	3.2 ± 0.2	$t(13) = -16.178$, $p < 0.001$
Sitting 2	10.2 ± 1.1	3.0 ± 0.2	$t(21) = -31.704$, $p < 0.001$

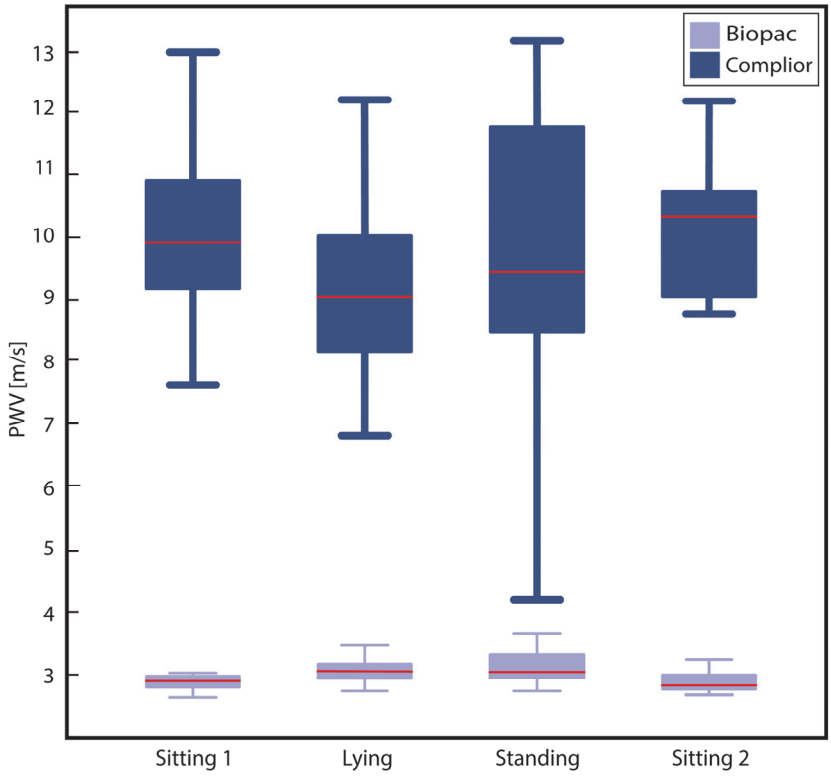

Figure 7.2: Boxplot of the PWVbiopac and PWVcomplior, with the median as red line and the minimum and maximum value

Figure 7.2 shows a boxplot of $PWV_{complior}$ and PWV_{biopac} for each position. The data consistently showed that PWV_{biopac} was much lower than $PWV_{complior}$.

Figure 7.3 and Table 7.3 present the Bland-Altman values and plot, showing good agreement between the two PWV measurement techniques.

The Pearson correlation between sitting Position 1 and Position 4 proved to be high and significant for PWV_{biopac} (0.778, $p < 0.001$). For $PWV_{complior}$ there was no

Table 7.3: Bland-Altman

Position	BIAS ± CI [m/s]	% of overall mean PWV [%]
Sitting 1	7.2 ± 2.7	37.6
Lying	6.2 ± 2.9	47.0
Standing	6.6 ± 4.3	64.4
Sitting 2	7.3 ± 2.1	29

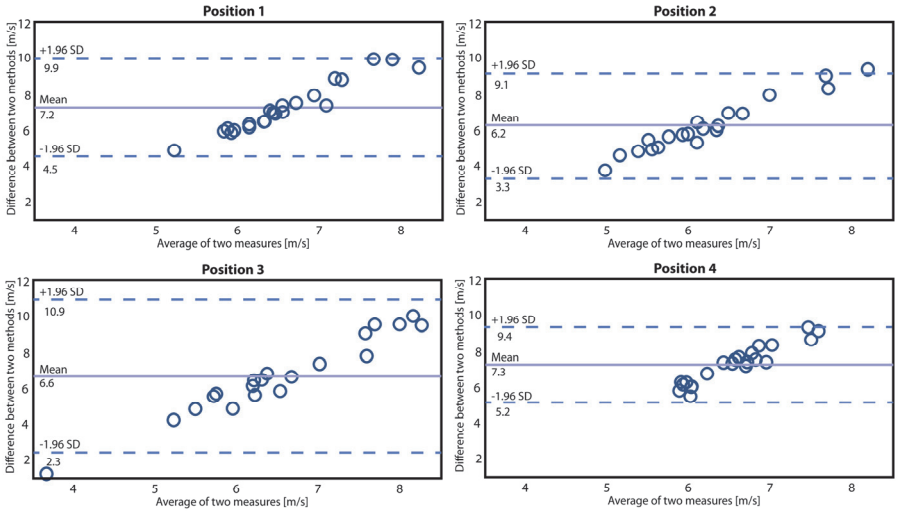

Figure7.3: Bland-Altman plots of $PWV_{complior}$ and PWV_{biopac} by the 4 positions. The dotted lines represent the 95% limits of agreement and the straight mean difference (bias) between $PWV_{complior}$ and PWV_{biopac}

significant correlation (0.141, p = 0.541).

The repeated measures ANOVA indicated that the four body positions were rated equally (F(3,45)=2.47, p=0.074), for the Complior. For the Biopac, the four body positions were not rated equally (F(3,39)=13,1, p=0.000).The post hoc tests of the Biopac-data revealed that Position 2 (lying) and Position 3 (standing) resulted in significantly higher PWV compared to Position 1 (sitting 1) ((p=0.000, p=0.025, respectively). There was no significantly difference between Position 2 (lying) and Position 3 (standing) (p=1.000).

7.4 Discussion

This study compared PWV values measured over the carotid-radial artery trajectory using the Complior system with PWV values measured between the R-peak of the ECG and the arrival of the PW in the left index finger tip using the Biopac system in healthy volunteers in three body positions: sitting, lying and standing. The PWV_{biopac} values were considerably lower than the $PWV_{complior}$ values, and this effect persisted in each position. This absolute difference might be explained for a minor part by the fact that PWV_{biopac} includes the PEP, whereas $PWV_{complior}$ does not. However, the PEP could account for no more than 1 m/s of the PWV_{biopac}. Therefore, the large absolute difference between PWV_{biopac} and $PWV_{complior}$ may more likely be explained by the difference in vessel compliance between the two trajectories. More peripheral vessels are narrower, thinner walled and more

compliant. Because the more peripherally measured PWV_{biopac} showed to be lower, it is hypothesized that the reduced vessel stiffness and wall thickness (both reducing PWV) outweigh the reduced vascular radii (which would increase the PWV). However, the $PWV_{complior}$ values agree with values reported in other studies. The mean $PWV_{complior}$ values (10.2 ± 1.4 m/s) were in the same range as those reported by Rajzer et al. [17] (10.1 ± 1.7 m/s). Although Raizer et al. measured PWV over the carotid-femoral trajectory, it is expected that PWVs over that trajectory will be similar to those in the carotid-radial trajectory, because of similar lengths and because the effects of differences in vessel radii and wall thicknesses are likely to cancel each other out, according to Equation 1. Furthermore, the current results also agree with those of McEleavy, who measured a PWV of 9.0 ± 1.2 m/s in the carotid-radial trajectory [18]. For the PWV_{biopac} no other studies reporting PWV between the heart and a fingertip were found, however the time between the R-peak of the ECG and arrival of the foot of the PW at the fingertip (called pulse transit time) (283 ± 21 ms) was in the same range as reported previously by van Velzen et al. (273 ± 20 ms) [16] and by Kortekaas et al. (271 ± 28 ms) [13].

Table 7.2 shows that the PWV_{biopac} was consistently and significantly lower than $PWV_{complior}$ for all positions (1 to 4). However, the Bland-Altman plots (Figure 7.3) show that the bias is small and the values are scattered around the mean, leading to the conclusion that there is a good agreement between the $PWV_{complior}$ and PWV_{biopac} values, but they simply differ in magnitude.

The PWV was slightly, but significantly higher when lying or standing as compared to sitting (with no significant difference between lying and standing), when measured by the Biopac system over the heart-fingertip trajectory. PWV may increase when vessels become stiffer and narrower due to contraction, but although this effect could be induced when standing up, it is less likely to happen when lying down. There was no significant effect of the different positions for the $PWV_{complior}$, which suggests that the $PWV_{complior}$ is less suitable to detect such small PWV changes or it is less sensitive to changing positions. The Pearson correlation results show much better agreement between repetitions of the sitting position at different moments for the Biopac system than for the Complior system. This suggests that when doing longitudinal PWV measurements, the Biopac system should be preferred, provided that the same position is consistently used during successive measurements.

When using the Biopac system, the measured PWV includes the PEP. The PEP is known to vary during position changes. PEP variations caused by subject movement or stress were avoided during the current study. Kortekaas et. al showed a variability of the PEP in healthy volunteers in rest of 58.5 ± 13.0 ms [13]. Over the distances travelled by the PWs in the current study, these PEP durations could account for no more than 1 m/s of the PWV_{biopac}. Consequently, PEP variations are unlikely to explain any variations in this study.

Limitations of the two tested techniques include the challenge of accurately positioning the sensors, and the discrepancy between the measured distance between the sensors and the actual path length travelled by the PWs. When measuring the PWV more locally, such as between the wrist and a position at the lower arm, the discrepancy between the distance between the sensors and the actual path length travelled by the PWs should diminish.

Furthermore, the utilized piezoelectric sensors in the Complior and PPG sensors in the Biopac system were quite sensitive to motion and positioning disturbances. This sensitivity to disturbances poses a potential limitation on the usability of these techniques in clinical practice. Moreover, the Complior system is not always comfortable for the subject: use of the clip on the neck was sometimes experienced as uncomfortable, whereas the sensor required for the Biopac system a photoplethysmography sensor on the finger and three ECG-leads on the wrists and right ankle are more comfortable than the Complior sensor and are generally available in hospitals. Using this system could benefit patients and clinical practice. Although the '7Step PW Filter' algorithm used to eliminate distorted PWs functioned well, the availability of a PPG sensor less sensitive to disturbances and not requiring measuring sensor distances, would greatly simplify measuring PWs in awake and moving patients. Obviously, this is less relevant when measuring PWs in patients under general anaesthesia.

7.5 Conclusion

In conclusion, this study demonstrated that PWV values were consistently and significantly lower when measured with the Biopac system than when measured with the Complior system. Yet, despite the difference in absolute PWV values, the two systems did agree fairly well. This suggests that as long as the difference in PWV magnitudes are taken into account, either system could be used to measure PWV changes in time. However, when basing diagnosis on absolute PWV values, one should be very much aware of how the PWV was measured and with what

system. In the future, clinical practice could greatly benefit if software for calculating PWV is embedded in the commonly used anaesthesia monitors, enabling PWV measurements using a standard ECG and a standard pulse oximeter. This might allow PWV measurements to become a widely available diagnostic tool, and an easy-to-use, non-invasive, safe and quick method for objectively assessing arterial stiffness as a reliable prognostic parameter for cardiovascular morbidity and mortality.

7.6 References

1. Cruickshank, K., et al., Aortic pulse-wave velocity and its relationship to mortality in diabetes and glucose intolerance: An integrated index of vascular function? Circulation, 2002. 106(16): p. 2085-2090.
2. Blacher, J., et al., Impact of aortic stiffness on survival in end-stage renal disease. Circulation, 1999. 99(18): p. 2434-2439.
3. Laurent, S., et al., Aortic stiffness is an independent predictor of all-cause and cardiovascular mortality in hypertensive patients. Hypertension, 2001. 37(5): p. 1236-1241.
4. Avolio, A.P., et al., Effects of aging on changing arterial compliance and left ventricular load in a northern Chinese urban community. Circulation, 1983. 68(1): p. 50-58.
5. Bramwell, J.C. and A.V. Hill, The Velocity of the Pulse Wave in Man. Proceedings of the Royal Society of London Series B, Containing Papers of a Biological Character, 1922. 93(652): p. 298-306.
6. Asmar, R., et al., Assessment of arterial distensibility by automatic pulse wave velocity measurement: Validation and clinical application studies. Hypertension, 1995. 26(3): p. 485-490.
7. Wilkinson, I.B., et al., Reproducibility of pulse wave velocity and augmentation index measured by pulse wave analysis. Journal of Hypertension, 1998. 16(12 SUPPL.): p. 2079-2084.
8. Safar, H., et al., Aortic pulse wave velocity, an independent marker of cardiovascular risk. Arch Mal Coeur Vaiss, 2002. 95(12): p. 1215-1218.
9. Jatoi, N.A., et al., Assessment of arterial stiffness in hypertension: Comparison of oscillometric (Arteriograph), piezoelectronic (Complior) and tonometric (SphygmoCor) techniques. Journal of Hypertension, 2009. 27(11): p. 2186-2191.
10. Heesch, C.M., Reflexes that control cardiovascular function. Am J Physiol, 1999. 277(6 Pt 2): p. S234-43.
11. Weissler, A.M., W.S. Harris, and C.D. Schoenfeld, Systolic time intervals in heart failure in man. Circulation, 1968. 37(2): p. 149-159.
12. Newlin, D.B. and R.W. Levenson, Pre-ejection period: Measuring beta-adrenergic influences upon the heart. Psychophysiology, 1979. 16(6): p. 546-553.

13. Kortekaas, M.C., et al., Small intra-individual variability of the pre-ejection period justifies the use of pulse transit time as approximation of the vascular transit. PLoS One, 2018. 13(10).
14. Clifford, G.D., Rpeakdetect function (ECG toolbox). 2008.
15. Van Velzen, M.H.N., et al., Effect of heat-induced pain stimuli on pulse transit time and pulse wave amplitude in healthy volunteers. Physiological Measurement, 2015. 37(1): p. 52-66.
16. van Velzen, M.H.N., et al., Increasing accuracy of pulse transit time measurements by automated elimination of distorted photoplethysmography waves. Med Biol Eng Comput, 2017: p. 1-12.
17. Rajzer, M.W.M.M.W., Comparison of aortic pulse wave velocity measured by three techniques: Complior, SphygmoCor and Arteriograph. Journal of Hypertension, 2008. 26(10): p. 2001-2007.
18. McEleavy, O.D., et al., Higher carotid-radial pulse wave velocity in healthy offspring of patients with Type 2 diabetes. Diabetic Medicine, 2004. 21(3): p. 262-266.

Chapter 8

Effect of Multi Photodiode Array positioning on pulse wave velocity measurement quality

Solving issues encountered in clinical studies

Marit. H.N. van Velzen, Sjoerd P. Niehof, Egbert G. Mik, Arjo J. Loeve

The Multi Photodiode Array (MPA) has previously been tested in clinical studies that were intended to provide insight in PWV values in various populations. Unfortunately, all these studies showed highly fluctuating and unrealistic results. To explore how to optimize the MPA positioning, four aspects were explored: light pollution reduction, using collimators, shortening the light travel paths and optimizing the contact between the MPA and the finger. The optimal use condition of the MPA appeared to be: soft-side positioning of the MPA, locating the active photodiodes across the middle, fleshy side-part of the distal phalanx and using light contact pressure between the MPA and the finger. A new sensor holder concept was designed to standardize the placement of the MPA on the finger for easy and intuitive application of the optimal use condition.

8.1 Introduction

The Multi Photodiode Array (MPA) sensor has previously been tested in one study on healthy volunteers and two clinical studies that were intended to provide insight in PWV (pulse wave velocity) values in various populations. Unfortunately, most of these data had to be excluded:

1. The study on healthy volunteers (Erasmus MC ethical board approval MEC-2012-139, see also Chapter 7 [1] and Appendix 8.A) was intended as a comparison between three PWV measurement systems: Biopac, Complior and the new MPA (see Chapter 7). In this study, all data obtained from 25 healthy volunteers with the MPA, used to measure PWVs on the left middle finger and reading out 4 of its 16 available photodiodes (diodes 1, 6, 11 and 16, spaced 4 mm apart) distributed evenly over the MPA, were eventually excluded entirely because too many PWV values showed very fast fluctuations between extreme positive and at that time unexplainable negative values.
2. While the study above was running, the first clinical study on patients (Erasmus MC ethical board approval MEC-2014-344, see also Appendix 8.B) was initiated. In this study PWVs of 23 patients undergoing surgery under general anesthesia was measured during initiation of the anesthesia. The PWV was measured using the MPA affixed to the index finger contralateral to the side of the infusion catheter. PWVs were measured using 4 photodiodes (diodes 1, 6, 11 and 16, spaced 4 mm apart) distributed evenly over the MPA. Again, too many PWV values showed very fast fluctuations between extreme positive and at that time unexplainable negative values.
3. A second clinical study (Erasmus MC ethical board approval METC-2015-159, see also Appendix 8.C) was conducted in a last attempt to obtain usable clinical data and after once more validating that all hardware and software of the MPA system worked properly. In this study one MPA sensor was placed on the left index finger and one on the left big toe. From each MPA sensor 2 photodiodes (diodes 1 & 16, spaced 12 mm apart) were used to measure PWV. From many patients no suitable measurements could be obtained (due to their diseases the pulse waves had too small amplitudes or were too heavily distorted to be observed) and when PWVs could be properly measured, these data again showed very fast fluctuations between extreme positive and at that time unexplainable negative values.

These results were unexpected, because both the successful functional validation of the MPA [2] (Chapter 6), accompanying pilot measurements on healthy volunteers, and intermediate tests done by the authors showed perfectly fine PWV measurements in several pilot volunteers and even for test-PWVs much higher than would occur in the fingers. However, as the distances between the diodes on the MPA are relatively small and the time differences between arrival of the pulse waves at the successive diodes very short, it was suggested that maybe the peaks of the pulse waves were insufficiently accurately detected due to undersampling. This could indeed have been a viable explanation, easily solvable by using a faster (but more expensive) DAQ-card for the sensor readings. However, the functional validation of the MPA [2] (Chapter 6), already proved that the MPA could easily handle speeds up to 45 times higher than the PWV in a finger. This was further confirmed by using Equation 8.1 to calculate the number of samples ($N_{samples}$) between the arrival times of a pulse wave at diodes spaced 1.6, 3.2 and 4.8 mm ($d_{a\text{-}b}$) for PWVs of 0.5 to 2 m/s (PWV) at a sample frequency of 62.5 kHz (f_s). Table 8.1 shows that even in the worst case scenario with the sensors closest together (even 3.2 to 7.5 times closer than in the experiments) and a very high PWV of 2 m/s in the finger, there would still be 50 samples between the arrival times of the pulse waves at the two diodes.

Consequently, taking the functional validation and above calculations into account, technical flaws or undersampling were definitively ruled out as possible causes of the oddities observed in the three human subjects studies.

$$N_{samples} = \frac{d_{a-b} \cdot f_s}{PWV} \qquad (8.1)$$

When considering the anatomy of the finger, no reason could be found to assume that negative PWVs would be true values originating from pressurized blood flowing in a distal-proximal direction. Yet, a possible explanation for the data obtained from the three human subject studies emerged when looking at the placement of the MPA photodiodes and LED light sources on the finger (see Figure 8.1).

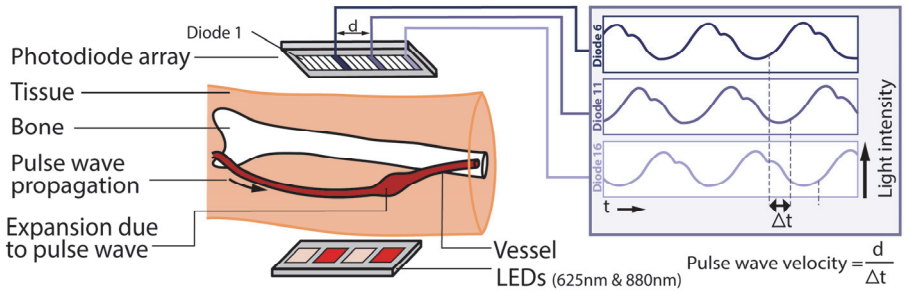

Figure 8.1: Schematic overview of the multi photodiode array (MPA) and illustration of the calculation of the pulse wave velocity.

It is apparent that light from the LEDs cannot reach the photodiodes in a straight line. The light has to travel around the bone through soft tissue and blood vessels, while being scattered and diffused along the way. Depending on the micro-anatomy in the finger and the travel path of the light from the individual LEDs, this implies that in this situation when a photodiode's signal shows a peak, it does not mean that at that time there was a maximum vessel expansion (e.g., due to a pressure pulse) at the line between that photodiode and its most directly opposing, closest LED. Therefore, due to this light-path effect, when a pressure pulse wave travels along the direction indicated in Figure 8.1, a signal peak may, perhaps contra-intuitively, occur earlier at a downstream photodiode than at an upstream diode.

Because of the light-path effect explained above, it was hypothesized that in order to enable reliable use of the MPA, a way had to be found to ensure or at least maximize the probability that the majority of the light that a photodiode receives originates from the LED directly across it. To clarify, in Figure 8.1 this would mean that each photodiode's signal is determined as much as possible by the light coming from the LED with the same number as the photodiode and by the anatomical structures directly between the photodiode and the LED.

Table 8.1: Number of samples between arrival times of pulse waves at different diodes on an MPA sensor for different PWVs at a sampling frequency of 62.5 kHz.

PWV [m/s]	**Diodes distance d_{a-b} 6-8**	**Diodes distance d_{a-b} 6-10**	**Diodes distance d_{a-b} 6-12**
2	50	100	150
1.5	67	133	200
1.0	100	200	300
0.5	200	400	600

The goal of this study was to explore how to optimize the detection of the LEDs' light by the photodiodes so that a peak in a photodiode signal truly corresponds to a maximum throughput of light over the line between that diode and its most directly opposing LED. Based on the considerations above and experiences during the development and testing of the MPA , four aspects were explored:

1. Removing light pollution coming from the measurement environment.
2. Using collimators to limit the field-of-view of the photodiodes
3. Shortening the light travel paths by placing the photodiodes and LEDs on the soft tissue palmar of the finger (Figure 8.2)
4. Optimizing the contact pressure between the MPA and the finger to avoid early light scattering and blood vessel occlusions

8.2 Methods

Throughout all of the tests described below, photodiodes 6, 8, 10 and 12 of the MPA were used and read out at 62.5 kHz (see Chapter 6 for further specifications of the data acquisition system). All tests were aimed at obtaining only realistic PWV values, corresponding with proximal-distal propagation of blood pressure pulse waves and an optimal line of sight between the photodiodes and their corresponding LEDs. The character, safety characteristics and durations of the tests were all such that no medical ethical committee review was needed.

To avoid over-idealization of results and to incorporate at least some anatomical variations, all tests were conducted on the left index fingers of authors MvV and AL. Subject 1 was a healthy female, 29 years old, 1.57 m body height, BMI 23.5, and Subject 2 was a healthy male, 35 years old, 1.74 m body height, BMI 23.1. Each PWV measurement consisted of placing the left index finger in a test setup (Figure 8.2) that held the MPA sensor to keep the position and contact pressure constant during each test.

After setting the test conditions (see the five descriptions below) and verifying that the MPA photodiodes showed undisturbed pulse waves (indicating that the finger wasn't squeezed too hard or too little and that the subject was properly holding still), the MPA data was acquired for 15-30 seconds. For each test the same data-filtering and PWV calculation methods were used as in Chapter 6, resulting in PWV values between each pair of read-out photodiodes (e.g., between 6 and 8, 6 and

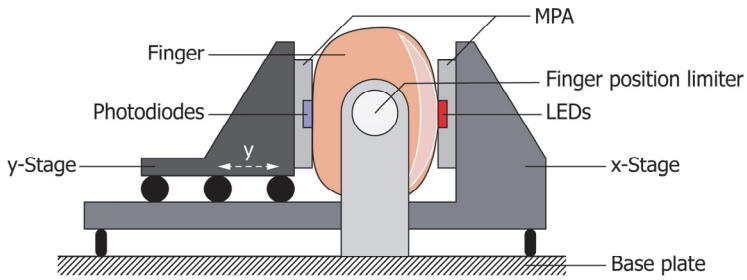

FRONT VIEW

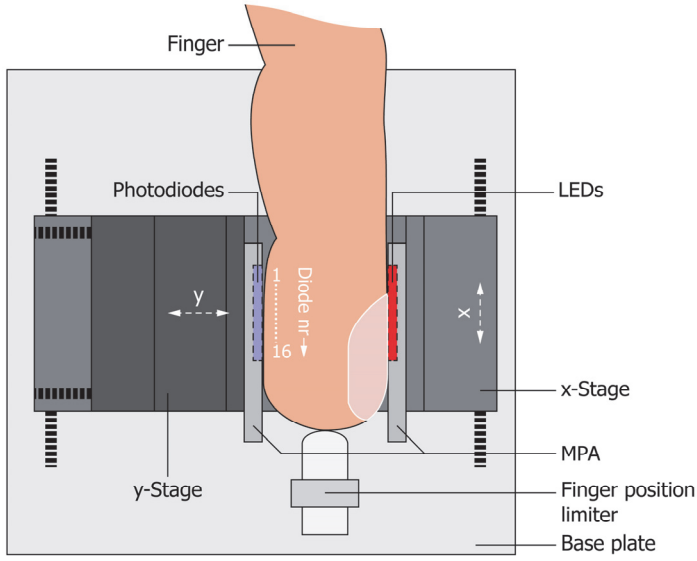

TOP VIEW

Figure 8.2: Setup used to systematically investigate and standardize the effect of MPA positioning along the finger axis and contact pressure with the finger on PWV measurement quality. The finger is placed with the nail towards the LEDs. The x-stage is used to control the placement of the MPA along the finger. The y-stage is used to control the contact pressure between the MPA and the finger. The finger position limiter is used to assure consistent positioning of the finger.

10, 6 and 12, 8 and 10 etc., each indicated by $PWV_{a\text{-}b}$ (with a-b indicating the photodiodes pair for which the PWV value is given) and from which the median PWV of all photodiode combinations (PWV_{med}) was determined.

8.2.1 Removing light pollution

The first test served to find out whether light coming from the environment—such as light from lamps or computer screens—would affect the PWV measurements. The PWV measurements on both subjects were done on each subject once with the MPA and finger open to environmental light as usual and once with a black, light blocking cloth draped over the entire setup, MPA and finger. Between the measurements with and without cloth, the subject sat still with their finger kept in the setup without any alterations. The measurements were conducted in an approximately 2.5x4 m large, well-lit hospital room with several computer screens in the close proximity of the test setup and three TL lights.

8.2.2 Using collimators

One way of limiting the amount of light that a photodiode receives from other directions than from their directly opposing LEDs might be found in limiting the field photodiode's field of view. To this purpose, a simple collimator was made, consisting of a black, opaque plate of acrylic glass, laser cut to the shape and dimensions shown in Figure 8.3. By placing the collimator over the MPA, with the openings over the active photodiodes and the other photodiodes blocked, their fields of view (the range of directions from which the photodiodes could receive light) were narrowed. PWV measurements were done on each subject once with

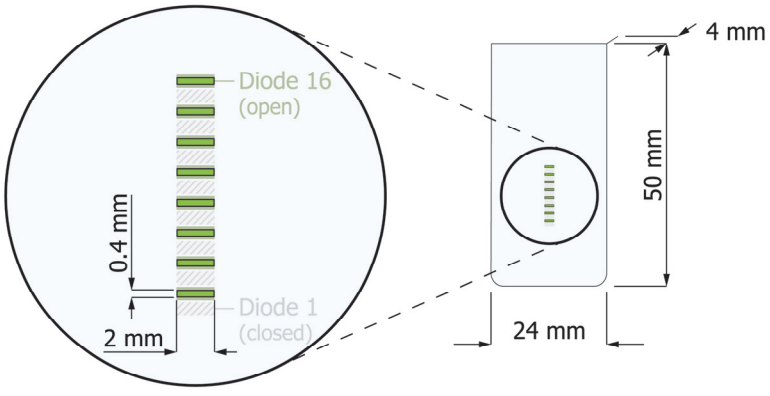

Figure 8.3: Dimensions of the collimator (mask that ensures that only light falling-in nearly perpendicular to the diode reaches a diode) used to narrow the fields of view of the photodiodes. The collimator is shown on the right half of the image. The circular inset on the left is a magnification of the area indicated on the collimator.

and once without the collimator in place.

8.2.3 Shortening light travel paths

Because tests in sections 8.2.1 and 8.2.2 did not provide satisfying results, some explorative tests were done to see if better results were obtained when placing the photodiodes and LEDs both along the soft tissue on the volar side of the finger. The reasoning behind this was that this would shorten the travel path of the light, not only in absolute sense, but also as compared to the travel path of light coming from other directions than straight across a photodiode. Furthermore, because the light then only has to span soft tissue, less disturbing structures (i.e. bone, which is highly scattering) blocked or scattered the light, enabling a more direct line of sight than for the positioning in Figure 8.1. To stably and reliably put the MPA in the new soft-side position, an approximately 1 cm thick layer of textile was placed under the finger (Figure 8.4).

Next, the effectiveness of the new soft-side position and its sensitivity to the sensor placement location along the axis of the finger were investigated. The left index finger of the test subject was placed initially with photodiode 16 at the proximal ridge of the distal phalanx, which put the active diodes (6, 8, 10 and 12) halfway the distal phalanx. The PWV acquisition was started, while after every 20 seconds, the x-stage of the setup was adjusted to move the MPA for 5 mm more proximally over the finger. At each 5 mm the sensor was kept in place and PWVs were measured for 20 seconds before moving to the next more proximal location until the sensor had moved 20 mm, finally locating the active photodiodes at the site where the medial and distal phalanx meet. This test was done on entirely on

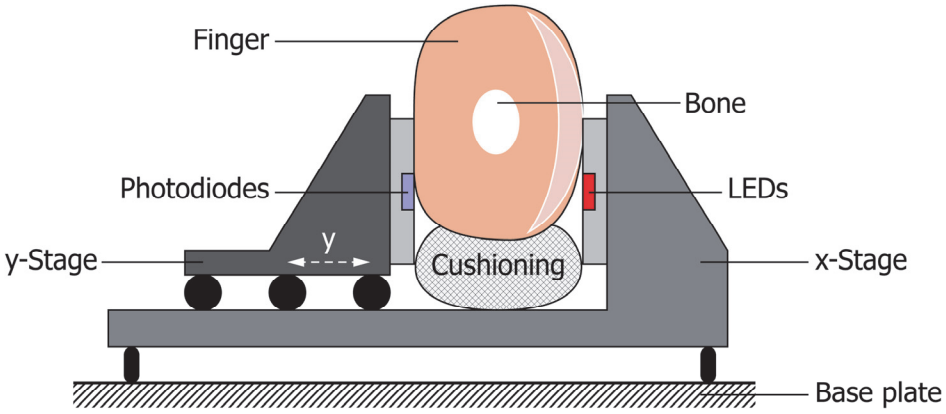

Figure 8.4: Front view of the adaptation used to obtain the soft-side positioning of the MPA with respect to the finger.

Subject 1 and only the two locations providing the most promising results were repeated on Subject 2.

8.2.4 Optimizing contact pressure

During the tests in 8.2.1 to 8.2.3 it was noticed that the contact pressure between the MPA and the finger could strongly affect the measured signals. When pressing too hard with the MPA not in the soft-side position, the pulse waves disappeared due to occlusion of the blood vessels. Yet, also when applying light or moderate pressure, sometimes good and clearly distinguishable pulse waves were visible in the MPA signals, but when calculating the PWVs from these signals these could ever still result in randomly scattered, unrealistically high or even negative PWV values. Therefore, the best sensor location from the test in section 8.2.3 was chosen and for that position the effect of finger-sensor contact pressure was further explored.

For both subjects the finger was placed as shown in Figure 8.4. The contact pressure between the MPA and the finger was varied by moving the y-stage of the setup in steps of 0.5 mm. Because both subjects had different sized fingers different pressure levels were used in different orders for both subjects:

Subject 1: The y-stage was initially put such that there was almost impalpable contact between the MPA and the subject's finger. At this pressure, PWVs were measured for 20 seconds. Next, the y-stage was tightened by 0.5 mm and another 20 seconds PWVs measurement was done. This was repeated until and including the pressure at which PWs became undistinguishable. After that, the y-stage was moved back again in two steps of 0.5 mm and at each level another 20 seconds measurement was taken.

Subject 2: A similar approach was taken as for Subject 1, but now the initial position of the y-stage was set to achieve a medium pressure level, comparable to that providing successful measurements in sections 8.2.1 to 8.2.4. From there, first the stage was loosened in three steps of 0.5 mm until there was almost impalpable contact and the PWs became undistinguishable. Then, the y-stage was tightened again in steps of 0.5 mm until the contact pressure became uncomfortable. At each contact pressure level a 20 seconds PWVs measurement was done.

8.3 Results

8.3.1 Removing light pollution

No effect of covering or not covering the measurement area was observed. All data showed comparable amplitudes and no observable improvements in the PWV values were found (see Figure 8.5).

8.3.2 Using collimators

The collimators did have an effect on the measured signals, but not in the way expected. The collimator reduced the amount of light reaching the sensor so strongly that the MPA signals became unusable.

8.3.3 Shortening light travel paths

Changing the MPA placement to the soft-side position enabled proper PWV measurements. Figure 8.6 shows the PWVs for the individual tested locations along the axis of the left index fingers for Subject 1 and 2. All locations (A to D) provided reasonably good results (few or no negative PWV values), but the locations where

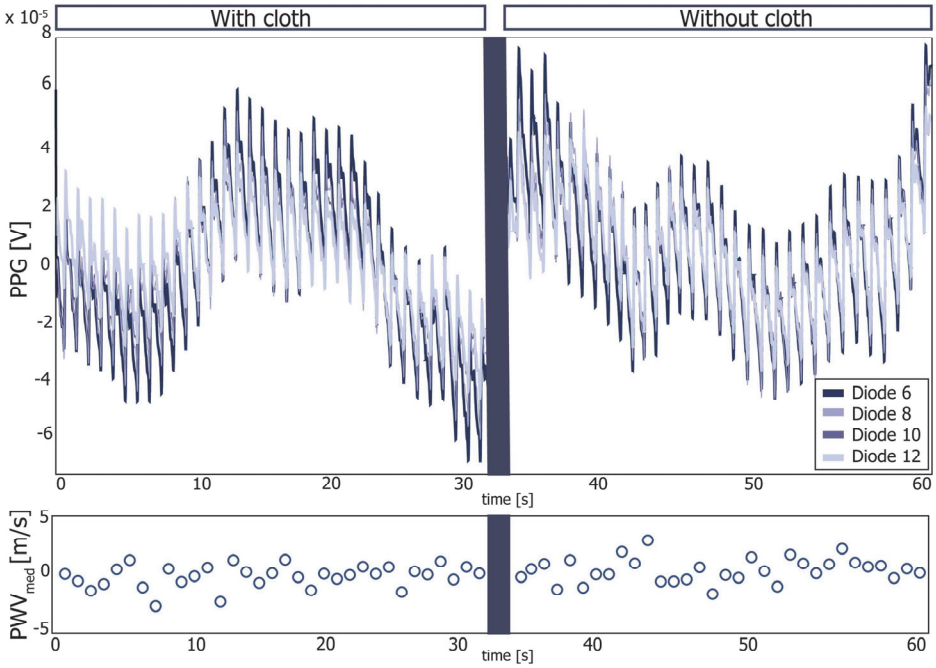

Figure 8.5: Amplitudes of photodiode signals and resulting PWV_{med} for tests with and without black opaque cloth covering the measurement area. The PWV values fluctuate around zero and are often negative.

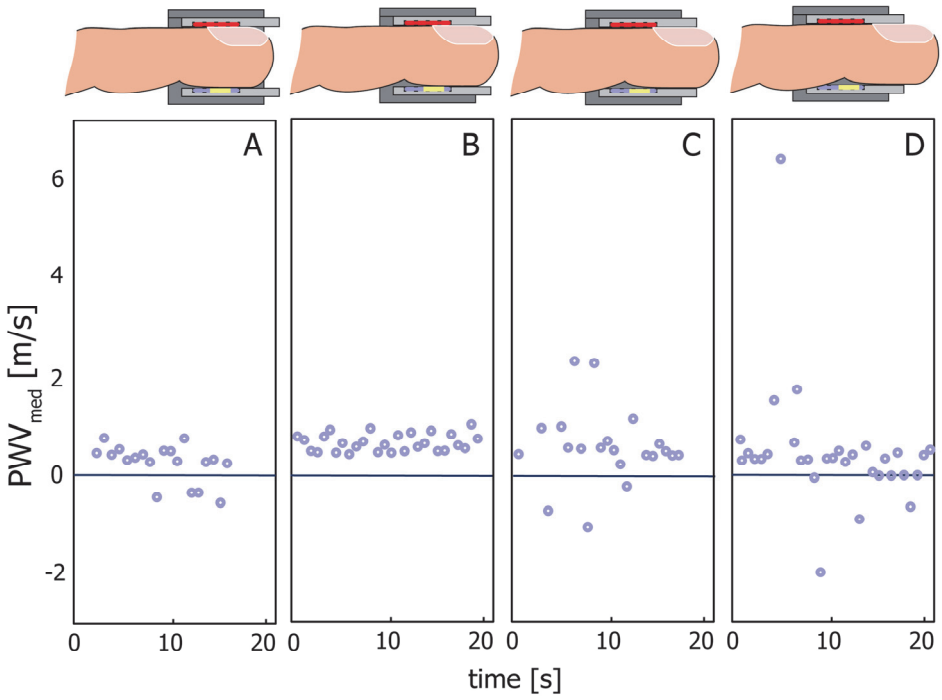

Figure 8.6: PWV_{med} measured during 20 s intervals at different positions along the axis of the left index finger. Gentle contact pressure between the MPA and the subjects' fingers was used. The position of the photodiode array of the MPA is expressed as the distance in millimeters that photodiode 16 on the array was moved from the ridge at the base of the distal phalanx towards the hand.

the active photodiodes got very close to or on the

distal-interphalangeal joint (C and D), the PWVs started to show more scattering. The best location, showing the little scattering and no negative PWVs appeared to be location B, where the active photodiodes (6, 8, 10 and 12 yellow area) spanned the soft side part of the fingertip.

8.3.4 Optimizing contact pressure

Figure 8.7 shows the PWVs obtained in Subjects 1 and 2 for the tested contact pressures created by tightening or loosening the y-stage. For both subjects it appeared that the best PWV measurements were obtained when applying light contact pressures (see Figure 8.7 for quantification). If pressures were too low, the data became very much scattered with many negative PWVs. Squeezing too hard may obstruct the blood flow, causing pulse waves to disappear or be malformed and making the calculated PWVs scatter and become unreliable.

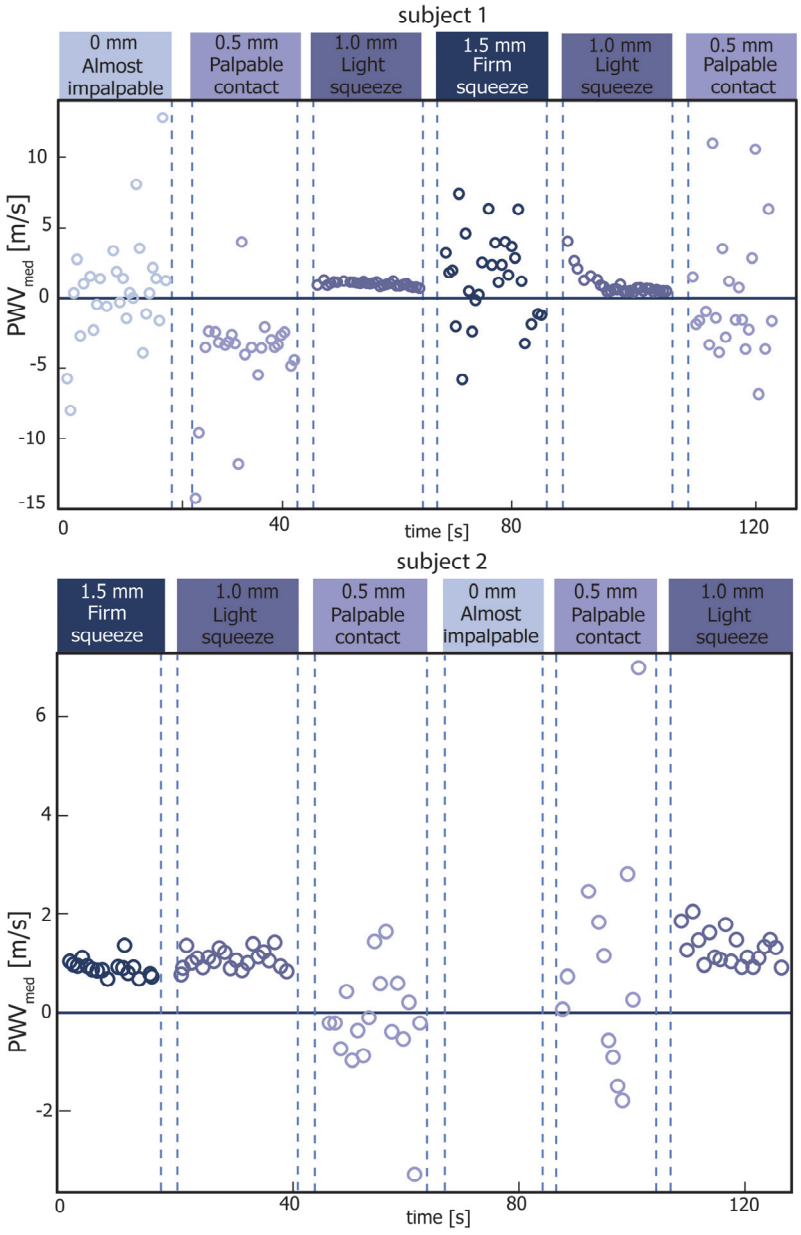

Figure 8.7: PWV_{med} measured during 20 s intervals and at different contact pressures with the MPA at the soft-side position (Figure 8.4) at location B from Figure 3. The contact pressures are expressed both in subjective terms as well as in the distance [mm] that the y-stage (Figure 8.2) was moved to squeeze the finger, starting from the 0-position providing almost impalpable contact between the MPA and the finger.

8.4 Discussion

This study aimed to establish how the MPA can be used or adapted in such a way that PWV measurements are less affected by light-path effects between the LED array and the photodiode array. The results showed that removing light pollution did not contribute to a solution in any way. Yet, the suitability of using collimators could not be excluded in this study. However, further exploring that solution would require stronger light sources and would make the design of the MPA more complex. As a simpler solution was found, the idea of using collimators was abandoned.

The key to achieving credible PWV measurements with little scattering and no negative values appeared to be simply in the positioning of the MPA on the finger. Avoiding disturbing (highly scattering, reflecting or absorbing) structures in the line of sight between LEDs and photodiodes and by making the line of sight shorter and more direct enabled true measurement of the light transmission fluctuations between a photodiode and the LED directly opposed to it. The new soft-side positioning of the MPA involved placing the photodiodes and LEDs such that the light was transmitted only through the soft-tissues on the side of the finger.

It appeared that, although the soft-side positioning shown in Figure 8.4 was much more robust than the original sensor positioning shown in Figure 8.1, the measurement quality still appeared to depend on the placement location of the active photodiodes along the fingertip and on the contact pressure between the sensor and the finger. When located too far to the tip of the finger, the most distal photodiodes loose contact with the finger, whereas locating the active photodiodes close to the site where the medial and distal phalanx meet, the joint structures seem to get in the line of sight, with both situations leading to scattered PWV measurements with negative values. The optimal use condition of the MPA provided consistently satisfying results and appeared to be:

- soft-side positioning of the MPA: locating the active photodiodes across the middle, fleshy side part of the distal phalanx,
- and using a light contact pressure.

The major limitation of the presented work is that it is of highly explorative nature. However, the robustness and user-friendliness of the optimal use condition described above was further substantiated in a study on 30 healthy volunteers (Erasmus MC ethical board approval MEC-2017-453). For this study a new sensor

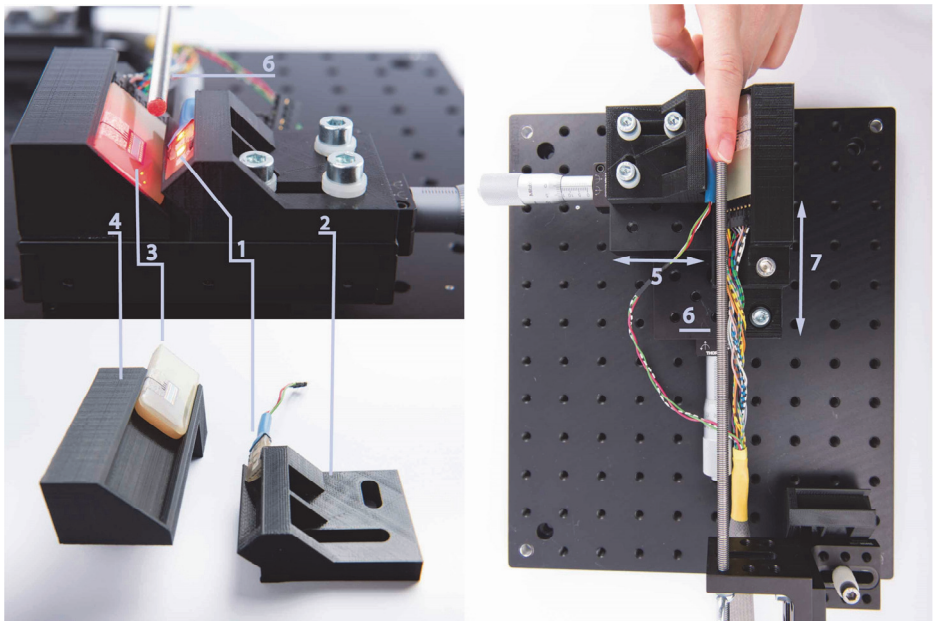

Figure 8.8: Test setup and sensor holder designed for the optimal use condition of the MPA, used to measure PWVs in 30 healthy volunteers. The main parts of the setup are: 1) LED array holder; 2) LED array; 3) Photodiode array; 4) Photodiode array holder; 5) y-stage, used to control distance between LEDs and photodiodes; 6) Finger position limiter; 7) x-stage, used to control photodiode array location along the finger. For further explanation, please see Chapter 9.

holder was designed (Figure 8.8) to standardize the placement of the finger on the MPA for the optimal use condition of the MPA (see Chapter 9 for further details). A standardized, light contact pressure was applied by placing an elastic tourniquet band at a preset pretension over the finger. During the study all participants could easily, rapidly, and consistently be placed in the setup. All measurements could be done without any adjustments to the setup, sensor placement or contact pressure.

The PWV measurements all showed good pulse waves, little scattering and positive PWVs, except for one subject who had extremely cold hands and later told to suffer from pernio, which perfectly explained why no proper pulse waves could be observed.

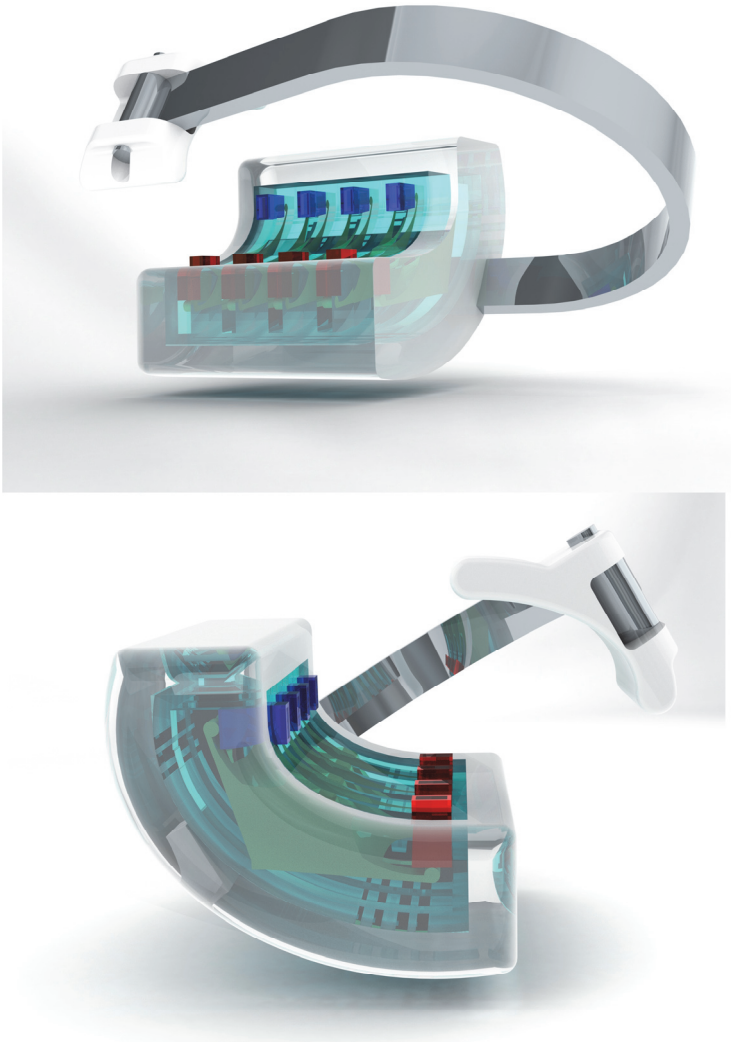

Figure 8.9: Artist impression of the MPA system used in a clinical-practice-ready medical device for integrated measurement of pulse rate, oxygen saturation and pulse wave velocity. Sensor location along the finger is standardized by using a position indicator combined with anti-slip edges and a self-locking limiter that prevents the finger from moving into the sensor clip once set at the correct distance. Contact pressure between the sensor and the finger is controlled by a self-balancing spring system.

An optimal use condition for the MPA was established and proved to be very suitable for human subject research. However, before being suitable for everyday clinical use, the MPA should be redesigned into a pulse-oximeter-like device that clips on the finger and ensures proper and consistent placement and contact

pressure independent of the caretaker or patient. An artist impression of how this future device could be designed is shown in Figure 8.9. In order for this design to function robustly and consistently, future research should provide more insight into the optimal contact pressure, location and orientation of the MPA on the finger.

8.5 Conclusions

The current study has brought the MPA from a pure research tool one step closer to a clinical-practice-ready diagnostic device. It was shown that soft-side positioning halfway the distal phalanx with some light pressure was the key to obtaining consistent and good quality measurements. Further developments will have to lift the MPA from a research tool to a user-friendly medical device for every-day clinical practice.

8.6 Acknowledgments

The authors would like to thank Arjan van Dijke of the Delft University of Technology for providing parts for the test setup.

8.7 References

1. van Velzen, M.H.N., et al., Comparison between pulse wave velocities measured using Complior and measured using Biopac. Journal of Clinical Monitoring and Computing, 2018. p1-7.
2. Van Velzen, M.H.N., et al., Design and functional testing of a novel blood pulse wave velocity sensor. Journal of medical devices, 2017. 12(1)

Appendix 8.A

First MPA tests on healthy volunteers

Chapter 7 [1] described the study that was conducted in healthy volunteers to measure the PWV with two different systems over different trajectories to investigate whether these provided comparable results. This study was initially intended as a comparison between three PWV measurement systems: Biopac, Complior and the MPA, but the MPA results were excluded because these provided no usable results at all. For reasons of completeness, these results are summarized below.

Materials & Methods

Twenty-five healthy volunteers, 20-30 years old, without any known history of atherosclerosis associated diseases (such as diabetes mellitus, hypertension, coronary artery disease, stroke, renal disorder) or injuries at the upper limbs were included in the study. This study was approved by the medical ethics committee of Erasmus University Medical Center Rotterdam, the Netherlands (approval number MEC-2012-139) and was conducted between 20 November 2014 and 17 December 2014. For further details about the study design, see Chapter 7.

The stripped MPA was used to measure PWVs on the left middle finger by reading out four of its sixteen available photodiodes (diodes 1, 6, 11 and 16, spaced 4 mm apart). The stripped MPA (see Appendix A) was placed as shown in Figure A.2 of Appendix A.

The data were analyzed using Matlab R2010a (The MathWorks, Inc. Matick, MA, USA) to calculate the PWVs from the PPG-signals. The PPG-signals were filtered with a fourth-order low-pass Butterworth filter with a cut-off frequency of 9 Hz. The PWV for each position (sitting 1, lying, standing, sitting 2) was determined for each pair of photodiodes i and j by dividing the distance between these photodiodes by the time difference between the arrival of the PPG-signals' peaks at the locations of these successive photodiodes. This was done for each combination of any two of the used photodiodes (photodiodes pairs 1-6, 6-11, 11-16, 1-11, 6-

16, 1-16). All distorted (and thus unusable) PWs were filtered out using the '7Step PW-Filter' [2]. The median PWV was calculated per heartbeat for each combination of any of two of the used photodiodes. The mean PWV was calculated for each position.

Results & Discussion

Figure 8A.1 shows three examples of typical PWV values measured in three of the volunteers. In each section of Figure 8A.1 the PWVs for each combination of any two of the used photodiodes are shown for position Sitting 1.

Figure 8A.1A shows a dataset in which almost all of the PWVs of each combination of any two of the used photodiodes are positive and around 2 m/s. The PWV between photodiodes 1 and 6 is most of the time negative, extremely high, or extremely low. Figure 8A.1B shows a dataset with mostly negative PWV values. The PWV between photodiodes 11 and 16 is the only one for which the PWV sometimes was positive. However, the PWV between photodiodes 11 and 16 is not stable and shows a very large variation (between -5 and 20 m/s). Figure 8A.1C shows a dataset in which the PWV values are scattered all over the plot, with PWV values between -50 and 50 m/s.

The results obtained in this study were unexpected, because both the successful functional validation of the MPA [3] (Chapter 6), accompanying pilot measurement on healthy volunteers, and intermediate tests done by the authors showed perfectly fine PWV measurements, even for test-PWVs much higher than would occur in the fingers. Although Figure 8A.1 shows only three examples, these data are representative for all healthy volunteers. The data obtained with the MPA were eventually excluded entirely because too many signals showed very fast PWV fluctuations between extreme positive and at that time unexplainable negative values. As the observed results remained unexplainable, it was recommended, and later decided, to first investigate how to optimize the PWV measurements using the MPA.

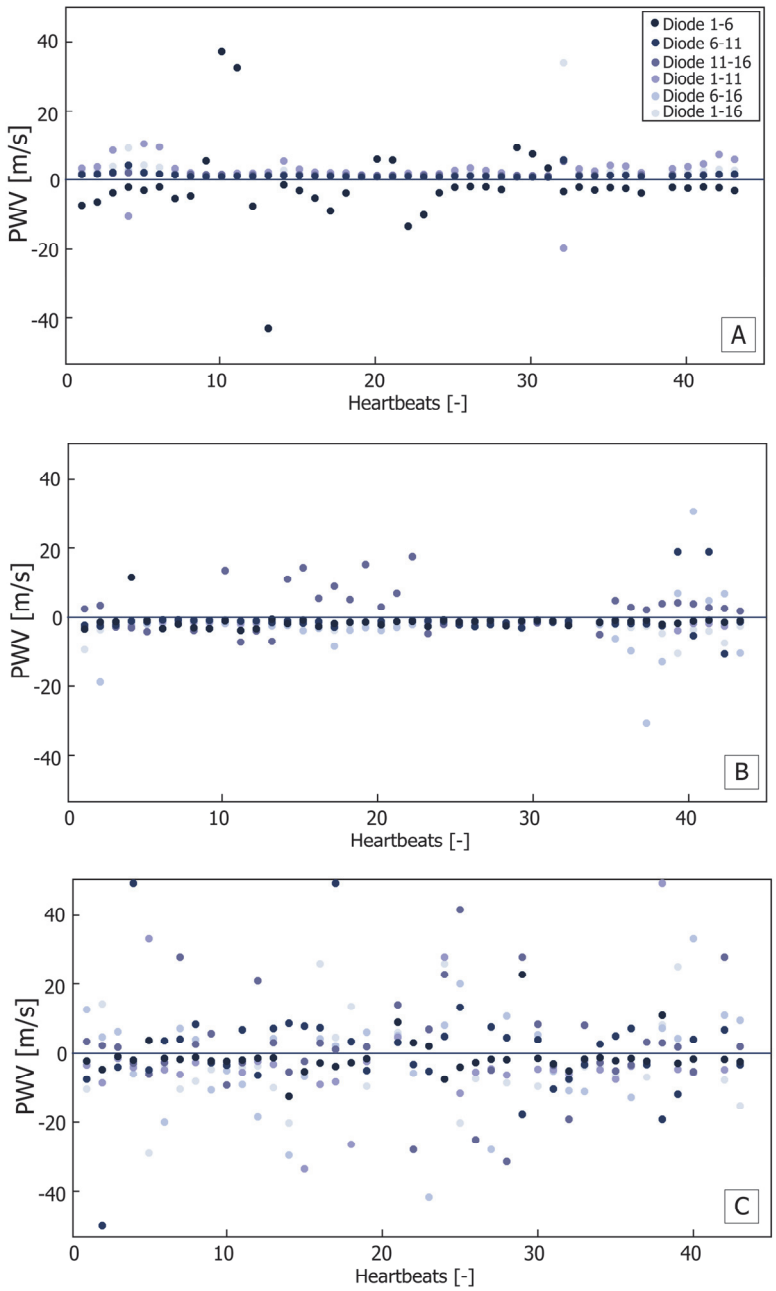

Figure 8A.1: Typical examples of PWVs measured with the MPA in three different volunteers (A, B and C).

References

1. van Velzen, M.H.N., et al., Comparison between pulse wave velocities measured using Complior and measured using Biopac. Journal of Clinical Monitoring and Computing, 2018. p1-7
2. Van Velzen, M.H.N., et al., Increasing accuracy of pulse transit time measurements by automated elimination of distorted photoplethysmography waves Med Biol Eng Comput, 2017: p. 1-12.
3 Van Velzen, M.H.N., et al., Design and functional testing of a novel blood pulse wave velocity sensor. Journal of medical devices, 2017. 12(1)

Appendix 8.B

MPA tests on anesthetized surgical patients

During induction of general anesthesia the compliance of vessels changes (in general: increases) because of loss of sympathetic drive and/or vascular tonus. The change in compliance of the vessels is perceptible in the pulse wave velocity (PWV) of the pressure pulse waves (PWs). The magnitude of the change in PWV may indicate a potential problem with the arterial stiffness, e.g. due to structural vascular changes or the use of medication. Ultimately, the Multi Photodiode Array (MPA) could aid in identifying patients at risk of cardiovascular events during or after general anesthesia. The aim of this study was to verify whether the MPA can be used to detect changes in PWV due to altered blood vessel compliance during induction of general anesthesia.

Materials & Methods

Twenty-three patients, 20-75 years old, without injuries at the upper limbs were included in this study. Any patient who was scheduled to receive general anesthesia could be included in this study. No specific exclusion criteria were applied as long as the measurements were technically feasible (i.e. presence of an accessible finger). This study was approved by the medical ethics committee of Erasmus University Medical Center Rotterdam, the Netherlands (approval number MEC-2014-344) and was conducted between 31 July 2014 and 7 May 2015.

Prior to transfer to the operating room, the patients were informed about the study and were asked questions concerning their general health. The stripped MPA-sensor (see Appendix A) was placed on the index finger, contralateral of where the infusion catheter was placed. During the measurement, the patient was lying in bed or on the operation table. A baseline PWV measurement was conducted on the preoperative holding for approximately 1 minute (M1). After that, the patient was transferred to the operation room and placed from the bed on the operation table. In the operation room, the PWV measurements started with a baseline measurement for approximately 1 minute before the anesthesia

had been induced (M2). During the entire procedure of induction of general anesthesia, continuing until 1 minute after the procedure the PWV was measured (M3). The anesthesiologist indicated whether general anesthesia had set in.

PWVs were measured using four photodiodes (diodes 1, 6, 11 and 16, spaced 4 mm apart). The data were analyzed using Matlab R2010a (The MathWorks, Inc. Matick, MA, USA) to calculate the PWV from the PPG-signals. The PPG-signals were filtered with a fourth-order low-pass Butterworth filter with a cut-off frequency of 9 Hz. The PWVs for each measurement period (M1, M2, M3) were determined per heartbeat for each pair of photodiodes *i* and *j* by dividing the distance between these photodiodes by the time difference between the arrival of the PPG-signals' peaks at the locations of these successive photodiodes. This was done for each combination of any two of the used photodiodes (photodiodes pairs 1-6, 6-11, 11-16, 1-11, 6-16, 1-16). Any distorted (and thus unusable) PWs were filtered out using the '7Step PW-Filter' [1]. The median PWV was calculated for each combination of any of two of the used photodiodes per heartbeat. The mean PWV was calculated of each measurement period.

Results & Discussion

Of all patients, only one showed consistent, positive and stable PWV-values during the three measurement periods (see Figure 8B.1 and Table 8B.1). This patient was a male, 29 years old, 1.86 m body height, BMI 23.7, smoking, American Society of Anesthesiologists score (ASA) II. The patient's blood pressure was 151/90 before start of induction of general anesthesia and the MPA was measured on the left index finger. All the other patients' PWV values showed the same patterns as in Appendix 8A (see Figure 8A.1) with fast fluctuations between extreme positive and at that time unexplainable negative values.

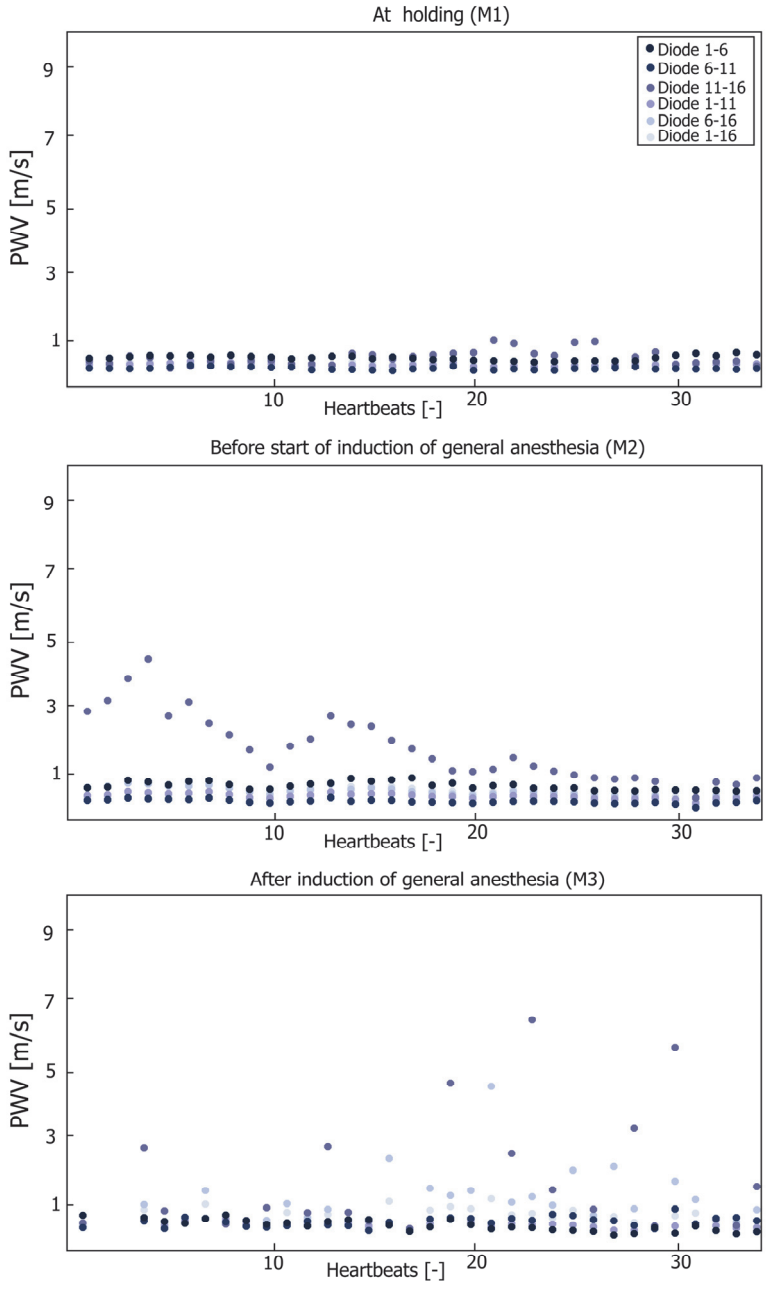

Figure 8B.1: PWV values of the single volunteer showing consistently positive and stable results during measurements at the holding, and before and after induction of general anesthesia.

Table 8B.1: The PWV values measured during each measurement period in the single volunteer who showed consistently positive and stable results.

	PWV [mean ± sd]
Measurement period 1 [m/s]	0.6 ± 0.1
Measurement period 2 [m/s]	0.8 ± 0.3
Measurement period 3 [m/s]	1.0 ± 0.2

Because only one patient could be included for the analyses, the study was considered failed and the results were not further analyzed. As the observed results remained unexplainable, it was recommended, and later decided, to first investigate how to optimize the PWV measurements using the MPA.

References

1. Van Velzen, M.H.N., et al., Increasing accuracy of pulse transit time measurements by automated elimination of distorted photoplethysmography waves Med Biol Eng Comput, 2017: p. 1-12.

Appendix 8.C

MPA tests on outpatients with vascular disease

The Ankle Brachial Index (ABI) is considered the gold standard indicator of peripheral artery disease (PAD) [1]. The gold standard for determining the ABI consists of taking the ratio between the systolic blood pressure at the ankle and the systolic blood pressure in the arm [2]. An ABI below 0.9 is a reliable indicator of compromised blood flow in the legs and is diagnostic for PAD [2, 3]. Furthermore, a decreased ABI is associated with an increased risk for cardiovascular events in general.

In clinical practice, ABIs are routinely measured using a Doppler blood flow detector and a sphygmomanometer, once on the arm and once on the leg. The sphygmomanometer cuff is inflated proximal to the artery of the extremity until the arterial pulse ceases. The cuff is then slowly deflated until the artery's pulse wave is re-detected by the Doppler probe. The pressure in the cuff at that moment indicates the systolic pressure of that artery. The same procedure is performed in both arms and legs. The ABI is calculated by dividing the systolic blood pressure at the ankle level by the systolic blood pressure at the arm.

It was hypothesized that the Multi Photodiode Array (MPA) may potentially aid in more objectively identifying patients with PAD by measuring the PWV instead of the ABI. Furthermore, the MPA may allow easier and simpler measurements than the method described above. Therefore, the aim of this study was to verify whether the MPA can detect changes in peripheral PW due to the presence of cardiovascular disease as determined by the gold standard ABI.

Materials & methods

A prospective, observational study was conducted. Fifty-two patients, older than 18 years, who were already scheduled for ABI measurement as part of their treatment for PAD at the department of Vascular Surgery in the Erasmus Medical Center, Rotterdam, the Netherlands, were included in this study after obtaining written informed consent. There were no specific exclusion criteria as long as the

measurement was technically feasible (i.e. presence of an accessible finger/arm/leg/toe). The study was approved by the Medical Ethics Committee of Erasmus University Medical Center Rotterdam (approval number MEC-2015-149) and was conducted between 5 June 2015 and 24 July 2015.

The standard ABI-procedure at the department of Vascular Surgery consist of:

1. Measuring the blood pressure (BP) on the left and right upper arms
2. Measuring the ABI on the left and right sides, using the Dopplex ABIlity device (Huntleigh Healthcare, Wales, United Kingdom).
3. Walking for maximum of 10 minutes on a treadmill.
4. Measuring the BP on the left arm.
5. Measuring the ABI on the left and right side, using the Dopplex ABIlity device (Huntleigh Healthcare, Wales, United Kingdom).

After starting the standard ABI-procedure, the PWV was measured two times for up to 1 minute, each time before the ABI-measurement (between steps 1 and 2 and between steps 4 and 5). Two Vamulec MPA sensors (see Appendix A) were used as shown in Figure A.3 of Appendix A: one on the left index finger and one on the left big toe.

From each Vamulec MPA-sensor two photodiodes (diodes 1 & 16, spaced 12 mm apart) were read out to measure the PWV. The data were analyzed using Matlab R2010a (The MathWorks, Inc. Matick, MA, USA) to calculate the PWV from the PPG-signals. The PPG-signals were filtered with a fourth-order low-pass Butterworth filter with a cut-off frequency of 9 Hz. Any distorted (and thus unusable) PWs were filter out using the '7Step PW-Filter' [3]. The mean PWV for each of the two measurement periods was determined by dividing the distance between photodiodes 1 and 16 by the time-difference between the arrival of the PPG-signals' peaks at the locations of these successive photodiodes.

Results & Discussion

Of the 52 patients, 17 patients were excluded from the analysis because they could not undergo the entire standard ABI-procedure. This was often due to a patient's inability to walk on the treadmill. Another reason sometimes occurring was that the patient had a shunt in the left arm, making the BP and ABI measurements on that arm impossible.

Table 8C.1: The ABI (ankle brachial index) classification and corresponding values.

Number of patients	Classification	ABI [mean ± sd]
2	Serious	0.5 ± 0.0
8	Moderate	0.7 ± 0.1
5	Mild	0.9 ± 0.1
16	Normal	1.2 ± 0.1
4	Incorrectly high	1.4 ± 0.1

The remaining 35 patients (20 male, 15 female) underwent the entire ABI-procedure. The Dopplex ABIlity device returned the ABI value and classification (Table 8C.1).

In many patients no suitable PWV-measurements could be obtained at all. In the classification groups 'serious', 'moderate' and 'mild' not a single patient had a usable PWV-measurement. In the group 'normal' there were nine usable PWV-measurements for the finger and eleven usable PWV-measurements for the toe. However, in only two patients a usable PWV-measurement could be obtained before and after walking the treadmill. In the group 'incorrectly high' there was one usable PWV-measurement for the finger and there were two usable PWV-measurements for the foot. For only one patient a usable PWV-measurement could be obtained before and after walking the treadmill.

The PWV-measurements were largely unusable because the patients showed hardly any undistorted PWs, which was likely caused by the patients' diseases. In the few patients who did show PWs that could be properly measured, the PWV-values still showed fast fluctuations between extreme positive and at that time unexplainable negative values, like in Appendices 8A & 8B.

Figure 8C.1 shows two typical examples of the data. One of the very few patients with usable results and one of the many patients with unusable results. Table 8C.2 shows the results of the ABI-measurement for these two example patients.

Patient A was one of the few showing usable PWV-measurements. Patient A was a male, 51 years old, 1.74 m body height, BMI 24.8, smoking, non-diabetes. All PWs (100%) proved to be of good quality according to the '7Step PW-filter' (see Chapter 2) before and after walking. The PWV values in the toe showed larger variations than in the finger.

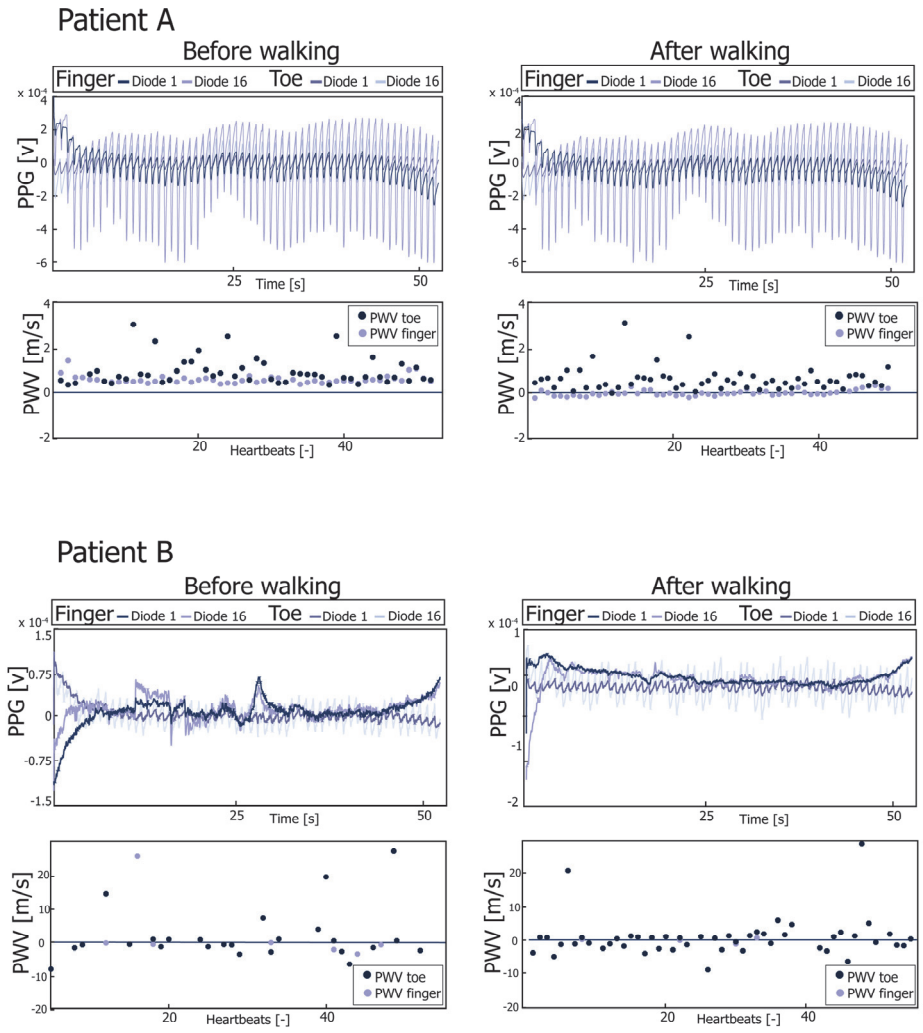

Figure 8C.1: The PPG (photoplethysmography) and PWV (pulse wave velocity) measured with the MPA during the ABI-procedure for two example patients.

Table 8C.2: The ABI (ankle brachial index) and PWV (pulse wave velocity) values obtained for the two example patients discussed in this appendix.

			Patient A	Patient B
Before walking	**ABI**		1.06	0.55
	PWV [mean ± SD]	**finger**	0.6 ± 0.2	-0.4 ± 10.2
		toe	0.8 ± 5.1	-0.6 ± 11.7
	PWV index [foot / hand]		1.3	1.3
After walking	**ABI**		1.08	0.95
	PWV [mean ± SD]	**finger**	0.6 ± 0.2	0.1 ± 0.8
		toe	1.2 ± 0.6	0.5 ± 11.2
	PWV index [foot / hand]		2.0	4.8

Patient B is an example of the unusable PWV-measurements, in which hardly any suitable values could be obtained at all. Patient B was a male, 80 years old, 1.77 m body height, BMI 28.7, smoking, non-diabetes. In this patient, mainly bad quality PWs were observed, with only 13% and 46% suitable PWs before walking and 7% and 93% suitable PWs after walking in the finger and toe, respectively. After walking there were only 4 PWs in the finger that passed the '7Step PW-filter' of the 55 PW in total. Consequently, there were too few PWV-values left for a reliable measurement.

Because almost all subjects had to be excluded during the analysis, this study was considered failed and the results were not further analyzed. As the observed results remained unexplainable, it was recommended, and later decided, to first investigate how to optimize PWV measurements using the MPA.

References

1. Weitz, J.I., et al., Diagnosis and treatment of chronic arterial insufficiency of the lower extremities: A critical review. Circulation, 1996. 94(11): p. 3026-3049.
2. Al-Qaisi, M., et al., Ankle Brachial Pressure Index (ABPI): An update for practitioners. Vascular Health and Risk Management, 2009. 5: p. 833-841.
3. Van Velzen, M.H.N., et al., Increasing accuracy of pulse transit time measurements by automated elimination of distorted photoplethysmography waves Med Biol Eng Comput, 2017: p. 1-12.

Chapter 9

Measuring pulse wave velocity with a novel, simple sensor on the finger tip: A feasibility study in healthy volunteers

Marit H.N. van Velzen, Sjoerd P. Niehof, Egbert G. Mik, Arjo J. Loeve

Submitted, 2019

The speed of pressure pulses traveling through the blood, the pulse wave velocity (PWV), is a metric that provides substantial information about the passive and active elasticity of the blood vessels. Therefore, PWV is a valuable parameter in the diagnosis of cardiovascular diseases. The purpose of this study was to investigate whether a novel, simple, easy- to use, photoplethysmography-based Multi Photodiode Array (MPA) provides PWV measurements that agree with measurements done with more complicated and harder-to-use systems currently used in clinical practice. An often-used vascular perturbation that changes the conduit artery vasomotor tone during reactive hyperemia was imposed on thirty healthy volunteers. The MPA was used alongside and its results compared to those of a commonly used measurement device, the Biopac-system, during flow-mediated dilation (FMD). This way it was investigated if measurements with these systems, measuring over two different vessel trajectories agree. The baseline absolute PWV values were significantly lower for the MPA as compared to the Biopac-system. Yet, the Bland-Altman plots show good agreement between the two measurement systems. Additionally, the Bland-Altman plot showed good agreement between the two PWV measurement techniques during the FMD. Measuring PWV with the MPA in clinical practice is feasible and provides reliable data in healthy volunteers. The MPA may substantially simplify PWV measurements and may enable long-term PWV monitoring as long as one is aware of the relation between PWV and the vascular trajectory over which it is measured.

9.1 Introduction

Worldwide, the number one cause of death is cardiovascular disease (CVD). Smoking, unhealthy diet, physical inactivity and excessive use of alcohol are the most important behavioural risk factors for CVD. Consequently, individuals may develop atherosclerosis, diabetes, heart failure or hypertension, most often related to a change in arterial stiffness. Arterial stiffness is deducted from the relationship between a change in blood pressure inside the artery and the successive change of arterial expansion [1]. Therefore, arterial stiffness, or its inverse the arterial compliance, is a reliable prognostic indicator of cardiovascular morbidity and mortality in the adult population [2-4]. When arterial stiffness increases, the speed with which pressure pulse waves (PWs) travel through the vessels, the pulse wave velocity (PWV) [5, 6], increases. Blood vessels should have proper arterial stiffness, because the elastic walls of the arteries attenuate the systolic pressure wave of each heartbeat. During the diastole, the potential energy stored in the elastic vessel walls is used to continue to propel the blood between successive heartbeats [1]. The gold standard for determining arterial stiffness consists of measuring the PWV. The PWV is inversely related to arterial distensibility [7-9] and directly related to the incremental elastic modulus $E_{inc,vessel}$ and vessel wall thickness h_{vessel}, and inversely related to the vessel radius r_{vessel} by the Moens-Korteweg equation (with ρ_{blood} the density of blood) [10]:

$$PWV = \sqrt{\frac{E_{inc,vessel} \cdot h_{vessel}}{2r_{vessel} \cdot \rho_{blood}}} \tag{9.1}$$

PWV is generally measured as an average speed of a PW between two locations on the body. Note that PWV is not the speed of blood, but of the pressure pulse traveling through the moving blood (comparable to a sound wave). The PWV can be measured both invasively and non-invasively and is highly reproducible [11]. However, available PWV measurement systems require quite advanced devices and highly trained operators and have several disadvantages in terms of usability [12].

The authors previously developed a device, further called the Multi Photodiode Array (MPA), that enables peripheral, non-invasive PWV measurements along a trajectory of 12.0 mm, without having the drawbacks of the currently available alternatives [12]. The MPA has been designed to enable comfortable measurements with a single, simple device without requiring highly trained operators. The MPA is based on photoplethysmography (PPG): a widely used

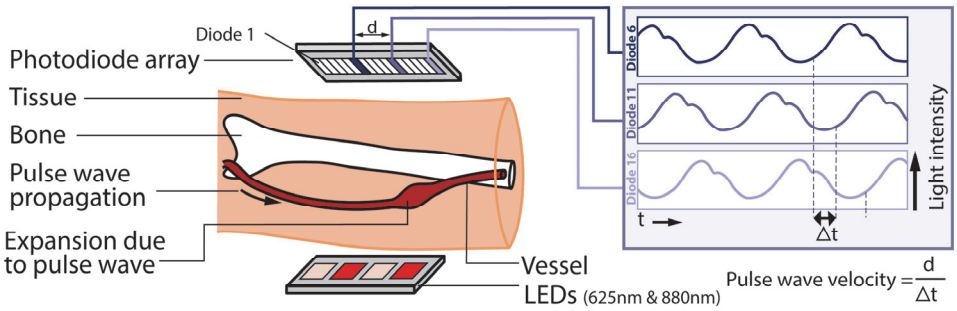

Fig. 9.1: Schematic overview of the multi photodiode array (MPA) and illustration of the calculation of the pulse wave velocity.

non-invasive optical technique for measuring volumetric expansion and contraction of vessels (Fig. 9.1) [13].

The maximum volumetric expansion at any point along a vessel occurs when the peak of a PW passes that point. Therefore, the PWV can be calculated using the time differences between the detection of the PW peaks at successive points along the vessel spaced a known distance apart. The technical functioning and measurement accuracy of the MPA have previously been validated in vitro [12]. However, because the MPA is utilized to measure PWV locally on a finger, it has yet to be investigated to what extent these local PWVs correspond with PWVs measured in conventional ways.

The goal of this study was to investigate whether the PWV values of the new developed MPA system correspond with PWV measurements obtained in clinical practice. To that purpose, the MPA was used synchronously with and its results compared to those of a commonly used measurement device, the Biopac-system (Biopac Systems, Inc. Goleta, USA). The Biopac-system measures PWV using photoplethysmography and ECG and measures PWV over the trajectory of the heart-fingertip vasculature. So both systems may provide similar information of vascular condition as the trajectories over which they measure PWV overlap. The MPA and the Biopac-system were compared during a well-known inducible physiological effect to investigate to what extent measurements with these systems and over those two different vessel trajectories agree.

9.2 Materials and methods

To investigate whether the MPA can measure physiological effects of the human body, a commonly used vascular perturbation that changes the conduit artery vasomotor tone during reactive hyperaemia [14, 15] was imposed on healthy

volunteers. Reactive hyperaemia can be measured using flow mediated dilation (FMD) [16], a technique that reflects the bioavailability of nitric oxide (NO) [17]. Characterized by reduced NO bioavailability, the endothelial dysfunction is part of the progression of cardiovascular diseases, such as hypertension, diabetes, heart failure or atherosclerosis [18, 19]. The observed decline in PWV during vasodilation after ischemia might be used as a marker of arterial distensibility and endothelial function [14, 15]. A quantitative change of the dilation of the artery can be measured with ultrasound. However, disadvantages of this technique are limited availability and requirement of a skilled operator. Moreover, the diameter and velocity are commonly measured with high-resolution B-mode and duplex ultrasound with the same transducer, which have competing requirements for an optimal measurement [20]. Alternatively, PWV measured with MPA could be easily measured continuously and without special training.

9.2.1 Study population

This study was approved by the medical ethics committee of Erasmus University Medical Center Rotterdam, the Netherlands (MEC-2017-453). A total of thirty healthy volunteers were included and then divided into two groups. The participants were between 19-63 years old without any known history of atherosclerosis associated diseases (such as diabetes mellitus, hypertension, coronary artery disease, stroke, renal disorder, arrhythmia) or injuries at the upper limbs. The healthy volunteers were included in this study after obtaining written informed consent from the subject. To determine the effect of age on the PWV, the study population was divided into 2 groups: a young group of participants aged between 18 and 35 years (n=20) and an older group aged above 55 years (n=10).

9.2.2 Protocol

The transit time of a PW traveling from within the left ventricle (LV) to easily accessible locations, such as the extremities or the neck, consists of 2 components: the PW propagation-time from the LV through the artery to the PW measurement location, and the isometric contraction time of the heart (pre-ejection period, PEP). The PEP is known to vary with cardiac preload and heart rate [21-23]. Therefore, all measurements were conducted in a quiet room under tranquil conditions at a room temperature of 22.4°C (SD 0.5°C). To further minimize any influences of a varying PEP or cardiac output during the measurement, the subjects were instructed not to talk or move during the measurement. Before the start of the measurement the subject's blood pressure and arm length (from the left middle finger to the sternoclavicular joint) was measured. The subjects were sitting on a

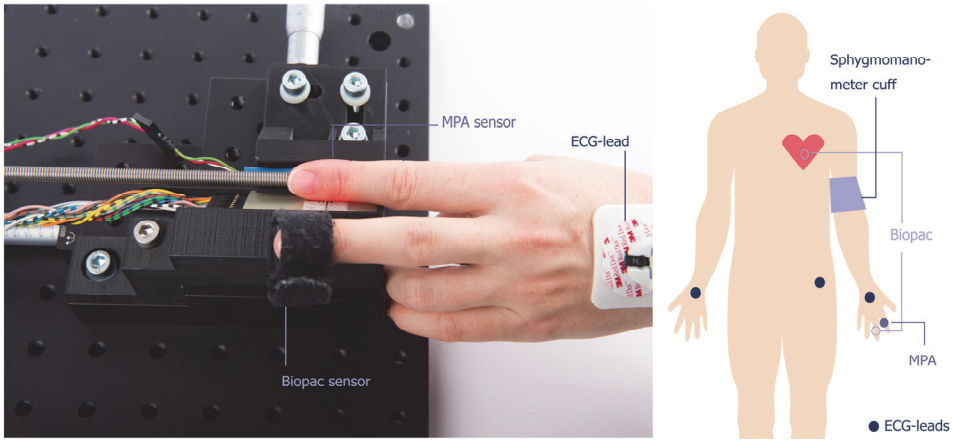

Fig. 9.2: Photograph and schematic view of placement of the both measurement systems and the sphygmomanometer cuff. MPA = Multi Photodiode Array; ECG = Electrocardiogram

chair with both hands resting on a pillow. To attain a cardiovascular steady-state before starting the measurement, the subjects had rested for at least 10 minutes in an upright sitting position.

A sphygmomanometer cuff was placed on the left upper arm for the FMD.

PWV was simultaneously measured using two systems: the new MPA and the Biopac-system. The Biopac-system consisted of a measurement device and analysis software. The measurement device contained a PPG-sensor (TSD200 with PPG100C amplifier, Biopac Systems, Inc, Goleta, USA), placed on the left middle finger, and three external ECG-leads (ECG100C amplifier, Biopac Systems, Inc, Goleta, USA) (see Fig. 9.2). The three ECG-leads were placed on the subject's both wrists and left hip. The PPG- and ECG-signals were simultaneously converted to digital signals using AcqKnowledge version 3.7.3 software (Biopac Systems, Inc, Goleta, USA), at a sampling frequency of 2 kHz. The MPA-system contained the MPA-sensor, consisting of an array of 4 red and infrared LEDs and an array of 16 photodiodes of which 4 were active. The left index finger was placed on the MPA using the setup shown in Fig. 9.2. The MPA-system read out 4 photodiodes (numbers 6, 8, 10, and 12 in the array, all spaced 1.6 mm apart) and converted the data to digital signals through a NI-USB 6229 Multifunction Data Acquisition system and LabVIEW 2010 software (both: National Instruments, Austin, TX, USA).

Before the start of the FMD the baseline PWV at rest was measured for 1 minute. Then reactive hyperaemia was induced by blocking the arterial blood supply with the sphygmomanometer cuff around the upper arm. The cuff was kept inflated for

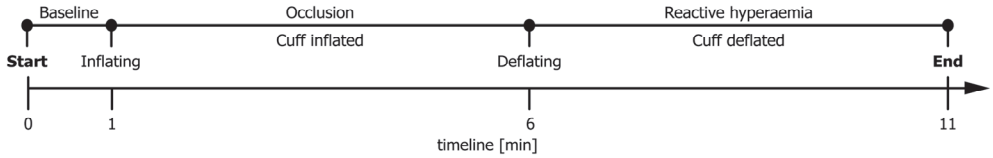

Fig. 9.3: Schematic representation of the measurement protocol used in the study comparing the MPA and the Biopac-system

5 minutes to approximately 50 mmHg above systolic blood pressure. This arterial occlusion activates the endothelium-dependent vasorelaxation, whereas after releasing the pressure in the cuff ischemia and shear stress on the endothelial cells of the blood vessel is induced. After 5 minutes, the cuff was rapidly deflated to 0 mmHg and the reactive hyperaemia was measured for 5 minutes. Summarizing, the PWV was recorded during a 1 minute baseline measurement, for 5 minutes during occlusion and 5 minutes after occlusion, see Fig. 9.3.

9.2.3 Pulse wave analysis

After obtaining the data, Matlab R2010a (The MathWorks, Inc., Matick, MA, USA) was used to analyse the data and to calculate the PWV from the signals received by the Biopac-system and MPA. All PPG-signals were filtered with a fourth-order low-pass Butterworth filter with a cut-off frequency of 9 Hz.

The PWV_{Biopac} was determined by dividing the distance between the PPG-sensor on the left middle finger and the sternoclavicular joint *(d)* by the calculated time-difference between the time instance of the R-peak of the ECG ($t_{ECG\ R\text{-}peak}(n)$) and the foot of the PW measured at the left index finger tip ($t_{PPG\ foot}(n)$):

$$PWV_{Biopac}(n) = \frac{d}{t_{PPG_{foot}}(n) - t_{ECG_{R-peak}}(n)} \tag{9.2}$$

where *n* is the sequence number of the heartbeats. To find the feet of the PWs, the maximum of the second derivative of each PW was taken [24-26]. The R-peaks in the ECG were found using the off-the-shelf Matlab function 'R-peakdetect' [27].

The PWV_{MPA} was determined for each pair of photodiodes *i* and *j* by dividing the distance between the photodiodes by the time-difference between the arrival of the PPG signals' feet at the locations of these successive photodiodes:

$$PWV_{MPA,i-j}(n) = \frac{d_{i-j}}{t_i(n) - t_j(n)} \tag{9.3}$$

where *n* is the sequence number of the heartbeats, d_{i-j} is the distance between two photodiodes and $t_i(n)$ and $t_j(n)$ are the times at which the feet of the PWs of heartbeat *n* arrived at those respective photodiodes. This was done for each combination of any two of the used photodiodes (photodiodes pairs 6-8, 8-10, 10-12, 6-10, 8-12, 6-12).

The utilized PPG-sensors were quite sensitive for motion and positioning artefacts, which sometimes distorted the shapes of the PWs in a way that they were rendered unsuitable for further analysis. Therefore, a custom-made Matlab algorithm, called '7Step PW-Filter', was implemented in the data analysis to filter out any PWs that strongly deviated in shape from a suitable PW [28]. Occasionally the PWV data showed inexplicably and unrealistically high or low PWV-values (e.g. >± 100 m/s). These extreme outliers were removed using the Matlab function 'Hampel'. The final $PWV_{MPA}(n)$ was calculated as the median PWV of all $PWV_{MPA,i-j}$ over all combinations of any pair of photodiodes used.

The median PWV after occlusion was calculated for each 30 s interval ($\tilde{P}WV_{30s,i}$) starting from the first PW after occlusion. The FMD for each 30 s interval ($FMD_{30s,i}$) was expressed as the relative change in PWV following hyperaemia, expressed as a percentage of the median baseline PWV ($\tilde{P}WV_{baseline}$):

$$FMD_{30s,i} = \frac{\tilde{P}WV_{30s,i}}{\tilde{P}WV_{baseline}} \cdot 100\% \tag{9.4}$$

These $\tilde{P}WV_{30s,i}$ were calculated for the MPA as well for the Biopac-system. Because in 4 subjects the values seemed to be heavily distorted (suspected to be caused by hand motion or strong coughing during the measurements), strong outliers (mean ± 3 SD) were removed.

9.2.4 Statistical analysis

The mean PWV ± standard deviation (SD) for the baseline were calculated. A Shapiro-Wilk test was used to check if the data were normally distributed. A Paired Sampled t-test was performed to assess the differences between the PWV of the

Table 9.1: Characteristics of the study population. Values are means ± SD or number (%) of participants

Variable	Young group (n=20)	Old Group (n=10)
Gender (male), no.(%)	8 (40)	5 (50)
Age [years]	27 ± 4	58 ± 3
Weight [kg]	77 ± 18	77 ± 15
Height [m]	1.72 ± 0.10	1.71 ± 0.05
Body mass index [kg/m²]	25.9 ± 5.6	26.1 ± 4.0
Blood pressure [mmHg]		
Systolic	132 ± 12	136 ± 17
Diastolic	87 ± 9	82 ± 11
Heart rate [bpm]	77 ± 15	69 ± 9
Smoker (yes), no. (%)	1 (5)	0 (0)
Distance from sternoclavicular to fingertip [cm]	85 ± 5	87 ± 5

Biopac- and MPA-systems during baseline and similarly for each 30s post-occlusion interval. Bland-Altman plots were used to assess the agreement between the PWV_{Biopac} and PWV_{MPA} for the baseline and for each 30 s post-occlusion interval. The analysis was performed using SPSS version 24.0 (SPSS, Inc., Chicago, IL, USA) and Matlab. The significance level adopted was $p<0.05$.

9.3 Results

Thirty subjects (13 male, 17 female) were included in this study. Table 9.1 presents the characteristic of the study population. The data of one male (Old group) and one female subject (Young group) were excluded from the analysis because there was too much noise in the signals to obtain any usable PWs.

Table 9.2: The PWV (Pulse Wave Velocity) values measured during baseline using the Biopac-system and MPA, and heart rate during the baseline measurements. MPA = Multi Photodiode Array

	Young group [Mean ± SD]	Elderly Group [Mean ± SD]	Paired sampled T-Test
PWV_{Biopac} mean [m/s]	3.2 ± 0.3	3.1 ± 0.2	t(6) = 0.898 p = 0.404
PWV_{MPA} mean [m/s]	0.9 ± 0.6	0.6 ± 0.2	t(5) = 1.787 p = 0.134
Heart rate mean [bpm]	75 ± 10	70 ± 9	t(6) = 0.649 p = 0.541
Paired sample T-Test	t(18) = 15.423 p < 0.001	t(5) = 19.769 p < 0.001	

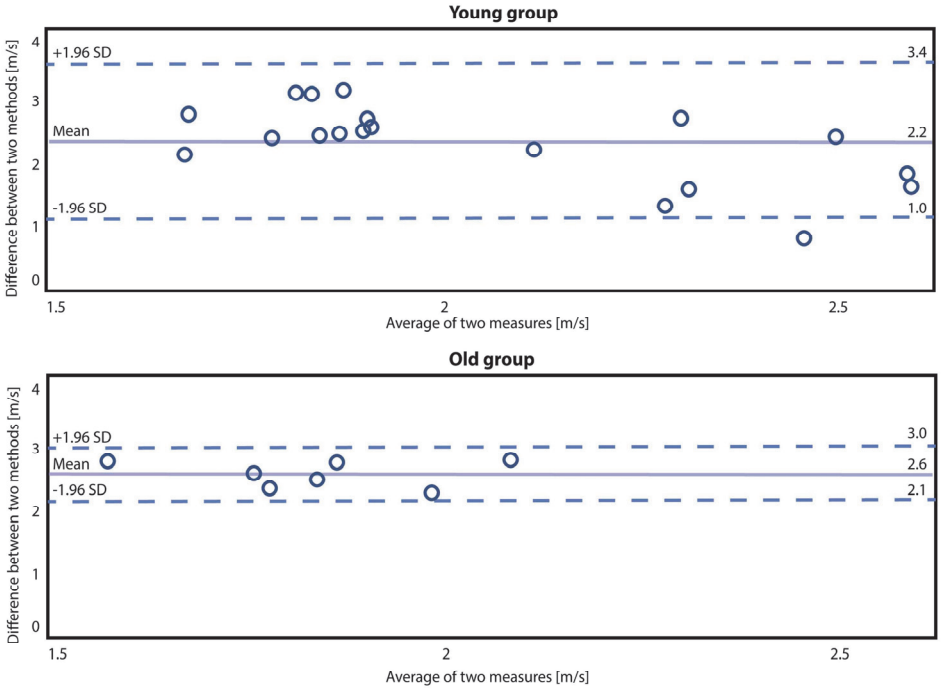

Fig. 9.4: Bland-Atman plots of the PWV_{Biopac} and PWV_{MPA} during baseline. The dotted lines represent the 95% limits of agreement and the solid lines represent the mean difference (bias) between PWV_{Biopac} and PWV_{MPA}.

Another male (Old group) had strong arrhythmia and was therefore excluded. For another female (Old group) the protocol appeared to not have been properly followed with regard to the positioning of the finger and was therefore excluded. Outlier removal removed most of the data of these subjects with irregularities due to coughing or moving and none of the subjects in whom no irregularities were observed, which further confirmed that these were in fact exceptions. For the Young group, the '7Step PW-Filter' to remove distorted unusable PWs filtered out 1.2% (median with Q1 = 0.6% and Q3 = 3.2%), the 'Hampel' filter to remove unrealistically high or low PWV-values, filtered out 0.8% (median with Q1 = 0.3 and Q3 = 1.3%). For the Old group, the '7Step PW-Filter' filtered out 1.3% (median with Q1 = 0.3% and Q3 = 7.5%), the 'Hampel' filter filtered out 0.6% (median with Q1 = 0.3 and Q3 = 1.2%).

Table 9.2 presents the mean PWVs and heart rates in absolute values for the baseline, as well as the results of the Paired Samples t-test, showing no significant differences between the two age groups. Fig. 9.4 shows the Bland-Altman plot for the agreement between the Biopac-system and MPA during the baseline

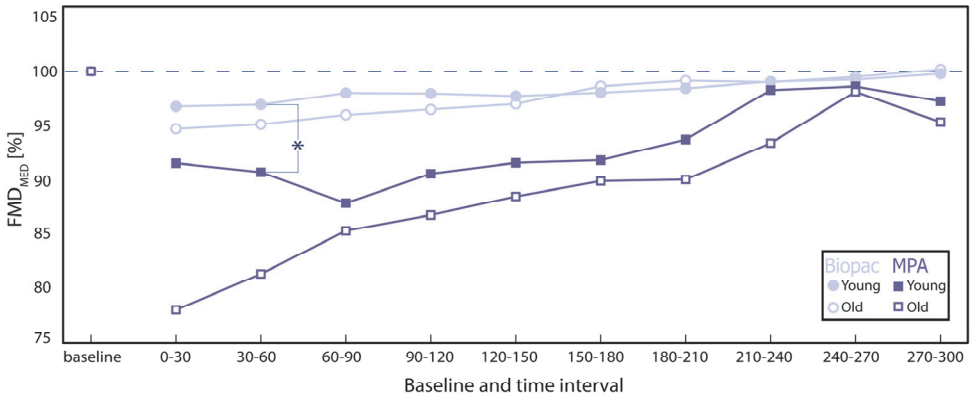

*Fig 9.5: FMD percentage per post-occlusion interval. The FMD percentage is the media PWV as percentage of the baseline PWV. Changes in PWV following hyperaemia were averaged per 30 s intervals, starting from the first PW after cuff release for each group. *) p <0.05 for difference between both systems. MPA = Multi Photodiode Array.*

measurements. The absolute PWV values were significantly lower for the MPA as compared to the Biopac-system. Yet, the Bland-Altman plots show good agreement between the two PWV measurement techniques.

A Paired Samples t-test was performed to assess the differences between the FMD_{Biopac} and FMD_{MPA} for each 30 s post-occlusion interval (Table 9.3). Fig. 9.5 shows the median PWV for the baseline and for each 30 s post-occlusion interval for both groups and both systems.

There was no significant difference between the two measurement systems following reactive hyperaemia after occlusion, except for the time-interval 30-60 s in the Young group (p = 0.042).

Additionally, the Bland-Altman plot showed good agreement between the two PWV measurement techniques (Fig. 9.6).

Table 9.3: FMD per time interval for the MPA and the Biopac-system for both age groups. Values are given as mean ± SD. FMD = flow mediated dilation; MPA = Multi Photodiode Array.

	FMD [%] Young group			FMD [%]Old group		
Time Interval [s]	**Biopac-system**	**MPA**	**Paired sample T-Test**	**Biopac-system**	**MPA**	**Paired sample T-Test**
0 – 30	94.7 ± 2.9	78.1 ± 31.4	t(15) = 2.071 p = 0.056	96.8 ± 2.1	91.6 ± 32.3	t(6) = 0.418 p = 0.691
30 - 60	95.1 ± 3.0	81.4 ± 25.4	t(16) = 2.214 **p = 0.042**	96.9 ±1.5	90.7 ± 28.2	t(6) = 0.566 p = 0.592
60 – 90	96.0 ± 2.8	85.4 ± 22.5	t(16) = 1.921 p = 0.073	98.0 ± 2.2	87.9 ± 19.2	t(5) = 1.192 p = 0.287
90 - 120	96.5 ± 2.7	86.8 ± 21.2	t(15) = 1.737 p = 0.103	98.0 ± 2.2	90.6 ±15.2	t(5) = 1.087 p = 0.327
120 – 150	97.0 ± 2.6	88.5 ± 21.7	t(15) = 1.504 p = 0.153	97.7 ± 2.3	91.6 ± 16.0	t(5) = 0.939 p = 0.391
150 - 180	98.6 ± 2.7	89.9 ± 16.5	t(13) = 2.131 p = 0.053	98.0 ± 2.3	91.8 ± 18.5	t(5) = 0.792 p = 0.464
180 – 210	99.1 ± 1.8	90.1 ± 20.4	t(13) = 1.592 p = 0.135	98.4 ± 2.1	93.7 ± 18.8	t(5) = 0.642 p = 0.549
210 – 240	99.0 ± 2.7	93.4 ± 19.0	t(14) = 1.207 p = 0.247	99.1 ± 1.8	98.3 ± 18.5	t(5) = 0.131 p = 0.901
240 – 270	99.5 ± 3.0	98.1 ± 24.3	t(14) = 0.795 p = 0.795	99.2 ± 2.0	98.6 ± 20.2	t(5) = 0.105 p = 0.920
270 -300	100.2 ± 3.0	95.3 ± 22.6	t(13) = 0.750 p = 0.466	99.8 ± 3.4	97.2 ± 17.2	t(5) = 0.457 p = 0.667

9.4 Discussion

This study compared PWV values measured in healthy volunteers over a 4.8 mm short peripheral vascular trajectory in the left index fingertip using the MPA system with PWV values measured between the R-peak of the ECG and the arrival of the PW in the left middle fingertip using the Biopac-system during reactive hyperaemia. The PWV_{MPA} and PWV_{Biopac} measurements showed good agreement, as shown by the Bland-Altman plots in Figure 9.4, but also a systematic difference. The PWV_{MPA} was consistently and considerably lower than PWV_{Biopac}. Looking at Equation 9.1 this difference may be explained by vessels being more compliant and thinner walled, yet also being smaller in diameter, closer to the periphery. This agrees with the results of Van Velzen et al., showing higher PWVs for the trajectory of the carotid-radial artery than for the heart-fingertip trajectory [29]. It seems that when the PWV is measured towards the periphery, the PWV decreases.

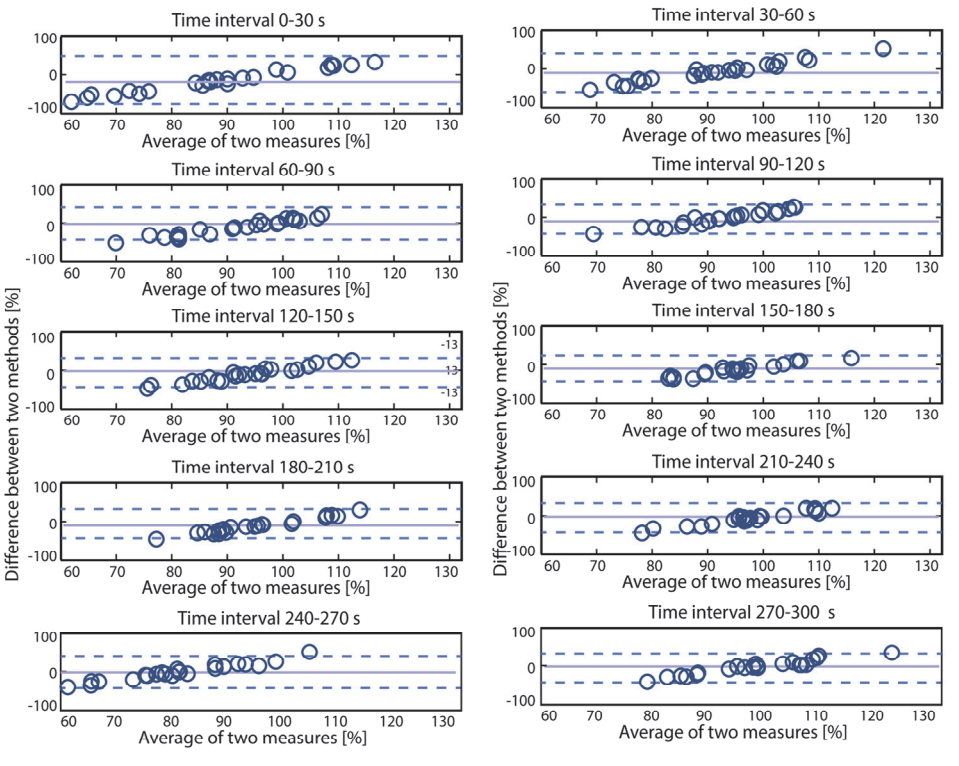

Fig 9.6: Bland-Atman plots for the agreement between the PWV_{Biopac} and PWV_{MPA} per post-occlusion interval. The dotted lines represent the 95% limits of agreement and the straight lines represent the mean difference (bias) between PWV_{Biopac} and PWV_{MPA}.

When eyeballing the results in Figure 9.5, it may seem as if there is a rather large difference between the relative change of PWV measured with the Biopac system compared to that measured with the MPA. Yet, these seemingly present differences were not statistically significant. This may have been a consequence of the standard deviations in the PWV_{MPA} results being relative large compared to those for the PWV_{Biopac}. This larger variability in PWV when using the MPA may have several causes, but the most likely cause (based on observations during the measurements) was that the MPA readings were quite sensitive to positioning and pressure of the finger on the sensor. Because this sensitivity was known in advance, all fingers were placed at the same spot on the sensor and kept in place using an elastic textile band with a gentle, standardized pre-tension. However, due to subject motion and slight variations in placement, variations may still occur. Therefore, the MPA sensor should be further developed into a user friendly device that facilitates standardized and stable placement of the MPA on the finger.

The FMD results in this study agreed with those of Cauwenberghs et al. when applying 5 min occlusions: a change in PWV with a maximum of -14.6% was found for the first 30 s post-occlusion time interval [30]. In that study, the PWV was measured over the brachial-radial trajectory by use of two oscillometric cuffs. As the Biopac-system measured the PWV over the heart-fingertip trajectory and the MPA over a mere 4.8 mm in the fingertip, it is fitting that the result of Cauwenberghs et al. is between the corresponding values for the Biopac-system (-5.3%) and for the MPA (-21.9%).When using the Biopac-system, the measured PWV includes the PEP. The PEP is known to vary during position changes. PEP variations caused by subject movement or stress were avoided as good as possible during the current study. Still, Kortekaas et. al showed a variability of the PEP in healthy volunteers at rest of 58.5 ± 13.0 ms [22]. Within the distances travelled by the PWs in the current study, these PEP durations could account for no more than 1 m/s of the PWV_{biopac}. Consequently, PEP variations are unlikely to explain the variations in this study.

Considering the relatively small sample size, the findings should be validated in a larger cohort of randomly recruited subjects. Furthermore, the study population mainly included healthy, Caucasian European participants, potentially limiting the generalizability of the findings to other ethnicities and patients. It would be of interest to perform these measurements in subjects with CVD. Furthermore, the utilized PPG sensor in the Biopac-system and the PPG sensor array in de MPA-system were quite sensitive to motion and positioning disturbances. This sensitivity

to disturbances poses a potential limitation on the usability of these techniques in clinical practice. Although the '7Step PW-Filter' algorithm used to eliminate distorted PWs functioned well, the availability of a MPA sensor less sensitive to disturbances and displacements would greatly simplify measuring PWVs and would be essential for application in clinical practice.

9.5 Conclusion

The results of this study demonstrated that the PWV values were consistently lower when measured with the MPA system than when measured with the Biopac-system, which fits the fact that they were measured over a more peripheral vascular trajectory. However, the measurements showed to be in good agreement. This suggests that as long as one is aware of the relation between PWV and the vascular trajectory over which the PWV is measured, either system could be used to reliably measure relative PWV values. When basing diagnoses or research outcomes on absolute PWV values, one should be very much aware of how the PWV was measured, with what system, and over which trajectory. Further research will have to be carried out to develop a better sensor to enable simple and consistent placement of the MPA on the finger. Next, a follow-up study should investigate whether the PWVs measured with the MPA on the finger can be used as an index for evaluation of aortic stiffness as a factor of cardiovascular risk.

9.6 References

1. Quinn, U., L.A. Tomlinson, and J.R. Cockcroft, *Arterial stiffness.* JRSM Cardiovasc Dis, 2012. 1(6): p. 1:18.
2. Blacher, J., et al., *Impact of aortic stiffness on survival in end-stage renal disease.* Circulation, 1999. 99(18): p. 2434-2439.
3. Laurent, S., et al., *Aortic stiffness is an independent predictor of all-cause and cardiovascular mortality in hypertensive patients.* Hypertension, 2001. 37(5): p. 1236-1241.
4. Cruickshank, K., et al., *Aortic pulse-wave velocity and its relationship to mortality in diabetes and glucose intolerance: An integrated index of vascular function?* Circulation, 2002. 106(16): p. 2085-2090.
5. Laurent, S., et al., *Expert consensus document on arterial stiffness: methodological issues and clinical applications.* Eur Heart J, 2006. 27(21): p. 2588-605.
6. Boutouyrie, P. and S.J. Vermeersch, *Determinants of pulse wave velocity in healthy people and in the presence of cardiovascular risk factors: Establishing normal and reference values.* European Heart Journal, 2010. 31(19): p. 2338-2350.

7. Cavalcante, J.L., et al., *Aortic stiffness: Current understanding and future directions.* Journal of the American College of Cardiology, 2011. 57(14): p. 1511-1522.
8. McDonald, D.A., *Regional pulse-wave velocity in the arterial tree.* Journal of applied physiology, 1968. 24(1): p. 73-78.
9. Asmar, R., et al., *Assessment of arterial distensibility by automatic pulse wave velocity measurement: Validation and clinical application studies.* Hypertension, 1995. 26(3): p. 485-490.
10. Bramwell, J.C. and A.V. Hill, *The Velocity of the Pulse Wave in Man.* Proceedings of the Royal Society of London Series B, Containing Papers of a Biological Character, 1922. 93(652): p. 298-306.
11. Wilkinson, I.B., et al., *Reproducibility of pulse wave velocity and augmentation index measured by pulse wave analysis.* Journal of Hypertension, 1998. 16(12 SUPPL.): p. 2079-2084.
12. Van Velzen, M.H.N., et al., *Design and functional testing of a novel blood pulse wave velocity sensor.* Journal of medical devices, 2017. 12(1): p. 7.
13. Allen, J., *Photoplethysmography and its application in clinical physiological measurement.* Physiol Meas, 2007. 28(3): p. R1-39.
14. Ellins, E.A., et al., *Validation of a new method for non-invasive assessment of vasomotor function.* European Journal of Preventive Cardiology, 2016. 23(6): p. 577-583.
15. Naka, K.K., et al., *Flow-mediated changes in pulse wave velocity: A new clinical measure of endothelial function.* European Heart Journal, 2006. 27(3): p. 302-309.
16. Corretti, M.C., et al., *Guidelines for the ultrasound assessment of endothelial-dependent flow-mediated vasodilation of the brachial artery: A report of the international brachial artery reactivity task force.* Journal of the American College of Cardiology, 2002. 39(2): p. 257-265.
17. Green, D.J., et al., *Flow-Mediated Dilation and Cardiovascular Event Prediction: Does Nitric Oxide Matter?* Hypertension, 2011.
18. Flammer, A.J., et al., *The assessment of endothelial function: From research into clinical practice.* Circulation, 2012. 126(6): p. 753-767.
19. Mordi, I., et al., *Endothelial dysfunction in human essential hypertension.* Journal of Hypertension, 2016. 34(8): p. 1464-1472.
20. Thijssen, D.H., et al., *Assessment of flow-mediated dilation in humans: a methodological and physiological guideline.* Am J Physiol Heart Circ Physiol, 2011. 300(1): p. H2-12.
21. Weissler, A.M., W.S. Harris, and C.D. Schoenfeld, *Systolic time intervals in heart failure in man.* Circulation, 1968. 37(2): p. 149-159.
22. Kortekaas, M.C., et al., *Small intra-individual variability of the pre-ejection period justifies the use of pulse transit time as approximation of the vascular transit.* PLoS One, 2018. 13(10).
23. Newlin, D.B. and R.W. Levenson, *Pre-ejection period: Measuring beta-adrenergic influences upon the heart.* Psychophysiology, 1979. 16(6): p. 546-553.

24. Kortekaas, M.C., et al., *Pulse transit time as a quick predictor of a successful axillary brachial plexus block.* Acta Anaesthesiol Scand, 2012. 56(10): p. 1228-1233.
25. Kortekaas, M.C., et al., *Comparison of bilateral pulse arrival time before and after induced vasodilation by axillary block.* Physiol Meas, 2012. 33(12): p. 1993-2002.
26. Teng, X.F. and Y.T. Zhang, *The effect of applied sensor contact force on pulse transit time.* Physiological Measurement, 2006. 27(8): p. 675-684.
27. Clifford, G.D., *Rpeakdetect function (ECG toolbox)*. 2008.
28. van Velzen, M.H.N., et al., *Increasing accuracy of pulse transit time measurements by automated elimination of distorted photoplethysmography waves.* Med Biol Eng Comput, 2017: p. 1-12.
29. van Velzen, M.H.N., et al., *Comparison between pulse wave velocities measured using Complior and measured using Biopac.* Journal of Clinical Monitoring and Computing, 2018.
30. Cauwenberghs, N., et al., *Flow-mediated slowing of brachial-radial pulse wave velocity: Methodological aspects and clinical determinants.* Artery Research, 2018. 21: p. 29-37.

Chapter 10

Discussion, recommendations, and conclusions

10.1 Introduction

The goal of this Ph.D. study was to develop and validate a non-invasive, photoplethysmography (PPG)-based device for peripheral measurement of the Pulse Wave Velocity (PWV), on the finger. In this chapter, the results, limitations, and recommendations that followed from the obtained achievements are discussed while following the stated aims, which are repeated below:

- to confirm the value of peripheral PWV measurements,
- to design and technically validate a PPG-based device for measuring PWV in the finger,
- to validate the developed device in clinical studies.

Part I - Substantiation, of this thesis showed the value of peripheral PWV measurements and presented a platform-independent and measurement-technique-independent algorithm for improvement of PWV measurements. Part II - Development & Validation, described the design, technical validation, testing, further improvement and final validation of the Multi Photodiode Array (MPA), the PWV measurement device developed during this Ph.D. study.

10.2 Substantiation

The literature study in Chapter 2 revealed that filtering techniques or methods that are used to eliminate unsuitable PWs are often not described and differ between studies. In fact, most studies do not report whether any or what kind of filtering algorithm was used to eliminated unsuitable PWs. Using unfiltered PPG-data may result in deviations in the calculated values with orders of magnitude close to commonly measured effect sizes in human subject studies. Yet, visually and manually selecting and removing unsuitable PWs is highly time consuming and therefore often undesirable or inconvenient in clinical practice. In order to obtain valid PW-based data, it is essential to only use PWs that contain the morphological landmarks on which the definition of Pulse Transit Time (PTT) is based. The '7-step PW-filter' algorithm was developed to apply 7 criteria to determine whether a PW matches the characteristics required to allow PTT/PWV-calculation. The '7Step PW-filter' offers objectivity and substantial time savings compared to manual elimination and can be implemented in many coding languages due to its simple and straight-forward concept.

The transit time of a PW traveling from within the heart to easily accessible locations, such as the extremities of the neck, consists of 2 components: the PW propagation-time from the heart through the artery and to the PW measurement location, Vascular Transit Time (VTT), and the isometric contraction time of the heart (pre-ejection period, PEP). In Chapter 3 it was shown in a study on both volunteers and patients that, when using the Biopac-system, the contribution of PEP to the PTT measured at the fingertip at rest is approximately 20%. The remaining 80% of the PTT is determined by the VTT. As the intra-individual variability of PEP is only minor, a change in PTT in a person at rest is most probably the result of a change in VTT. Thus, PTT at rest is an easy, non-invasive and accurate approximation of VTT for monitoring arterial stiffness. In order to further eliminate the effect of the PEP, measuring PWV on the finger may be a feasible approach.

After improving the PW measurement technique in Chapter 2 and confirming the limited effect of the PEP on PTT and PWV in Chapter 3, the remaining chapters of Part I were used to show two clinically relevant applications of such measurements. In Chapter 4 a patient study performed on 23 patients who were scheduled for elective unilateral upper limb surgery under axillary block demonstrated that PTT can provide a fast and objective alternative to the current methods for determining whether an axillary plexus block has set in properly. An axillary block is used to block the sensory and motion function of the arm which is essential for, e.g., hand or arm surgery in awake patients. This block also causes relaxation of the vascular musculature and dilatation of the blood vessels.. Early, reliable and objective assessment of a block can improve the efficacy of operating room time and minimize patients' fear of possible conversion to general anesthesia. Even when different local anesthetics are used with different onset times, measuring the PTT proved to be a much quicker an objective indication of the state of the vascular system than the conventional sensory test. This may enable an early additional intervention when necessary.

Another useful potential application of PTT measurements was found in the objective assessment of pain, which is commonly assessed subjectively by interpretations of patient behavior and/or reports from patients. Pain is a sensation that is highly subjective, but also has objective aspects. In Chapter 5 it was shown that a bilaterally significant decrease of PTT occurs in response to heat-induced pain stimuli in volunteers, who all underwent pain stimuli leading to similar pain scores. Furthermore, the pain response appeared to be centrally mediated. It was

concluded that PTT is a reliable indicator of pain-induced alterations of vasotonus and can be measured on a contralateral extremity in situations in which it is impossible or undesirable to measure directly on the affected extremity. In the future, PTT may be applied as an objective indicator of pain stimulus, either together with the standard self-report tests, or instead of it, when self-reporting is impossible.

10.3 Development & Validation

Although it was made clear in Part I that measuring the speed of PWs could be highly valuable and beneficial in clinical practice, the available techniques for obtaining these measurements were still far from ideal. Therefore, the Multi Photodiode Array (MPA) was developed. The MPA is a novel transmission photoplethysmography sensor with a single photodiode array. Chapter 6 describes its design and validation. The MPA was developed for PWV measurements on the finger, measures the pulse rate, pulse wave amplitude, and peripheral PTT, and could also measure SpO_2. The MPA was shown to enable reliably and accurately measuring PWVs with a maximum deviation of 3.0%, within clinically relevant ranges and even well beyond

A study on volunteers was set up to compare the MPA to two currently available and widely used, but harder to use systems for measuring PWVs: the Complior and the Biopac system. Chapter 7 described the results for the Complior and the Biopac system. However, the data obtained with the MPA showed unexplainably large variations, many negative PWV values and many unsuitable (and therefore removed) PWs. Therefore, the MPA results are only briefly shown and discussed in Appendix 8.A. Nonetheless, the comparison between the Complior and Biopac systems did provide valuable insights in the differences and similarities between measuring PWV from the carotid to the wrist (Complior) and measuring PWV from the heart to the fingertips (Biopac).

Two extensive patient studies (see Appendices 8.B and 8.C) with the MPA were also conducted. The study in Appendix 8.B consisted of PWV measurements on surgical patients during induction of general anesthesia. The study described in Appendix 8.C focused on measuring PWVs in further unspecified outpatients with vascular diseases who had their ankle brachial index measured. When analyzing the data after the experiments were done, the MPA appeared to have delivered erroneous data, which was not useable, but unnoticeably during the experiments. This appeared not to have been caused by technical malfunction, but failed use

condition. Furthermore, most of the patients with vascular diseases had such heavily affected vascular functions that the vast majority of PWs were too distorted to pass the '7Step PW filter'.

Despite failing to obtain proper PWV measurements with the MPA at that time, the studies described in Chapter 7 and Appendix 8.A-C did provide the onset to a thorough and systematic investigation of how the MPA should be used in practice. After all, Chapter 6 had already shown that the MPA properly functioned technically. The acquisition rate and accuracy of the MPA hardware and software proved to be more than sufficient to allow measuring the relatively low PWVs in the finger. Even PWVs twenty times higher could reliably be measured with four diodes simultaneously.

The Biopac and Complior systems have several disadvantages, such as hard to accurately position sensors, discomfort for the patient, the need for extra equipment in the hospital, and the discrepancy between the measured distance between the sensors and the actual path length travelled by the PWs. Therefore, the need for further developing the MPA was ever clear. In Chapter 8 the optimal use condition of the MPA was systematically investigated and it appeared that consistently satisfying PWV measurements could be obtained, provided that the following conditions were met:

- soft-side positioning of the MPA: locating the active photodiode array across the middle, fleshy side part of the distal phalanx,
- and using light contact pressure.

The robustness and user-friendliness of the optimal use condition was further substantiated in a study on 30 healthy volunteers, described in Chapter 9. In this study the MPA could easily, rapidly, and consistently be positioned with respect to the patient in such a way that proper PWs and PWVs were obtained. The PWV values were lower than the PWV_{Biopac} values found in Chapter 7, which were also lower than the $PWV_{Complior}$ values, so it seems that the more peripherally the PWV is measured, the lower the PWV will be. Obviously, this makes sense looking at the Moens-Korteweg; equation, this difference may be explained by vessels being more narrower, thinner walled and more compliant closer to the periphery with the reduced vessel stiffness and wall thickness apparently outweighing the reduced vascular diameter.

10.4 Recommendations

PWV measurements are widely used as an index of arterial stiffness [2] and for the evaluation of cardiovascular risk. A preferred clinical next step required further research, to investigate whether the PWVs measured with the MPA on the finger can be used as an index for evaluation of aortic stiffness as a factor of cardiovascular risk [3]. This will require that PWVs measured purely locally on the finger can be shown to correlate with the arterial conditions elsewhere in the vascular system. A subsequent step is to examine the reproducibility and variance of the PWV in cardiovascular risk patients when applying measurements over short trajectories at relevant locations, such as over a short section of the carotid artery or along the arm, instead of the currently used measurements over larger distances. Furthermore, PWV could be used in the future as a measurement of pain stimuli during general anesthesia.

Although the patient studies were aimed to find differences in PWV under various pathophysiological circumstances, the produced results were disappointing. Nonetheless, these studies provided useful insights and eventually led to the development of the optimal use condition described in Chapter 8. Yet, these studies also underlined the importance of always properly validating a medical device before using it on patients. This validation should not only cover functional tests, but also thorough testing of the use conditions of the device in situations and on populations in which the expected outcome is as clear as possible. Another valuable insight obtained through the patient studies, which is also a recommendation for further expansion of the applicability of the MPA, was that measuring the PWV is unlikely to provide useful results in patients with vessels seriously affected by vascular disease. However, the MPA might still be used in combination with the 7Step PW-filter to determine the PW quality ratio 'PWQR' as:

$$PWQR = \frac{S - U}{S + U} \tag{10.1}$$

In which 'S' is the number of suitable PWs and 'U' is the number of unsuitable pulse waves. The PWQR will limit to 1 if $S >> U$ or if U=0, and to -1 for the inverse situation. So, boldly stated, as long as proper application of the MPA is guaranteed, a PWQR of 1 would indicate healthy vessels and a PWQR of -1 would indicate unhealthy vessels.

In November 2015, 10 months after we first presented the functional testing of the MPA system at a conference, a conference paper was published by Nabeel et al. presenting PWV measurements on the carotid using reflective Hall sensors and photoplethysmography (PPG) sensors at 20 mm distance [1]. Although that system has clear similarities with the MPA system, it is not suitable for prolonged measurements without causing discomfort and requires adding extra devices to the vast number of equipment already present in the hospital. It would be advantageous if PWV measurements could be performed while integrated into currently available medical devices. One of the simplest potentially suitable devices broadly used in the clinic are the commonly available finger clip PPG-sensors used for SpO_2 and pulse rate monitoring, which basically already are MPA sensors with only a single photodiode. Clinical practice would particularly benefit from such a simple PWV measuring device because its use and presence is already familiar to clinicians, while being comfortable for patients and easy-to-use. Because of its simplicity and the elimination of the need for any other measurement systems, such as ECG, for measuring PWV, using the MPA will reduce the need for trained staff and costly equipment, and will allow for comfortable continuous monitoring.

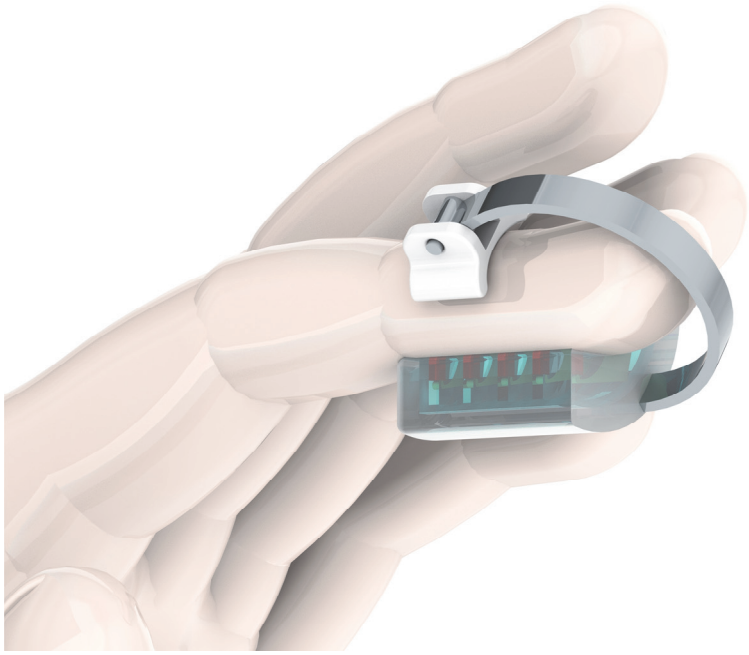

Figure 10.1: Artist impression of the m-MPA clip used in a clinical-practice-ready medical device for integrated measurement of pulse rate, oxygen saturation and PWV.

Therefore, for future clinical use, the MPA should be further designed into a pulse-oximeter-like device that clips on the finger and ensures proper and consistent placement and contact pressure independent of the caretaker or patient. An artist impression of how this future device, called the m-MPA (modular MPA) could be designed is shown in Figure 10.1. The device consists of a basic housing in which several identical sensing modules can be placed in a linear array. The modules contain the sensors and transmitters for measuring PWV, SpO_2, pulse rate, temperature, or whatever physiologic signal could be measured by any sensor put in such a module. Contact pressure between the sensor and the finger is controlled by a self-balancing spring system, which also defines the positioning of the finger with respect to the sensor.

10.5 Concluding remarks

Although there is still much to investigate before the MPA is ready for broad clinical use for non-invasive, easy and comfortable measurement of peripheral PWVs, the achievements reached through the work described in this thesis suggest that the MPA could readily be made useful in clinical practice. It would be advantageous if PWV measurements could be performed while the MPA is integrated into currently available medical devices, such as standard pulse-oximeters. It has been demonstrated that the MPA functions as intended and that clinical practice is likely to benefit from the MPA in a broad range of applications, such as objectively confirming axillary blocks, pain and vascular diseases.

In short, this Ph.D. study consisted of: developing and validating a novel data filtering algorithm; building several new measurement setups; designing, building and validating five different versions of MPA prototypes; 5 clinical studies on a total 115 volunteers; and 4 clinical studies on a total of 135 patients. With respect to the goals stated in Chapter 1, the following achievements were reached:

- the value of the peripheral PWV measurements were confirmed through volunteer and patient studies and the quality of PWV data acquisition was improved with the 7Step PW-filter.
- the Multi Photodiode Array (MPA), a PPG-based device for measuring PWV in the finger was designed, built and technically validated for PWV ranges well exceeding clinically relevant ranges.
- the MPA was validated for PWV measurements in human volunteers in a controlled clinical study.

Overall, the results of this thesis indicate that the novel, PPG-based, MPA allows accurate and reliable PWV measurements within all clinically relevant ranges. Some important advantages of the MPA as compared to other PWV measurement systems are that the MPA is easy-to-use, non-invasive, and provides objective data. Additionally, the MPA combined with the 7Step PW-filter may help assessing vascular condition through the newly suggested pulse wave quality ratio. In the future, the MPA may substantially simplify PWV measurements and enable long-term monitoring of vascular health, which may contribute to improving prevention, diagnosis and treatment of cardiovascular diseases.

10.6 References

1. Nabeel, P.M., J. Joseph, and M. Sivaprakasam. Arterial compliance probe for local blood pulse wave velocity measurement. in Proceedings of the Annual International Conference of the IEEE Engineering in Medicine and Biology Society, EMBS. 2015.
2. Asmar, R., et al., Assessment of arterial distensibility by automatic pulse wave velocity measurement: Validation and clinical application studies. Hypertension, 1995. 26(3): p. 485-490.
3. Mancia, G., et al., 2013 ESH/ESC guidelines for the management of arterial hypertension: The Task Force for the management of arterial hypertension of the European Society of Hypertension (ESH) and of the European Society of Cardiology (ESC). European Heart Journal, 2013. 34(28): p. 2159-2219.

Appendix A

Designs of MPA sensors and holders

During this Ph.D. study six different versions of the MPA and its holder (sensor units) were designed and manufactured in order to accomplice optimal placement of the MPA on the finger and measurement of the finger pulse wave. In this appendix these six developed sensor units are explained:

- MPA placed in an original SpO_2 clip
- Stripped MPA
- Vamulec
- Smart sensor holder
- Soft-side positioning holder
- m-MPA clip

MPA placed in an original SpO_2 clip

Figure A.1 shows the MPA sensor (developed by M.H.N. van Velzen) placed in an original, commercially available SpO_2 clip (Datascope SpO_2 sensor) that normally contains only a single LED and photodiode for measuring heartbeats and oxygen saturation levels of the blood. This was done to investigate the possibility of placing all the components of the MPA system into an SpO_2 clip. All the 16 signals from the photodiode array were read out through the PPG100C amplifier (Biopac System, Inc, USA) at a sampling frequency of 2 kHz. During the research described in this thesis it appeared that this sampling frequency was too low to measure all 16 PPG-signals and their PWV-values accurately enough. However, this simple adaptation of the SpO_2 clip did prove the feasibility of incorporating the MPA-technology in a simple-to-use finger clip.

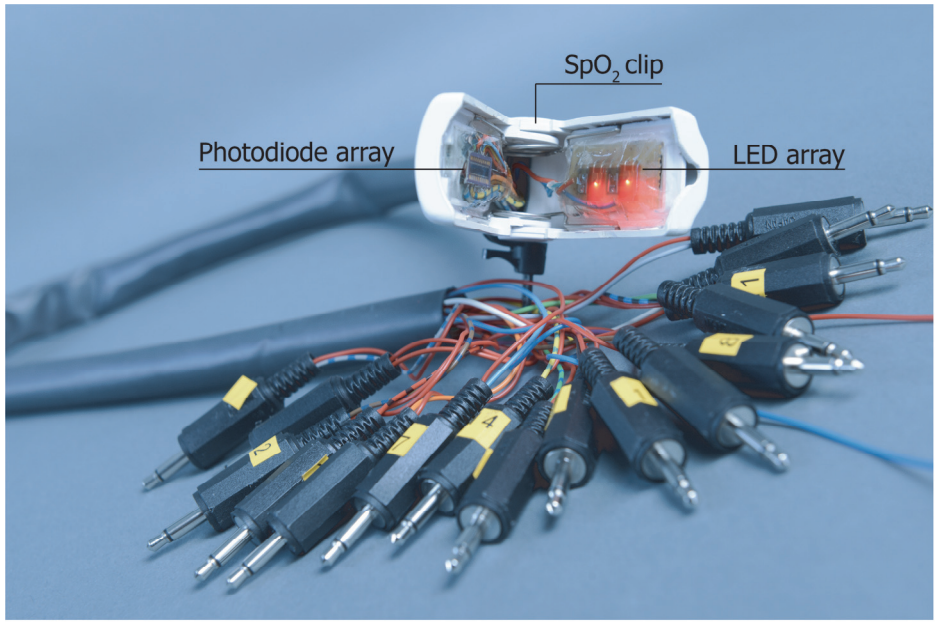

Figure A.1: The MPA placed in an original SpO_2 clip

Stripped MPA

To investigate how the MPA should best be positioned on the finger, a stripped version of the MPA was built (developed by M.H.N. van Velzen). The stripped MPA consists of two independent sides, the LED array (with two infrared and two red LEDs) and the photodiode array (see Figure A.2). All of the 16 analogue signals from the photodiode array were converted to digital signals through a NI-USB 62289 Multifunction Data Acquistion system and LabVIEW 2010 software (both: National Instruments, Austin, TX, USA). This data acquisition-system has a 250 kHz sampling rate and 32 analog, 16-bit input channels and was used with all of the designs of MPA and holders, except for the 'MPA placed in an original SpO_2 clip' (see previous section).

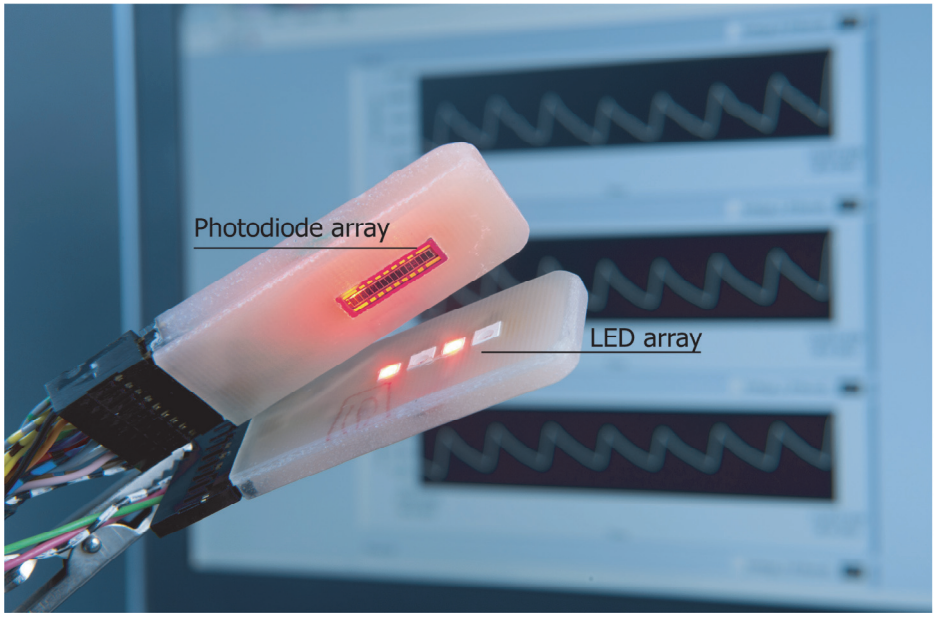

Figure A.2: The stripped MPA, used to investigate how the MPA should best be positioned on the finger.

Valumec

Figure A.3 shows the "Vamulec". The Vamulec was developed by G. van Geest during his master graduation process of Integrated Product Design at the faculty of Industrial Design Engineering, Delft University of Technology, supervised by the author of this thesis. The Vamulec is a clip consisting of two elements: the body and the roller. The body is a cylinder, ending in two lips that contain the LEDs and the photodiode array of the MPA. The finger is placed between these two lips. The roller is rolled over the two lips, which presses the LEDs and photodiode array down onto the finger. The Vamulec was designed to keep the sensor stably positioned on a variety the finger sizes during use. However, because of the change to a different positioning method (see Chapter 8), further use and development of the Valumec was abandoned.

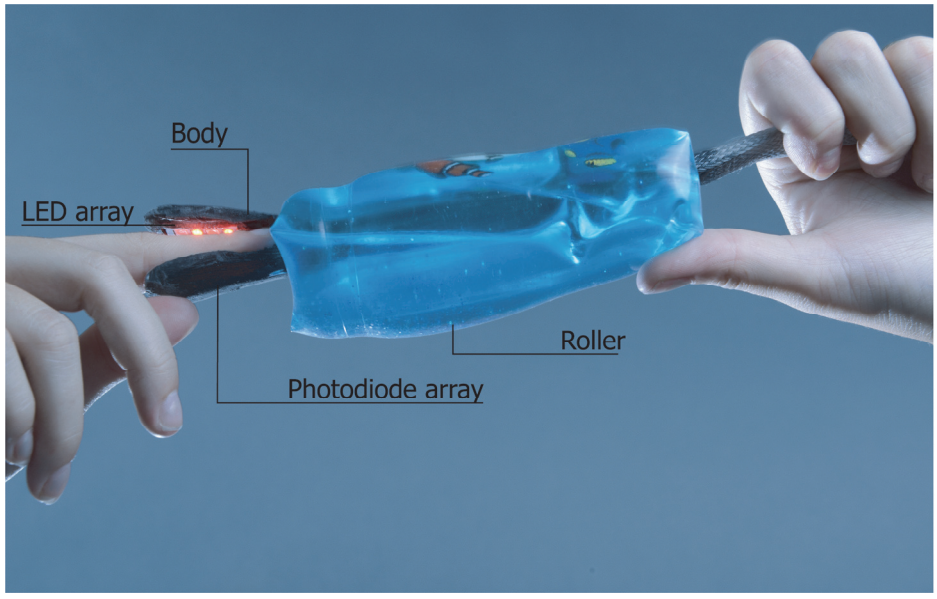

Figure A.3: The Vamulec placed on a finger

Smart sensor holder

The "smart sensor holder" (Figure A.4) was the outcome of the research project done by five students (J. Floor, K. Braham, G. Klarenbeek, D. Koot and J. Vergeer) of the minor Technical Multidisciplinary Design, University of Applied Science Utrecht, supervised by the author of this thesis. The smart sensor holder is a holder in which three stripped MPA-sensors can be placed on three different positions between the lower arm and the fingertip. The distance between the MPA-sensors is measured using potentiometers, allowing accurate measurement of the PWV over the entire lower arm. Although being less easy-to-use and offering less flexibility, the smart sensor holder does enable PWV measurements over various trajectories in the lower arm.

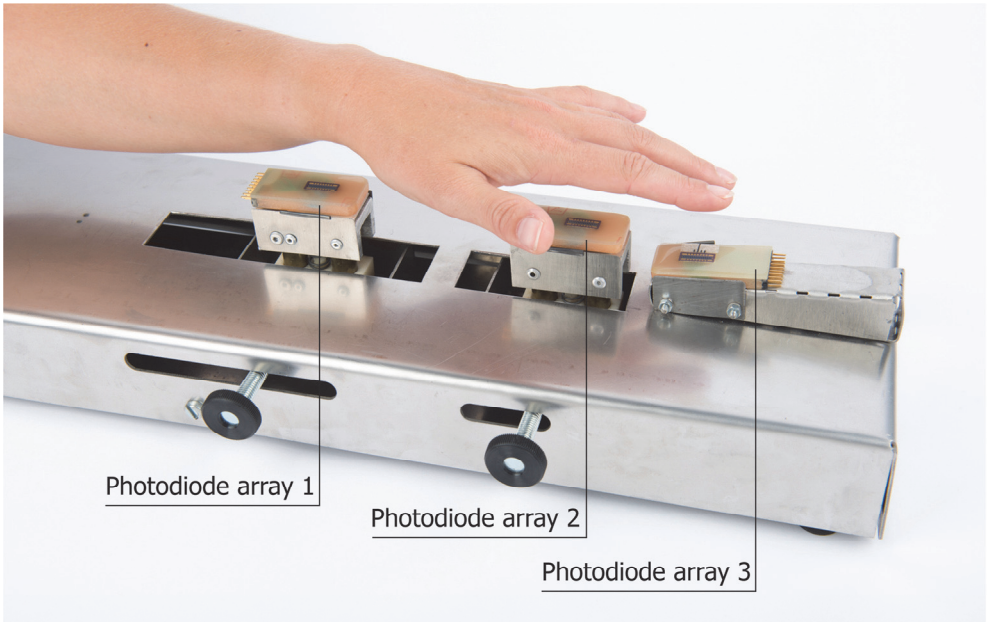

Figure A.4: The smart sensor holder with the fingertip, wrist and lower arm each lying on one of the three MPA-sensors.

Soft-side positioning holder

The presented research in Chapter 8 showed what the optimal use conditions of the MPA are to provide consistently satisfying results. This optimal use condition consisted of:

- soft-side positioning of the MPA: locating the active photodiodes across the middle, fleshy side part of the distal phalanx,
- and using a light contact pressure.

In Figure A.5 the new sensor holder is shown (developed by M.H.N. van Velzen and A.J. Loeve), which was designed to standardize the placement of the finger on the MPA for the optimal use condition of the MPA. This soft-side positioning holder was used on 30 healthy volunteers (see Chapter 9).

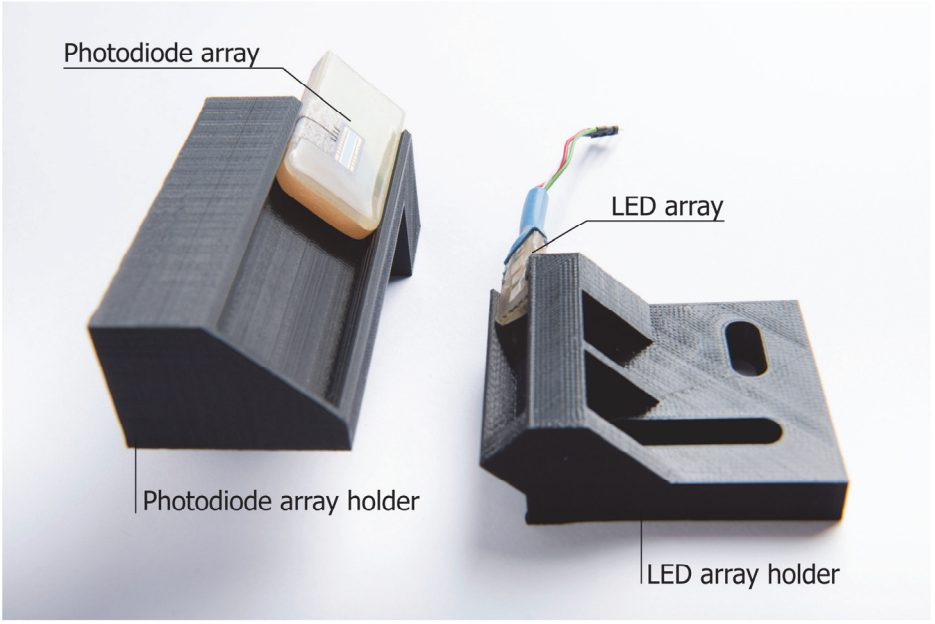

Figure A.5: Soft-side positioning holder designed for the optimal use condition of the MPA, used to measure PWVs in healthy volunteers (see Chapter 9).

m-MPA clip

An optimal use condition for the MPA was established and proved to be very suitable for human subject research, called the m-MPA clip (modular-MPA clip) (see Chapter 9). For future clinical use, the MPA should be redesigned into a pulse-oximeter-like device that clips on the finger and ensures proper and consistent placement and contact pressure independent of the caretaker or patient. An artist impression of how this future device could be designed to look like (made by M.H.N. van Velzen and A.J. Loeve) is shown in Figure A.6. The device consists of a basic housing in which any desired number of identical sensing modules can be placed in a linear array. An extensible finger positioning clamp ensures proper contact pressure and positioning of the finger on the MPA. See Chapter 8 for further details.

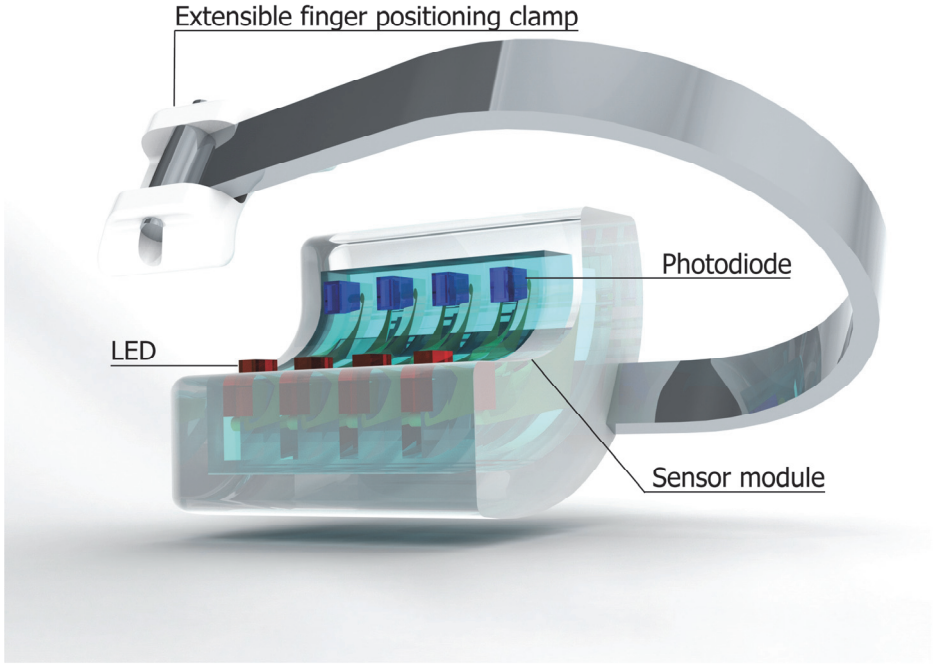

Figure A.6: Artist impression of the m-MPA clip, in which the MPA system is integrated for measurement of pulse rate, oxygen saturation and pulse wave velocity.

Summary

THE SPEED OF WAVES

Measuring the velocity of pressure pulse waves traveling through peripheral blood vessels

Worldwide, cardiovascular diseases (CVDs) are the number one cause of death. Smoking, unhealthy diet, physical inactivity and excessive use of alcohol are the most important behavioural risk factors of CVDs. As an effect, individuals may develop hypertension, diabetes, heart failure or atherosclerosis, most often related to a change in arterial stiffness. Considering the wide spread of CVDs in the world, there is a strong need for, besides adopting prevention, an easy and quick prognostic indicator of this disease to support early diagnosis.

Arterial stiffness is most commonly used to express the viscoelastic properties of the arterial wall and is expressed as the relationship between change in pressure and change in volume. Arterial stiffness is a reliable prognostic indicator of cardiovascular morbidity. The gold standard for determining arterial stiffness is measuring the pulse wave velocity (PWV), which is the speed of the pressure pulse traveling through the moving blood. The goal of this Ph.D. study was to develop and validate a non-invasive, photoplethysmography (PPG)-based device for peripheral measurement of the PWV on the finger. To that purpose, the following aims were formulated:

- to confirm the value of peripheral PWV measurements,
- to design and technically validate a PPG-based device for measuring PWV in the finger,
- to validate the developed device in clinical studies.

The Ph.D. study existed of two complementary parts: Part I – Substantiation, illustrates the value of peripheral PWV measurements and provides a platform-independent and measurement technique independent algorithm for improvement of PWV measurements. Part II - Development & Validation, describes the design, technical validation, testing, further improvement and final validation of the Multi

Photodiode Array (MPA), the PWV measurement device developed during this Ph.D. study.

Literature study revealed that filtering techniques that are used to eliminate unsuitable pulse waves (PWs) are often not described in articles using PWs to determine physiological parameters for research or diagnostic purposes. Using unfiltered PPG-data may result in deviations in the calculated values from the actual values. In order to obtain valid measurements, it is essential to only use PWs that contain the morphological landmarks on which the definition of a PW is based. A '7Step PW-filter' algorithm was developed to apply 7 criteria to PW data to determine whether a PW matches the characteristics required to allow pulse transit time (PTT) or PWV-calculations.

PTT, the propagation time of a PW going from the heart tot the peripheral arteries, consist of 2 components: the isovolumetric contraction time (pre-ejection period 'PEP') and the PW propagation time through the vessel. The PEP is known to vary with cardiac preload and heart rate. When measuring PTT or PWV with a method that includes the PEP, the PEP contributes approximately 20% of the measured value. PTT/PWV at rest is an easy-to-use, non-invasive and accurate physiological parameter for monitoring arterial stiffness. In order not to suffer from the PEP, a system that allows measuring the PWV without including the PEP would be beneficial.

PTT/PWV measurements are valuable in various clinical applications. For upper limb surgery, an axillary plexus block is used to desensitize and demobilize the arm and deactivate the vascular walls. The axillary plexus block affect the sympathetic nerves resulting in relaxation of the arterial wall muscle and vasodilatation, and change the state of the vascular system. By measuring the change of PTT during an axillary plexus block the condition of the vascular system can be determined much quicker and more objectively than by the conventional, subjective sensory test.

Pain is commonly assessed subjectively by interpreting patient behaviour and/or by report from patients. Pain is a sensation that is highly subjective, but also has objective aspects. An experiment on 25 volunteers showed that the PTT decreases centrally in response to heat-induced pain stimuli. This suggests that the PTT is reliable parameter of pain-induced alterations of vasotonus and can be measured on a contralateral extremity in situations in which it is impossible or undesirable to measured directly on the affected extremity.

A novel sensor, called "Multi Photodiode Array" ('MPA'), was designed for peripheral, non-invasive PWV measurements along a trajectory of 12 mm on the finger. The MPA basically is a transmission PPG sensor with a single row photodiode array instead of a single photodiode. The MPA can simultaneously measure the pulse rate, pulse wave amplitude, and peripheral PTT, and could also measure SpO_2. The MPA was shown to deliver reliable and accurate PWV measurements with a deviation below 3% within clinically relevant ranges.

Biopac and Complior are two existing systems that are generally used to non-invasively measure the PWV in the large arteries over a long trajectory. A study was conducted on healthy volunteers to investigate whether comparable results are provided by these systems, which both measure PWV over similar, but different trajectories. The results showed that the two systems correlated well, but the Biopac returned consistently lower PWV values than the Complior. This suggests that as long as the difference in PWV magnitude is taken into account, either system could be used to measure PWV changes over time.

During the course of the research it was observed that the MPA positioning on the finger could strongly affect the quality of the PWV measurements. Therefore, an explorative study was conducted to find the optimal use condition of the MPA. Four aspects were explored: light pollution reduction, using collimators, shortening the light travel paths between the LEDs and photodiodes in the MPA, and optimizing the contact pressure of the MPA on the finger. The optimal use condition of the MPA appeared to be: soft-side positioning of the MPA, locating the active photodiodes across the middle, fleshy side part of the distal phalanx and using light contact pressure. The robustness and user-friendliness of the established optimal use condition was further substantiated in a final clinical validation study on 30 healthy volunteers of various ages and builds. That study showed that the MPA could be placed easily, rapidly, and consistently, irrespective of the volunteer.

Overall, the results in this thesis suggest that the novel, PPG-based, MPA allows accurate and reliable PWV measurements within clinically relevant ranges. Some important advantages of the MPA as compared to other PWV measurement systems are that the MPA is easy-to-use, non-invasive, and provides objective data. In the future, the MPA may substantially simplify PWV measurements and enable long-term monitoring of vascular health, which may contribute to improving prevention, diagnosis and treatment of CVDs.

Marit van Velzen, 2019

Samenvatting

DE SNELHEID VAN GOLVEN

Het meten van de snelheid van bloeddrukgolven
die door perifere bloedvaten bewegen

Wereldwijd zijn hart- en vaatziekten (HVZ) doodsoorzaak nummer één. Roken, ongezond eten, niet sporten en overmatig alcoholgebruik zijn belangrijke factoren voor HVZ. Als gevolg daarvan kan men hypertensie, diabetes, hartkwalen of aderverkalking ontwikkelen. Gezien de grote omvang van HVZ wereldwijd, is het van groot belang dat er onderzoek gedaan wordt naar een makkelijke en snelle methode voor het opsporen van deze aandoeningen om een tijdige diagnose te kunnen stellen.

Arteriële stijfheid is de meest gebruikte maat voor de viscoelastische eigenschappen van de vaatwanden wordt bepaald uit de relatie tussen de verandering van de bloedvatdiameter als gevolg van een drukverandering in het vat. Daardoor is de arteriële stijfheid een reële indicator voor cardiovasculair morbiditeit. De gouden standaard voor het bepalen van arteriële stijfheid is het meten van de "pulse wave velocity" (PWV), oftewel de snelheid waarmee een bloeddrukpuls door het bloed in de vaten reist. Het doel van dit promotieonderzoek was het ontwikkelen en valideren van een niet-invasief, fotoplethysmografie (PPG)-gebaseerd apparaat voor het perifeer meten van de PWV in de vinger. Daarvoor zijn de volgende doelen gesteld:

- het onderbouwen van het nut van perifere PWV-metingen,
- het ontwerpen en technische valideren van een PPG-gebaseerd apparaat voor het meten van de PWV in de vinger,
- het ontwikkelde apparaat in klinische studies valideren.

Het promotieonderzoek bestaat uit twee delen: Deel I - Onderbouwing laat zien wat de waarde is van perifere PWV-metingen en biedt een platform- en meettechniek-onafhankelijk algoritme voor verbetering van PWV-metingen. Deel II - Ontwikkeling & Validatie beschrijft het ontwerp, technische validatie, testen,

verdere verbetering en uiteindelijke validatie van de Multi Photodiode Array (MPA), het PWV-meetinstrument dat tijdens dit promotieonderzoek is ontwikkeld.

Uit literatuurstudie is gebleken dat filtertechnieken die worden gebruikt om voor analyse ongeschikte bloeddrukgolven (PW's) te elimineren vaak niet worden beschreven in artikelen die PW's gebruiken om fysiologische parameters te bepalen voor onderzoek of diagnostische doeleinden. Het gebruik van ongefilterde PPG-data kan leiden tot afwijkingen in de berekende waarden ten opzichte van de werkelijke waarden. Om geldige PWV-waarden te verkrijgen, is het van essentieel belang om alleen PW's te gebruiken die de morfologische oriëntatiepunten bevatten waarop PWV is gedefinieerd. Een '7Step PW-filter'-algoritme is ontwikkeld om te bepalen of een PW overeenkomt met de zeven karakteristieken die vereist zijn om pulse transit time (PTT) en PWV-berekening mogelijk te maken.

Pulse transit time is de voortplantingstijd van een PW die van het hart naar de perifere vaten gaat en omvat mede de isovolumetrische samentrekkingsduur (pre-ejectieperiode, PEP). Het is bekend dat de PEP varieert met de hartvoorspanning en hartslag. Wanneer de PTT of PWV gemeten wordt met een methode waarbij de PEP wordt meegenomen, is de bijdrage van de PEP ongeveer 20% van de gemeten waarde. PTT in rust is een eenvoudige, niet-invasieve en nauwkeurige fysiologische parameter voor het monitoren van de arteriële stijfheid. Om invloed van de PEP uit te sluiten, zou een systeem dat het mogelijk maakt de PWV te meten zonder de PEP mee te nemen gunstig zijn.

PTT/PWV metingen zijn waardevol in verschillende klinische toepassingen. Voor een operatie aan de bovenste ledematen kan een axillair plexusblok gebruikt worden om de arm ongevoelig te maken en de vaatwanden te deactiveren. De blokkade beïnvloedt de sympathische zenuwen resulterend in ontspanning van de slagaderlijke wandspier en vasodilatatie, en verandert de toestand van het vasculaire systeem. Door de verandering van PTT te meten tijdens een blokkade kan veel sneller en objectiever de toestand van het vasculaire systeem gemeten worden dan met conventionele, subjectieve, sensorische tests.

Pijn wordt vaak subjectief beoordeeld door interpretaties van het gedrag en/of meldingen van patiënten. Pijn is een sensatie die zeer subjectief is, maar ook objectieve aspecten heeft. Een test op 25 vrijwilligers liet zien dat de PTT centraal daalt als gevolg van een door warmte geïnduceerde pijnpuls. Dit suggereert dat de PTT een betrouwbare parameter is voor door pijn geïnduceerde veranderingen van

vasotonus en kan worden gemeten aan de contralaterale zijde in situaties waarin het onmogelijk of onwenselijk is om direct op de aangedane extremiteit te meten.

Een nieuwe sensor, genaamd "Multi Photodiode Array", is ontworpen voor perifere, niet-invasieve PWV metingen over een traject van 12 mm op de vinger. De MPA is een transmissie-PPG-sensor met een fotodiode-array voor PWV-metingen. De MPA kan tegelijkertijd ook de pulsfrequentie, pulsgolf-amplitude, perifere PTT en SpO_2 meten. Het is aangetoond dat de MPA betrouwbare en accurate PWV metingen levert met een afwijking van minder dan 3% binnen klinische relevante bereiken

Biopac en Complior zijn twee bestaande systemen die worden gebruikt om niet-invasief de PWV in de grote slagaders over een lang traject te meten. Er is een studie uitgevoerd bij gezonde vrijwilligers om te onderzoeken of vergelijkbare resultaten worden geleverd door deze systemen, die beide de PWV meten over vergelijkbare, maar verschillende trajecten. De resultaten toonden aan dat de twee systemen goed gecorreleerd zijn, maar dat de Biopac consistent lagere PWV waarden ten opzichte van de Complior leverde. Dit suggereert dat, zolang het verschil in PWV-waarde wordt meegenomen, beide systemen gebruikt kunnen worden om PWV-veranderingen over de tijd te meten.

Tijdens het onderzoek werd vastgesteld dat de positionering van de MPA op de vinger de kwaliteit van de PWV metingen sterk kon beïnvloeden. Daarom is een verkennend onderzoek uitgevoerd om de optimale gebruiksconditie van de MPA te vinden. Vier aspecten werken onderzocht: vermindering van lichtverstoring, gebruik van collimators, kortere lichtroutes tussen de LED's en fotodiodes en de optimalisatie van de contactdruk van de MPA op de vinger. De optimale gebruiksconditie van de MPA bleek te zijn: zachte-zijdepositionering van de MPA, lokaliseren van de actieve fotodiodes over het middelste, vlezige deel van de zijkant van de vinger en gebruikmakend van lichte contactdruk. De robuustheid en gebruiksvriendelijkheid van de optimale gebruiksconditie is verder onderbouwd in een klinische validatiestudie op 30 gezonde vrijwilligers van verschillende leeftijden. Uit de studie bleek dat de MPA gemakkelijk, snel en consistent kon worden geplaatst, ongeacht de vrijwilliger.

Over het algemeen suggereren de resultaten in dit proefschrift dat de nieuwe, op PPG gebaseerde, MPA accurate en betrouwbare PWV metingen mogelijk maakt binnen een klinisch relevante bereik. Enkele belangrijke voordelen van de MPA in vergelijking met andere PWV-meetsystemen zijn dat de MPA gemakkelijk in gebruik is, niet-invasief is en objectieve informatie levert. In de toekomst kan de

MPA-sensor PWV metingen aanzienlijk vereenvoudigen en langdurige monitoring van vasculaire gezondheid mogelijk maken, wat kan bijdragen aan het verbeteren van de preventie, diagnose en behandeling van hart- en vaatziekten.

Marit van Velzen, 2019

Met dank aan

Promotor	Prof. dr. Robert Jan Stolker
Copromotoren	dr. ing. Sjoerd Niehof
	dr. Bert Mik
Promotiecommissie	Prof. dr. I. Reijs
	Prof. dr. J. Dankelman
	Prof. dr. H. Verhagen
	Prof. dr. F. Huyghen
	Prof. Dr. ir. J. Harlaar
	Prof. dr. T. Leeuwen
	Dr. ir. A. v.d. Giessen
Paranimfen	Arjo & Minke
Collega's Experimentele Anesthesiologie	Floor, Harold, Jacqueline, Mariska
	Minke, Patricia & Sander
Collega's ErasmusMC	Emmy, Eva, George, Judith,
	Nadia & Shoista
Collega's TUDelft MisitLab	Annetje, Arjan, Arjo, Hoda,
	Julie, Kirsten, Linda, Listte,
	Nick, Roos & Tonke
Collega's JBZ	Alina, Bas, Jeroen & Nanneke
Beste Vrienden	Arjo & Jikke
Grootste Fan	Irma
Zussen	Jette & Irrin
Ouders	Lieneke & Albert

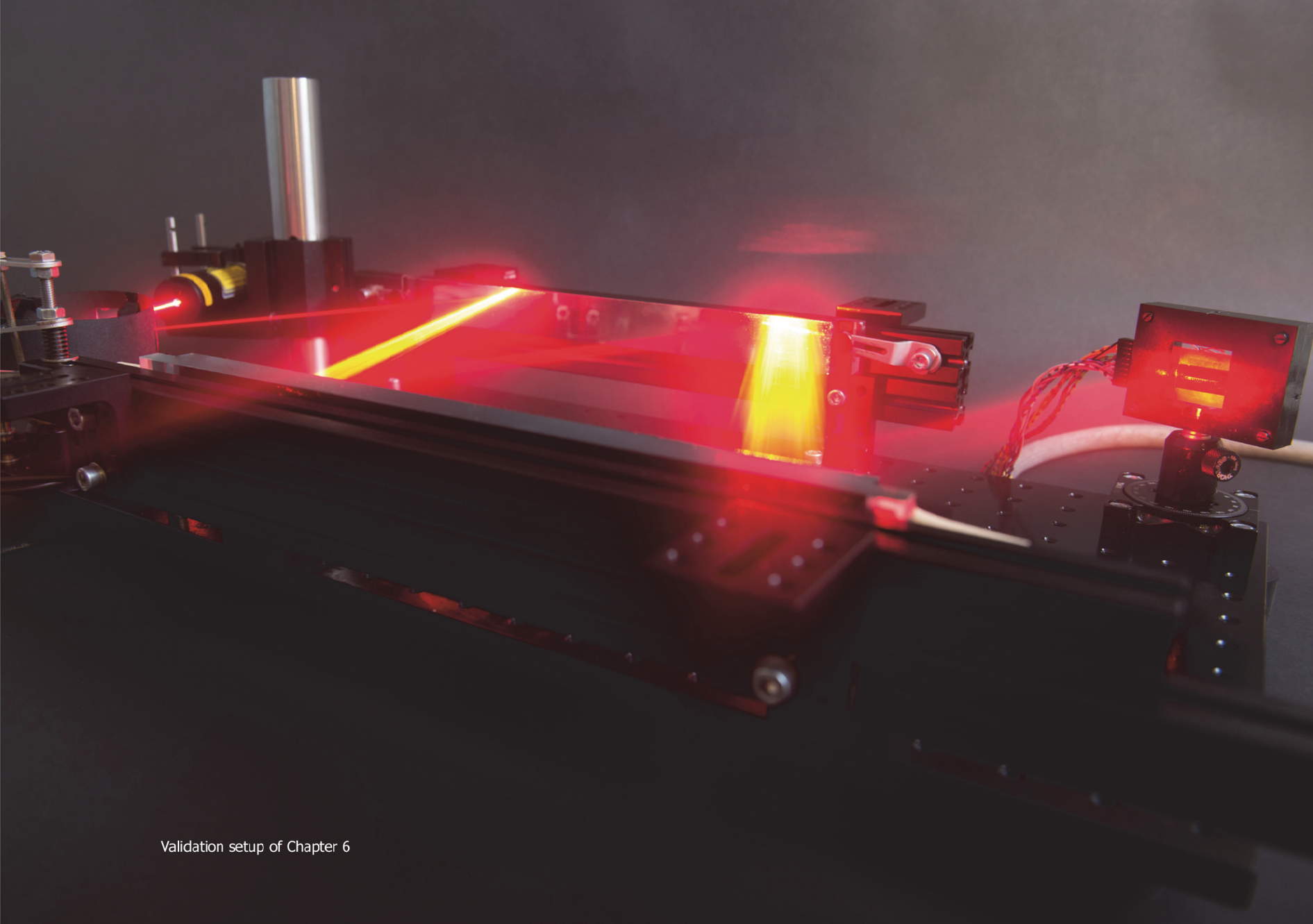

Validation setup of Chapter 6

Publications

Scientific publications

VAN VELZEN M.H.N., NIEHOF S.P., MIK E.G. ,LOEVE A.J. 2019. Measuring pulse wave velocity with a novel, simple sensor on the finger tip: A feasibility study in healthy volunteers. *Submitted*

KORTEKAAS M.C., **VAN VELZEN M.H.N.,** GRÜNE F., NIEHOF S.P., STOLKER R.J., HUYGEN F.J.P.M. 2018. Small intra-individual variability of the pre-ejection period justifies the use of pulse transit time as approximation of the vascular transit time. *PLOS ONE*

VAN VELZEN M.H.N., STOLKER R.J., LOEVE A.J., NIEHOF S.P., MIK E.G. 2018. Comparision between pulse wave velocity measured using Complior and measured using Biopac. *Journal of Clincial Monitoring and Computering*

HEMELRIJK S.D., DIRKES M.C., **VAN VELZEN M.H.N.,** BEZEMER R., VAN GULIK T.M., HEGER M. 2018. Exogenous hydrogen sulfide gas does not induce hypothermia in normoxic mice. *Scientific Reports Nature*

VAN VELZEN M.H.N., & LOEVE A.J., MIK E.G., NIEHOF, S.P. 2017. Design and functional testing of a novel blood pulse wave velocity sensor. *Journal of Medical Devices*

VAN VELZEN M.H.N., LOEVE A.J., NIEHOF S.P., MIK E.G. 2017. Increasing accuracy of pulse transit time measurements by automated elimination of distorted photoplethysmography waves. *Medical & Biological Engeneering & Computing*

VAN VELZEN M.H.N., LOEVE A.J., KORTEKAAS M.C., NIEHOF S.P., MIK E.G., STOLKER R.J. 2015. Effect of heat-induced pain stimuli on pulse transit time and pulse wave amplitude in healthy volunteers. *Physiological Measurement*.

KAMBIZ S., VAN NECK J.W., COSGUN S.G., **VAN VELZEN M.H.N**., JANSSEN J.A.M.J.L., AVAZVERDI N., HOVIUS S.E.R., WALBEEHM E.T. 2015. An early diagnostic tool for diabetic peripheral neuropathy in rats. *PLOS ONE*

KLIJN E., **VAN VELZEN, M.H.N.**, LIMA A.P., BAKKER J., VAN BOMMEL J. GROENEVELD A.B.J. 2015. Tissue perfusion and oxygenation to monitor fluid responsiveness in critically ill, septic patients after initial resuscitation: a prospective observational study. *Journal of Clinical Monitoring and Computing*.

KORTEKAAS M.C., NIEHOF S.P., **VAN VELZEN M.H.N**., GALVIN E.M., HUYGEN F.J.P.M. STOLKER R.J. 2012. Pulse transit time as a quick predictor of a successful axillary brachial plexus block. *Acta Anaesthesiologica Scandinavica.*

KORTEKAAS M.C., NIEHOF S.P**., VAN VELZEN M.H.N**., GALVIN E.M., STOLKER R.J. HUYGEN F.J.P.M. 2012. Comparison of bilateral pulse arrival time before and after induced vasodilation by axillary block. *Physiological Measurement*.

Scientific presentations

VAN VELZEN M.H.N, EGGENKAMP M., DE GRAAF S., QUINTEN M., SIMONS T., LOEVE A.J., VAN DER GIESSEN A.G. **'***Sprint Splint', rapidly customized, patient specific wrist splint.***.** BioMedical Engineering (BME) 7th Annual Congress 2019, Egmond aan Zee, Netherlands, *poster presentation*

VAN VELZEN M.H.N, VAN DE VEN J. 2016. *De mogelijkheden met 3D printen binnen het ziekenhuis.* Wetenschapsmiddag Jeroen Bosch Ziekenhuis 2016, 's Hertogenbosch, *E-poster pitch*

VAN VELZEN M.H.N, LOEVE A.J., MIK E.G., NIEHOF S.P., STOLKER R.J. *Functional testing of a novel pulse wave velocity sensor***.** BioMedical Engineering (BME) 5th Annual Congress 2015, Egmond aan Zee, Netherlands, *oral presentation*

VAN VELZEN M.H.N, LOEVE A.J., KORTEKAAS M.C., NIEHOF S.P., MIK E.G., STOLKER R.J. *Can pulse transit time be used as an indicator of pain?* 10ste Wetenschapsdag Anesthesiologie 2013, Hotel Theater Figi Zeist, the Netherlands, *oral Presentation*

VAN VELZEN M.H.N, LOEVE A.J., KORTEKAAS M.C., NIEHOF S.P., MIK E.G., STOLKER R.J. *Can a simple photodiode be used to detect pain?* Society for Medical Innovation and Technology (SMIT) 25nd International Congress 2013, Baden-Baden, *oral presentation*

VAN VELZEN M.H.N, LOEVE A.J., KORTEKAAS M.C., NIEHOF S.P., MIK E.G., STOLKER R.J. *Effect of heat-induced pain stimuli on Pulse Transit Time* BioMedical Engineering (BME) 4th Annual Congress 2013, Egmond aan Zee, Netherlands, *poster presentation*

VAN VELZEN M.H.N, MIK E.G., NIEHOF S.P., STOLKER R.J. *Assessment of the Multi Photodiode Array (MPA) functionality – Preliminary results* Society for Medical Innovation and Technology (SMIT) 23nd International Congress 2012, Barcelona Spain, *poster presentation*

VAN VELZEN M.H.N, KORTEKAAS M.C., NIEHOF S.P., STOLKER R.J. *Measuring vascular transit time with a new photoplethysmography-sensor*. BioMedical (BME), 3rd Annual Congress 2011, Egmond aan Zee, the Netherlands, *oral presentation*

About the author

Marit van Velzen is geboren op 2de Paasdag 1988. Zij groeide op met haar ouders en haar 2 zusjes in Heesch. In 2005 behaalde ze haar HAVO diploma bij Instituut de Boer in Arnhem. Daarna startte zij de studie Technische Natuurkunde aan de Fontys Hogeschool in Eindhoven met als studierichting Medische Technologie. Haar afstudeeronderzoek deed zij bij de afdeling Experimentele Anesthesiologie van het Erasmus MC genaamd 'Kloppende optimalisatie'. Na het behalen van haar ingenieursdiploma in 2009 kreeg zij de kans om haar onderzoek, naar een betere fotoplethysmografie sensor, voort te zetten. In Februari 2011 begon zij deeltijd aan haar promotieonderzoek bij de afdeling Anesthesiologie, Laboratorium voor Experimentele Anesthesiologie onder begeleiding van prof. dr. Robert Jan Stolker. Sinds November 2015 is zij fulltime werkzaam als Medische Technoloog Adviseur bij het Jeroen Bosch Ziekenhuis te 's-Hertogenbosch.

Marit van Velzen was born in Heesch, the Netherlands, on Easter Monday 1988. In 2005 she obtained her HAVO diploma at the Instituut de Boer in Arnhem, the Netherlands, and proceeded studying Technical Physics with a specialization in Medical Technology at the Fontys University of Applied Science, Eindhoven, the Netherlands. Her bachelor research was carried out at the Department of Anesthesiology at Erasmus MC called 'Throbbing optimization'. After she received her Bachelor of Science in 2009, she was invited to continue her research to improve the photoplethysmography sensor. In 2011 she started as a Ph.D. student at the Department of Anesthesiology, Laboratory of Experimental Anesthesiology under supervision of prof. dr. Robert Jan Stolker. Since November 2015 she has been working as a Medical Engineer Adviser at the Jeroen Bosch Hospital in 's-Hertogenbosch, the Netherlands.

Ph.D. Portfolio

Summary of Ph.D. training and teaching

Name PhD candidate	Marit H.N. van Velzen
Erasmus MC Department	Anesthesiology
Research school	COEUR
PhD Period	2011 – 2018
Promotor	Prof. dr. R.J. Stolker
Supervisors	dr. E.G. Mik & dr. ing. S.P. Niehof

1. PhD Training	Year	ECTS
General courses		
BROK (Basiscursus Regelgeving en Organistatie voor Klinisch onderzoekers) Erasmus University	2010	1.0
Reanimatie course	2011	0.1
Photoshop and Illustrator course	2013	0.6
Laser safety in the medical sector	2014	0.3
Workshop Solidworks Tekenen, Assemblies & Werktekeningen	2014	0.9
Her-registratie BROK	2014 & 2018	0.8
Forensic Engineering; learning from failures	2017	0.6
Seminar and Workshops		
Master Class Cardiac Output, Erasmus MC, Rotterdam	2010	0.1
LabVIEW programming courses, National Instruments	2011 & 2012	0.3
Course: Patient Oriented Research: design, conductance, analysis and clinical implications	2010 & 2012	0.6
Systematic literature research course, Erasmus MC, Rotterdam	2012	0.5
Social and Didacting skills, Erasmus MC, Rotterdam	2012	0.3
Workshops PhD Days, Erasmus MC, Rotterdam	2012	0.1
EDICA Düsseldorf	2012 -2018	1.0
Symposia Scientific Integrity ERIM, Erasmus MC, Rotterdam	2012	0.1
Study design: beyond simple randomization, Erasmus MC, Rotterdam	2012	0.1

(Inter) national conferences

Attendance		
TREND consortium congress	2010	0.6
Dutch Society of Anesthesiology Research day, Ede	2010 & 2012	0.8
STW Annual Congress	2012	0.3
IMDI MedTechWest Event, Delft	2013 & 2015	0.3
Society for Medical Innovation and Technology (SMIT), Delft	2016	0.3
Presentation		
Bio Medical Engineering (BME) Egmond aan Zee, oral presentation	2011	1.6
Society for Medical Innovation and Technology (SMIT), Barcelona, poster presentation	2012	1.9
Dutch Society of Anesthesiology Research day, Zeist, oral presentation	2013	1.6
Society for Medical Innovation and Technology (SMIT), Baden-Baden, oral presentation	2013	1.9
Bio Medical Engineering (BME) Egmond aan Zee, poster presentation	2013	1.6
Bio Medical Engineering (BME) Egmond aan Zee, oral presentation	2015	1.6

2. Teaching	**Year**	**ECTS**
Lecturing		
Elective courses of medical students, Erasmus MC, Rotterdam	2013 - 2014	1.0
Supervising projects		
Supervising Junior Science students	2009 - 2012	3.5
Supervising medical students (research projects)	2011 – 2013	1.0
Supervising student of Clinical Technology students‘, Delft University of Technology	2017 - 2018	5.0
Supervising students		
'Research for improving DNIC measurement device'', Daniel Stolk & Marco Evenaars, Healthcare technology, University of Applied Science Rotterdam	2010 - 2011	5.0
‘Design of an improved photoplethysmographic-clip', Gerjan van Geest, Industrial Design Engineering, Delft University of Technology	2012	5.0
'Smart Sensor Holder'', Minor group, Technical students of University of applied science Utrecht	2014	1.0
‘Evaluatieonderzoek aanschaftraject MICT’, Anne Vonk, Healthcare technology, University of Applied Science Rotterdam	2016	3.0

'Vervanging oorthermometer', Bianca Wolvekamp, Middenkader Engineering ROC Albeda College	2016	1.0
'Beveiliging van patiëntengegevens bij toekomstige ziekenhuisverplaatste zorg', Michiel Nijholt, Healthcare technology, University of Applied Science Tilburg	2017	5.0
'Vervanging videomonitoren op de OK', Marléne van Mil, Healthcare technology, University of Applied Science Tilburg	2017	3.0
'3D geprinte lichtpenhouder voor op OK', Tommie van Houtum, Middenkader Engineering ROC Oss	2017	1.0
'Physical factors contributing to adverse effects in infusion processes: A systematic review', Michiel Adriaanse, BioMedical Engineering,Delft University of Technology	2018	1.0

NJUTA

ISBN 978-94-6375-331-9

51°47'58.5"N 5°28'53.3"E

2018SEP21 7.6°C 4-6 Bft